CHAPTER 1

Long-Lived Compounds

Lead Authors:
C. Clerbaux
D.M. Cunnold

Coauthors:
J. Anderson
A. Engel
P.J. Fraser
E. Mahieu
A. Manning
J. Miller
S.A. Montzka
R. Nassar
R. Prinn
S. Reimann
C.P. Rinsland
P. Simmonds
D. Verdonik
R. Weiss
D. Wuebbles
Y. Yokouchi

Contributors:
P. Bernath
D. Blake
T. Blumenstock
J. Butler
P.-F. Coheur
G. Dutton
D. Etheridge
L. Froidevaux
P. Krummel
J. Mühle
S. O'Doherty
D. Oram
E. Remsberg
R. Rhew
J.M. Russell III
C. Trudinger
D. Waugh
R. Zander

CHAPTER 1

LONG-LIVED COMPOUNDS

Contents

SCIENTIFIC SUMMARY

- **The fully amended and revised Montreal Protocol is continuing to be very successful in reducing the emissions and atmospheric abundances of most ozone-destroying gases. By 2005, the total combined abundance of anthropogenic ozone-depleting gases in the troposphere had decreased by 8-9% from the peak value observed in the 1992-1994 time period.**

Tropospheric Chlorine

- **Total tropospheric chlorine-containing chemicals (approximately 3.44 parts per billion (ppb) in 2004) continued to decrease.** Recent decreases (−20 parts per trillion per year (ppt/yr) or −0.59% in 2003-2004) have been at a slightly slower rate than in earlier years (−23 ppt/yr or −0.64% in 1999-2000) primarily because of the reduced contribution from methyl chloroform. The declines in total chlorine (Cl) during 2000-2004 were slightly faster than projected for these years in the Ab (most likely, or baseline) scenario of the previous (2002) Assessment (WMO, 2003).

- **Chlorofluorocarbons (CFCs), consisting primarily of CFC-11, -12, and -113, accounted for 2.13 ppb (~62%) of total Cl in 2004 and accounted for a decline of 9 ppt Cl from 2003-2004 (or nearly half of the total Cl decline in the troposphere over this period).** Atmospheric mixing ratios of CFC-12, which account for about one-third of the current atmospheric chlorine loading, have been constant within 1% (5 ppt) since 2000, and some in situ and Northern Hemisphere column measurements show that peak values were attained in 2003. CFC-11 mixing ratios are decreasing at approximately 0.8%/yr (1.9 ppt/yr) and CFC-113 mixing ratios are decreasing by approximately 1%/yr (0.8 ppt/yr), which is twice as fast as in 1999-2000.

- **Hydrochlorofluorocarbons (HCFCs), which are substitutes for CFCs, continue to increase in the atmosphere. HCFCs accounted for 214 ppt or 6% of total tropospheric chlorine in 2004 versus 180 ppt of Cl (5% of total Cl) in 2000.** HCFC-22 is the most abundant of the HCFCs and is currently (2000-2004) increasing at a rate of 4.9 ppt/yr (3.2%/yr). HCFC-141b and HCFC-142b mixing ratios increased by 1.1 ppt/yr (7.6%/yr) and 0.6 ppt/yr (4.5%/yr) over this same period or at about half the rates found for these two gases in 1996-2000. The rates of increase for all three of these HCFC compounds are significantly slower than projected in the previous Assessment (6.6, 2.6, and 1.6 ppt/yr for HCFC-22, HCFC-141b, and HCFC-142b, respectively) (WMO, 2003). HCFC-123 and -124 are currently measured, but contribute less than 1% to total chlorine from HCFCs.

- **Methyl chloroform (CH_3CCl_3) has continued to decrease and contributed 13.5 ppt (or more than half) of the overall decline observed for total tropospheric Cl in 2003-2004. It is currently still the largest contributor to the decline in tropospheric chlorine.** Globally averaged surface mixing ratios were 22.6 ppt in 2004 versus 46.4 ppt in 2000.

- **An imbalance exists between the emissions inferred from the atmospheric measurements and the emissions needed to account for the stratospheric and ocean sinks and the more recently discovered soil sink of CCl_4.** CCl_4 continues to decline at an approximately steady rate of 1 ppt/yr (about 1%/yr).

- **The globally averaged abundance of methyl chloride of 550 ± 30 ppt is the same as that given in the previous Assessment, and there has been no consistent trend in the atmospheric values in recent years.** Mixing ratios at midlatitudes of the two hemispheres are 5-10% lower than the high values measured in 1997-1998 (which were probably related to large-scale effects of forest fires). Firn air measurements show an increase of approximately 50 ppt (10%) from 1940 to 1990.

Stratospheric Chlorine and Fluorine

- **The stratospheric chlorine burden derived by the ground-based total column and space-based measurements of inorganic chlorine is now in decline. This is consistent with the decline in tropospheric chlorine from long-lived halocarbons (CFCs, carbon tetrachloride, methyl chloroform, HCFCs, methyl chloride, and halon-1211).** The burden of total stratospheric chlorine derived from satellite measurements agrees, within ±0.3 ppb (about 12%), with the amounts expected from surface data when the delay due to transport is considered. The uncertainty in this burden is large relative to the expected chlorine contribution from shorter-lived gases (0.05 to 0.1 ppb, see Chapter 2).

LONG-LIVED COMPOUNDS

- **Column and satellite measurements of hydrogen fluoride continued to show the reduction in the upward trend that began in the late 1990s.** This reduction is consistent with the change in tropospheric fluorine burden derived from CFCs, HCFCs, and hydrofluorcarbons (HFCs).

Total Tropospheric Bromine

- **Total organic bromine from halons and methyl bromide (CH_3Br) peaked in about 1998 at 16.5 to 17 ppt and has since declined by 0.6 to 0.9 ppt (3 to 5%).** This observed decrease was solely a result of declines observed for methyl bromide. Bromine (Br) from halons continues to increase, but at slower rates in recent years (+0.1 ppt Br/yr in 2003-2004).

- **Atmospheric amounts of methyl bromide declined beginning in 1999, when industrial production was reduced.** By mid-2004, mixing ratios had declined 1.3 ppt (14%) from the peak of 9.2 ppt measured before 1999. Reported production of methyl bromide for emissive uses decreased by 50% during this same period.

- **Both the recently observed decline and the 20th-century increase inferred for atmospheric methyl bromide were larger than expected.** Although industrial emissions of methyl bromide were thought to account for 20 (10-40)% of atmospheric methyl bromide during 1992-1998 (i.e., before production was reduced), the observations are consistent with this fraction having been 30 (20-40)%. This suggests that fumigation-related emissions could have a stronger influence on atmospheric methyl bromide mixing ratios than estimated in past Assessments, though uncertainties in the variability of natural emission rates and loss, and in the magnitude of methyl bromide banked in recent years, influence our understanding of this sensitivity.

- **Mixing ratios calculated from updated emission estimates are in good agreement with the measurements for halon-1211 but they exceed all the halon-1301 measurements since 1980 by more than 10%.** Atmospheric increases in halon-1211 (0.06 ppt/yr or 1%/yr) in 2000-2004 were about half those in 1996-2000. It is currently unclear whether atmospheric mixing ratios of halon-1301 continue to increase.

Equivalent Effective Stratospheric Chlorine (EESC) and Effective Equivalent Chlorine (EECl)

- **The decrease in EECl over the past 10 years has been 20% of what would be needed to return EECl values to those in 1980 (i.e., before the Antarctic stratospheric ozone hole).** EECl has decreased at a mean rate of 29 ppt EECl per year from 1994 to 2004 in the lower atmosphere. This amounts to a total decline of 277 ppt or 8-9% for EECl over this period. The reduction in stratospheric EESC is somewhat less because it takes a few years for near-surface trends to be reflected in the stratosphere. These declines are slightly larger than projected in the previous Assessment primarily because of the decline in methyl bromide.

- **The decline in the short-lived methyl chloroform and methyl bromide contributed the most to the decline in the effective equivalent chlorine in the atmosphere.** The total decline was about 120 ppt between 2000 and 2004, of which about 60 ppt was due to the decline of methyl chloroform and about 45 ppt due to methyl bromide. The CFCs together accounted for less than 23 ppt of this decline. The contribution of HCFCs was 12 ppt in the other direction, i.e., an increase.

Emission Estimates

- **Global emissions of CFC-11 (88 Gg/yr), CFC-12 (114 Gg/yr), and CFC-113 (6 Gg/yr) in 2003 were approximately 25%, 25%, and 3% of their maximum values around 1986.** Emissions of CFC-11, CFC-12 and CFC-113 have all continued to decrease since 2000.

- **Reported regional emission estimates for CFCs, methyl chloroform, and CCl_4 have been summed for the first time.** Differences between developed and developing regions are indicative of the differing schedules of phase-out. However, the patchiness in the present coverage (especially in developing regions such as Southeast Asia) and the uncertainties in the regional estimates, mean that useful comparisons between summed regional emissions and global emissions derived from trends cannot currently be made. Regional emission estimates of methyl chloroform indicate that global emissions after 2000 may have been roughly 22 Gg/yr, which is not statistically different from the estimate of 12.9 Gg/yr (for 2002) obtained from industry/United Nations Environment Programme data.

- **While emissions of HCFC-22 have remained nearly constant from 2000 to 2004, emissions of HCFC-141b and HCFC-142b decreased by approximately 15% over the same period.**

- **HFC-23 emissions estimated from atmospheric measurements have increased from about 6 Gg/yr in 1990 to about 13 Gg/yr in 2001 (an increase of approximately 120%).** These emissions are a byproduct of HCFC-22 production.

Hydrofluorocarbons (HFCs)

- **The atmospheric abundances of all measured HFCs are increasing due to their rapid introduction as CFC and HCFC replacements.** HFC-134a concentrations reached 30 ppt in 2004 and are increasing at 3.9 ppt/yr (13%/yr). Globally averaged concentrations of HFC-125 and HFC-152a were both approximately 3.1 ppt in 2004, increasing by about 23%/yr and 17%/yr, respectively. HFC-23 mixing ratios in the Southern Hemisphere were 18 ppt in 2004, having increased at a mean rate of 0.7 ppt/yr (4%/yr) in 2001-2004.

Sulfur Hexafluoride (SF$_6$)

- **Measurements of SF$_6$ suggest its global average concentration in 2003 was 5.2 ppt and it was growing by 0.23 ppt/yr (4%/yr).** Similar percentage rates of increase have been estimated from column measurements over Switzerland. Temporal extrapolation of the past 20 years of measurements results in significantly smaller atmospheric concentrations in the future than those produced in the most likely emission scenario from the previous Assessment.

1.1 INTRODUCTION

Ozone depletion observed in the stratosphere over the past three decades has resulted from the accumulation of trace gases in the atmosphere. This was due to industrial activities and to a much-reduced extent to agricultural practices, which led to increases in the concentrations of chlorine, bromine, nitrogen, and hydrogen radicals in the stratosphere. These radicals are produced from long-lived source gases that, because their atmospheric lifetimes are long compared with the transport time to reach the stratosphere, are able to be transported intact into the stratosphere. The Montreal Protocol and its Amendments and Adjustments have, however, led to reductions in the tropospheric abundances of the chlorine- and bromine-containing source gases as a result of reductions in the production and consumption of manufactured halogenated source gases.

Direct observations of most chemical species that cause stratospheric ozone depletion began in the late 1970s or later. The ground-based in situ and flask measurements have provided the most complete picture of the evolution of these species because of the regularity of the measurements. The complete 20th century and earlier pictures of the accumulation of ozone-depleting chemicals in the atmosphere also rely on calculations based on historic emission estimates, and analysis of air trapped in polar firn and ice or measurements of air archives. Ground-based remote sensing techniques, in particular numerous Network for the Detection of Atmospheric Composition Change (NDACC, formerly Network for the Detection of Stratospheric Change or NDSC) sites equipped with Fourier transform infrared (FTIR) instruments, have also provided multidecadal information of relevance to this chapter. Satellite observations have also provided information on the most abundant ozone-depleting substances since the mid-1980s. Although the long-term trends are difficult to measure with space-based techniques due to the generally short lifetime of the space missions, they can be inferred by combining data from multiple instruments operating in different years. This method was applied by Harries et al. (2001), using data from the Infrared Radiation Interferometer Spectrometer (IRIS) sensor in 1970 and the Interferometric Monitor for Greenhouse Gases (IMG) sensor in 1997, to identify the long-term changes in the Earth's outgoing longwave radiation, notably due to the rise of the chlorofluorocarbons (CFCs) in that time period. More recently, Rinsland et al. (2005) have compared data from the Atmospheric Trace Molecule Spectroscopy (ATMOS) missions in 1985 and 1994 and the Atmospheric Chemistry Experiment - Fourier Transform Spectrometer (ACE-FTS) data in 2004 to determine lower-stratospheric trends of several target species during the last two decades.

The atmospheric history of ozone-depleting substances in years before regular measurements began have been examined using Antarctic firn air samples (Butler et al., 1999; Sturges et al., 2001; Sturrock et al., 2002; Trudinger et al., 2004; Reeves et al., 2005). These analyses have revealed that atmospheric mixing ratios of the various CFCs and halons underwent large increases beginning in the 1950s to 1970s. As a result of international production and consumption restrictions, all of these gases now exhibit substantially reduced rates of atmospheric growth, and, for many of them, mixing ratio declines. The hydrochlorofluorocarbons (HCFCs) first appeared in the atmosphere in the 1960s to the 1980s and their mixing ratios continued to increase through 2004. Firn air results also indicate that nearly all of the CFCs, halons, methyl chloroform, and carbon tetrachloride (CCl_4) present in today's atmosphere are the result of anthropogenic production, though the existence of small natural sources or some anthropogenic production and use in years predating the oldest firn air samples cannot be ruled out.

This chapter provides a scientific update to various sections of Chapter 1 of the previous World Meteorological Organization Assessment Report (WMO, 2003; hereafter referred to as *WMO 2002*). It reports the measurements of long-lived compounds obtained from many typical observation means (Table 1-1), including firn air analysis, ground-based in situ and remote sensing stations, and satellite observations, for ozone-depleting substances and for other climate-related gases through 2004. The latter gases, which include the hydrofluorocarbons, are also discussed in Section 1.4, because they can contribute indirectly to ozone change and ozone recovery through their effects on the radiative forcing of the atmosphere. Trace gases with lifetimes shorter than 0.5 years (in particular nitrogen and hydrogen radicals) are reported in Chapter 2. The observations provide important constraints on past emissions and thereby on future emissions. Chapter 1 compares the current observed trends with the expectations based on standard emission scenarios. Further results on EECl (effective equivalent chlorine) and EESC (equivalent effective stratospheric chlorine) calculations from assumed future emission scenarios and for calculations of the remaining banks may be found in Chapter 8. The reader is referred to Table 1-4 for the chemical formulae of the gases discussed.

LONG-LIVED COMPOUNDS

Table 1-1. Measurements of long-lived compounds. *

Name	Technique
Location	
Firn air	
Law Dome	
Antarctica	Firn ice
On-Site Sampling — Ground-Based	
AGAGE – Advanced Global Atmospheric Gases Experiment	
Cape Grim, Tasmania (41°S, 145°E)	In situ GC measurements
Cape Matatula, Samoa (14°S, 171°E)	
Ragged Point, Barbados (13°N, 59°W)	
Mace Head, Ireland (53°N, 10°W)	
Trinidad Head, United States (41°N, 124°W)	
SOGE – System for Observation of Halogenated Greenhouse Gases in Europe	
Jungfraujoch, Swiss Alps (46.5°N, 8.0°E)	In situ GC measurements
Ny Ålesund, Norway (78°N, 11.5°E)	
Monte Cimone, Italy (44° N, 10.5°E)	
NOAA/ESRL – National Oceanic and Atmospheric Administration/Earth System Research Laboratory	
South Pole, Antarctica [1,2,3,4]	Flasks-GC, and in situ-GC
Palmer Station, Antarctica [4]	Flasks-GC
Cape Grim, Tasmania [2,3,4]	Flasks-GC
Cape Matatula, Samoa [1,2,3,4]	Flasks-GC, and in situ-GC
Mauna Loa, United States [1,2,3,4]	Flasks-GC, and in situ-GC
Cape Kumukahi, United States [2,3,4]	Flasks-GC
Niwot Ridge, United States [1,2,3]	Flasks-GC, and in situ-GC
Wisconsin, United States [2,4]	Flasks-GC
Harvard Forest, United States [4]	Flasks-GC
Barrow, United States [1,2,3,4]	Flasks-GC, and in situ-GC
Alert, Canada [2,3,4]	Flasks-GC
UCI – University of California at Irvine	
40-45 Pacific sites from 71°N to 47°S sampled approximately twice per season. www.physsci.uci.edu/~rowlandblake/ samplinglocationsmap.html	Flasks-GC
UEA – University of East Anglia	
Cape Grim, Tasmania	Flasks-GC, Archived air
Remote Sensing — Ground-Based	
Kiruna, Sweden (67.8°N, 20.4°E)	Ground-based infrared FTS
Jungfraujoch, Swiss Alps (46.5°N, 8.0°E)	Total column measurements
Kitt Peak, Arizona (32.0°N, 111.6°W)	
Izaña, Tenerife (28.3°N, 16.5°W)	
Remote Sensing — Satellite	
HALOE - Halogen Occultation Experiment	
U.S. experiment (1991-2005)	Infrared gas filter correlation
Latitudinal coverage from 80°S to 80°N/1 year	and broadband filter
	radiometry (solar occultation)
	Stratospheric-mesospheric profiles
IMG - Interferometric Monitor for Greenhouse Gases	
Japanese experiment (1996-1997)	Spaceborne infrared FTS (nadir)
Global coverage	Tropospheric columns

Table 1-1, continued.

MIPAS - Michelson Interferometer for Passive Atmospheric Sounding
    European experiment (launched in 2002)   Spaceborne infrared FTS (limb)
    Global coverage   Strato-mesospheric profiles
ACE/FTS - Atmospheric Chemistry Experiment
    Canadian experiment (launched in 2003)   Spaceborne infrared FTS (solar occultation)
    Latitudinal coverage from about 80°S to 80°N/1 year   Upper troposphere to the lower thermosphere
MLS - Microwave Limb Sounder
    U.S. experiment (launched in 2004)   Microwave sounder (limb)
    Latitudinal coverage from 82°N to 82°S daily   Upper troposphere to the lower thermosphere

[*] The list provided here is restricted to the measurements reported in this chapter. GC = gas chromatographic.

[1] Data from in situ instruments at these stations are used by NOAA to derive global tropospheric means for CFCs and CCl_4.
[2] Data from flasks collected at these stations are used by NOAA to derive global tropospheric means for CH_3CCl_3.
[3] Data from flasks collected at these stations are used by NOAA to derive global tropospheric means for HCFCs and halons.
[4] Data from flasks collected at these stations are used by NOAA to derive global tropospheric means for CH_3Br.

1.2 HALOGENATED OZONE-DEPLETING GASES IN THE ATMOSPHERE

1.2.1 Updated Atmospheric Observations of Ozone-Depleting Gases

In this section, measurements of halogenated gases by the ground-based networks are summarized. As indicated in Table 1-1, these network measurements include those by the Advanced Global Atmospheric Gases Experiment (AGAGE), the System for Observation of Halogenated Greenhouse Gases in Europe (SOGE, although the measurements used here were from Jungfraujoch and Ny Ålesund only), the National Oceanic and Atmospheric Administration / Earth System Research Laboratory (NOAA/ESRL, formerly NOAA/CMDL) and the University of California at Irvine (UCI). In a number of cases this also includes measurements of air samples collected at Cape Grim, Australia since 1978 that have been archived (Langenfelds et al., 1996). The section extends the time series described in *WMO 2002* (Montzka and Fraser et al., 2003) beyond 2000 and emphasizes the measurements from 2001 to the end of 2004. The time series for these gases shown in the Figures and Tables throughout this Chapter are from monthly means of data from individual sites that have been combined to produce monthly hemispheric and global means. Annual means of these are also used in some Figures and Tables.

Table 1-2 shows annual means of the measured ozone-depleting halocarbons. The precisions and accuracies of the measurements may mostly be judged by the differences between the reported values. Only for CFC-12, HCFC-22, and halon-1301 are the differences in the trends observed by the various groups statistically significant. All uncertainties are one sigma unless otherwise specified. Terms used to describe measured values throughout Chapter 1 are mixing ratios (for example parts per trillion, ppt, pmol/mol), mole fractions, and concentrations. These terms have been used interchangeably and, as used here, they are all considered to be equivalent.

Methyl chloride and methyl bromide have substantial natural sources and the emissions of these gases are also discussed in their subsections. The emissions of the other halocarbons are discussed in Section 1.3.

1.2.1.1 CHLOROFLUOROCARBONS (CFCs)

CFC-11 (CCl_3F), CFC-12 (CCl_2F_2), and CFC-113 (CCl_2FCClF_2) are routinely measured by the three ground-based gas-sampling networks (see Table 1-1) using gas sampling techniques. Results from these independent laboratories generally agree to within 2% (Figure 1-1). CFC-11 and CFC-12 are also measured using ground-based infrared solar absorption spectroscopy, such as at the Jungfraujoch station. From space, CFCs have been measured by a variety of shuttle- or satellite-based instruments operating in the infrared spectral region. Most of these data concern CFC-11 and CFC-12. They were obtained from thermal infrared nadir sounders (Harries et al., 2001; Coheur et al., 2003; Dufour et al., 2005), limb instruments (Bacmeister et al., 1999; Hoffmann et al., 2005), or solar occultation sounders (Khosrawi et al., 2004; Rinsland et al., 2005).

Recent measurements from the gas sampling networks indicate that the CFC-12 global trend is now approximately zero, and two of the three networks plus the remote sensing measurements at Jungfraujoch indi-
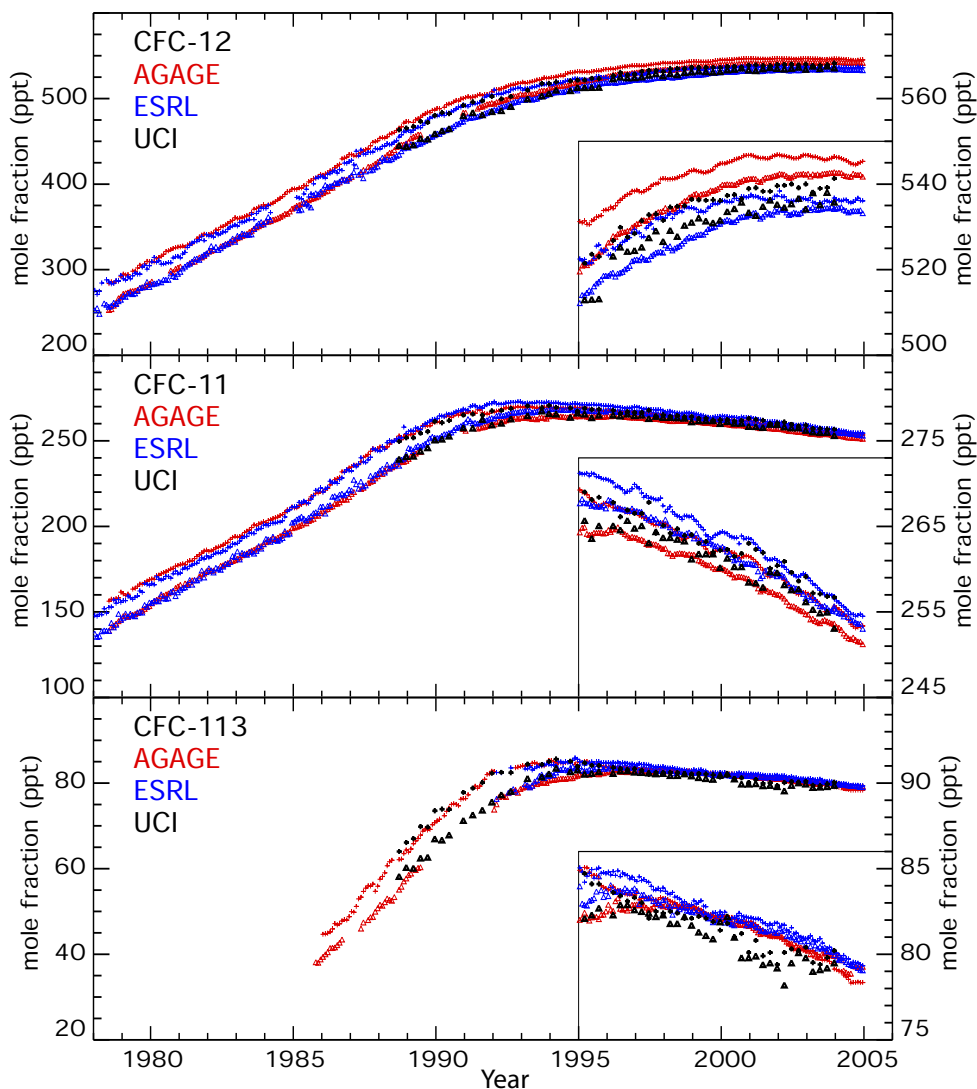
Figure 1-1. Hemispheric monthly means of the major chlorofluorocarbons CFC-12, CFC-11, and CFC-113 (crosses for Northern Hemisphere and triangles for Southern Hemisphere). Measurements from the AGAGE network (Prinn et al., 2000 updated), the NOAA/ESRL network (Montzka et al., 1999 updated; Thompson et al., 2004), and UCI (D.R. Blake et al., 1996; N.J. Blake et al., 2001) are shown. To increase visibility, recent measurements are depicted on a larger scale in the inserts (the scales are on the right-hand sides of the panels).

cate that Northern Hemispheric mole fractions are now decreasing. These observations are consistent with the analyses of Rinsland et al. (2005) using ATMOS and ACE satellite data. The measured annual column change above Jungfraujoch in 2003-2004 is -0.11×10^{14} molec cm^{-2} (-0.16%/yr) (Zander et al., 2005) compared with 0.50×10^{14} molec cm^{-2} ($+0.71\%$/yr) in 1998 (*WMO 2002*) and 0.27×10^{14} molec cm^{-2} ($+0.39\%$/yr) in 1999-2000. Trends from column measurements in %/yr should be almost directly comparable with trends for similar periods derived from the sampling networks, because of the long lifetimes of the species being discussed. Averaged over

Kiruna (68°N) and Izaña (28°N), the column trend from 2000 to 2005 is $-0.09 \pm 0.10\%$/yr (update from Kopp et al., 2003, and Schneider et al., 2005). Since the CFC-12 lifetime is approximately 100 years, the measured rate of change indicates that there are still significant emissions of CFC-12. Differences between measured Northern Hemisphere and Southern Hemisphere mole fractions have been decreasing since approximately the end of the 1980s (Figure 1-1). The hemispheric difference in 2004 was still approximately 3 ppt (0.6%), indicating that the remaining emissions are still occurring predominantly in the Northern Hemisphere.

Table 1-2. Mole fractions and growth rates of ozone-depleting gases.

Chemical Formula	Common or Industrial Name	Annual Mean Mole Fraction (ppt)			Growth (2003-2004)		Laboratory, Method
		2000	2003	2004	(ppt yr)	(% yr)	
CFCs							
CCl_2F_2	CFC-12	543.0	544.2	543.8	−0.6	−0.1	AGAGE, in situ
		534.1	535.2	535.0	−0.2	0.0	NOAA*
		535.6	537.9	539.7	1.8	0.3	UCI
CCl_3F	CFC-11	260.6	254.9	253.1	−1.8	−0.7	AGAGE, in situ
		262.5	256.6	254.7	−1.9	−0.7	NOAA*
		261.2	256.1	253.7	−2.4	−0.9	UCI
		263.9	257.3	254.7	−2.7	−1.0	SOGE, in situ (Europe)
CCl_2FCClF_2	CFC-113	81.8	79.6	78.7	−0.9	−1.1	AGAGE, in situ
		82.1	80.5	79.5	−0.9	−1.2	NOAA*
		81.1	79.5	79.1	−0.4	−0.5	UCI
$CClF_2CClF_2$	CFC-114 including -114a	17.21	17.24	17.31	0.07	0.4	AGAGE, in situ (Cape Grim only)
	CFC-114		14.90	14.72	−0.18	−1.2	UCI
$CClF_2CF_3$	CFC-115	8.10	8.26	8.34	0.08	1.0	AGAGE, in situ
		8.19	8.18	8.29	0.11	1.3	SOGE, in situ (Europe)
HCFCs							
$CHClF_2$	HCFC-22	142.8	159.0	163.9	4.9	3.0	AGAGE, in situ
		141.7	157.9	162.1	4.2	2.6	NOAA, flasks
			161.9	169.1	7.2	4.4	UCI
CH_3CCl_2F	HCFC-141b	12.82	16.70	17.42	0.72	4.2	AGAGE, in situ
		12.66	16.58	17.18	0.60	3.6	NOAA, flasks
		15.05	18.57	19.20	0.60	3.2	SOGE, in situ (Europe)
CH_3CClF_2	HCFC-142b	12.46	14.74	15.38	0.64	4.2	AGAGE, in situ
		11.72	13.99	14.53	0.54	3.8	NOAA, flasks
$CHCl_2CF_3$	HCFC-123	0.050	0.060	0.064	0.004	6.5	AGAGE, in situ (Cape Grim only)
$CHClFCF_3$	HCFC-124	1.40	1.63	1.64	0.01	0.1	AGAGE, in situ
		1.46	1.71	1.72	0.01	0.1	SOGE, in situ (Europe)
Halons							
CBr_2F_2	halon-1202	0.044	0.040	0.038	−0.002	−5.1	UEA, flasks (Cape Grim only)
$CBrClF_2$	halon-1211	4.12	4.28	4.33	0.05	1.2	AGAGE, in situ
		3.98	4.13	4.15	0.02	0.0	NOAA, flasks
		4.43	4.68	4.77	0.09	1.9	UEA, flasks (Cape Grim only)
		4.32	4.52	4.62	0.08	1.8	SOGE, in situ (Europe)
$CBrF_3$	halon-1301	2.95	3.04	3.14	0.10	3.2	AGAGE, in situ
		2.57	2.61	2.60	−0.01	0.0	NOAA, flasks
		2.26	2.38	2.45	0.07	2.9	UEA, flasks (Cape Grim only)
		3.04	3.06	3.16	0.10	3.2	SOGE, in situ (Europe)
$CBrF_2CBrF_2$	halon-2402	0.425	0.427	0.427	0.0	0.0	UEA, flasks (Cape Grim only)
		0.48**	--	0.48			NOAA, flasks

Table 1-2, continued.

Chemical Formula	Common or Industrial Name	Annual Mean Mole Fraction (ppt)			Growth (2003-2004)		Laboratory, Method
		2000	2003	2004	(ppt yr)	(% yr)	
Chlorocarbons							
CH_3Cl	Methyl chloride	532.1	523.4	527.8	4.4	0.8	AGAGE, in situ (Ireland/Cape Grim average)
		529.5	523.0	526.0	3.0	0.6	SOGE, in situ (Europe)
CCl_4	Carbon tetrachloride	96.4	93.5	92.6	−0.8	−1.0	AGAGE, in situ
		100.2	97.2	96.1	−1.1	−1.1	NOAA*
		99.2	96.3	95.1	−1.2	−1.2	UCI
CH_3CCl_3	Methyl chloroform	45.6	26.5	22.0	−4.5	−18.6	AGAGE, in situ
		45.8	26.5	22.0	−4.5	−18.7	NOAA, flasks
		47.7	28.3	23.9	−4.4	−16.8	UCI
		44.3	26.7	22.2	−4.5	−18.5	SOGE, in situ (Europe)
Bromocarbons							
CH_3Br	Methyl bromide	10.3	8.8	9.1	0.3	3.3	AGAGE, in situ (Ireland only)
		8.7	8.1	7.9	−0.2	−2.4	NOAA, flasks

All values are estimates for the global troposphere unless specified otherwise.

* These NOAA values consist of a combination of flask and in situ measurements.

** Earlier halon-2402 data from NOAA are for 1996, not 2000.

The sampling networks indicate that global mole fractions of CFC-11 decreased by approximately 2.0 ± 0.1 ppt/yr (0.8%/yr) from 2000 to 2004 (Table 1-2). This rate of decrease is larger than that reported in *WMO 2002* (Montzka and Fraser et al., 2003), 1.4 ppt/yr (0.5%/yr), for 1996 to 2000. Zander et al. (2005) indicate that the CFC-11 column change and the corresponding annual trend have remained constant since the late 1990s over the Jungfraujoch, amounting to -1.85×10^{13} molec cm^{-2} (−0.59%/yr in 2004). A slightly smaller downtrend is to be expected in the CFC-11 column than in the surface measurements, by approximately 0.1%/yr, because the proportion of CFC-11 that is in the stratosphere is predicted to have been continuing to increase slowly. The decline in the tropospheric CFC-11 mole fractions from 2000 to 2004 is approximately 20% less than that projected in the Ab (baseline, most likely) scenario of *WMO 2002* (Table 1-14, Chapter 1, WMO (2003)). The measured hemispheric difference for CFC-11 has been decreasing (Figure 1-1), but it was still approximately 2 ppt (0.8%) in 2004. This and the 45-year lifetime of CFC-11 indicate that significant Northern Hemispheric emissions are still occurring.

CFC-113 has decreased by approximately 1% (0.8 ppt) from 2003 to 2004. This is larger than the rate of decrease of 0.5%/yr reported for 1999-2000 in *WMO 2002*

(Montzka and Fraser et al., 2003). Since the lifetime is estimated to be 85 years, the recent decrease indicates that global emissions of CFC-113 are now small. Consistent with this, the hemispheric gradient is less than 1 ppt (Figure 1-1). A global decrease of CFC-113 of 1%/yr provides an upper limit to its atmospheric lifetime of 100 years.

CFC-114 ($CClF_2CClF_2$) and CFC-115 ($CClF_2CF_3$) have been measured in Cape Grim (41°S) air samples since 1978. As noted by Sturrock et al. (2001), and by Mangani et al. (2000) for Antarctica, the mixing ratio of CFC-114 was not changing in the atmosphere in mid-2000. Recent measurements indicate that there have only been small but insignificant changes of CFC-114/-114a (Table 1-2). In contrast, CFC-115, which is used with HCFC-22 ($CHClF_2$) in refrigeration blends, has continued to increase at about 1%/yr (0.08 ppt/yr), which is only half of the growth rate reported in *WMO 2002* (Montzka and Fraser et al., 2003).

1.2.1.2 HYDROCHLOROFLUOROCARBONS (HCFCS)

Measurements of HCFCs from the gas sampling networks have been updated through 2004 (O'Doherty et al., 2004; Krummel et al., 2004). Furthermore, recent remote measurements of HCFC-22 (Rinsland et al., 2005) and HCFC-142b (Dufour et al., 2005), which show gen-

eral consistency with the AGAGE and the NOAA/ESRL values, have recently become available from the ACE satellite mission.

Global mixing ratios of the three most abundant HCFCs have all increased due to sustained emissions (resulting from their being substitutes for CFCs and other ozone-depleting substances (ODSs) (Figure 1-2). The annual global mole fraction of HCFC-22 (CHClF$_2$) was

approximately 165 ppt in 2004, with an averaged annual growth rate of about 4.9 ± 0.5 ppt/yr ($3.2 \pm 0.3\%$/yr) (2000-2004, with more weight being given to the more precise trend estimates from AGAGE and NOAA/ESRL).

Combined vertical column abundances of HCFC-22 above Kiruna (68°N) and Izaña (28°N) yield a trend of $3.5 \pm 0.3\%$/yr (1.1×10^{14} molec cm^{-2} yr^{-1}) for 2000-2004 (updated from Kopp et al., 2003; Schneider et al., 2005).
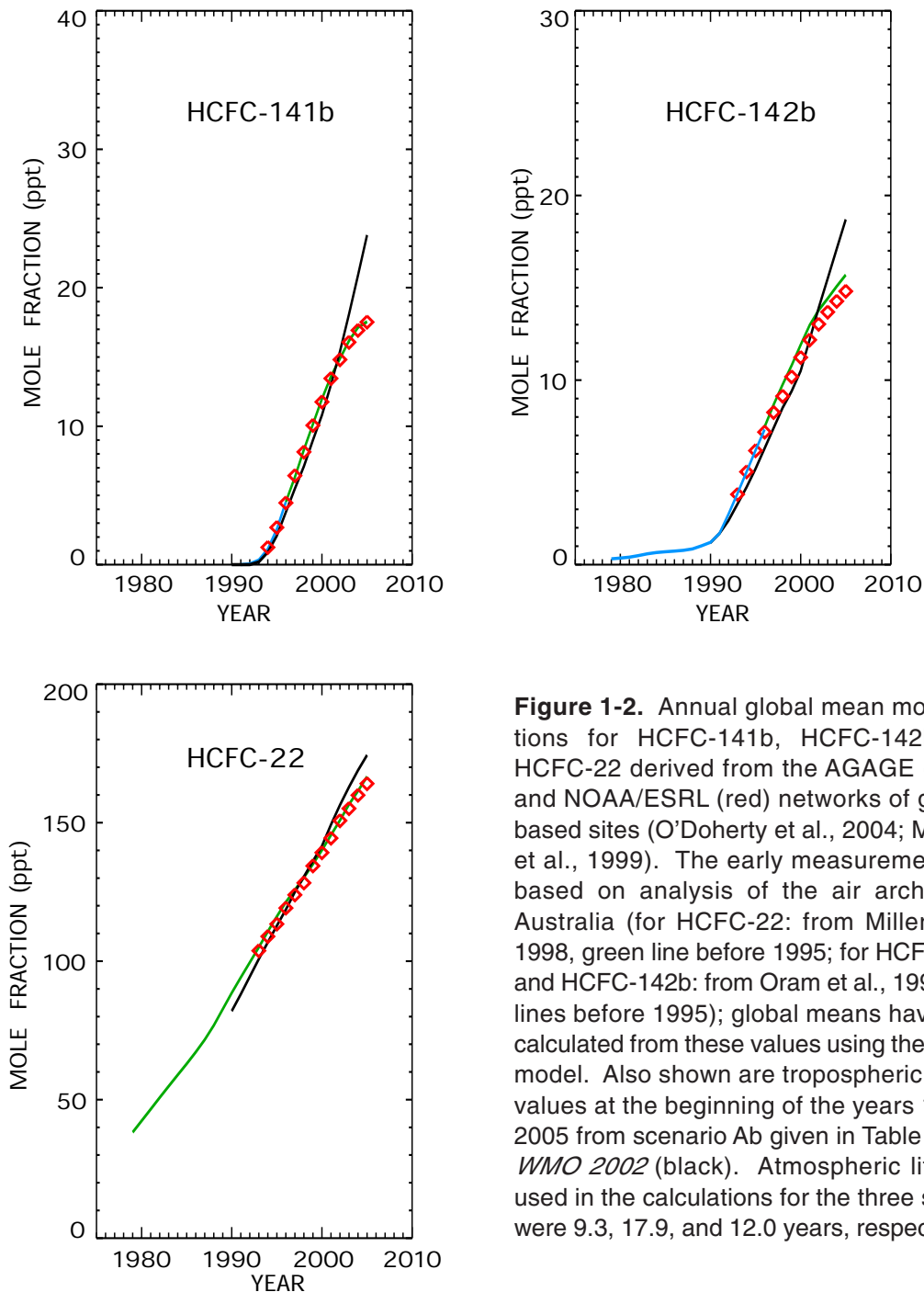

Figure 1-2. Annual global mean mole fractions for HCFC-141b, HCFC-142b, and HCFC-22 derived from the AGAGE (green) and NOAA/ESRL (red) networks of ground-based sites (O'Doherty et al., 2004; Montzka et al., 1999). The early measurements are based on analysis of the air archived in Australia (for HCFC-22: from Miller et al., 1998, green line before 1995; for HCFC-141b and HCFC-142b: from Oram et al., 1995, blue lines before 1995); global means have been calculated from these values using the 12-box model. Also shown are tropospheric annual values at the beginning of the years 1990 to 2005 from scenario Ab given in Table 1-14 of *WMO 2002* (black). Atmospheric lifetimes used in the calculations for the three species were 9.3, 17.9, and 12.0 years, respectively.

Column abundances above the Jungfraujoch station (last reported for 1986 to 2001 in Figure 1-2 of *WMO 2002*) have been measured since 1986. The column abundances found at the extremes of the Jungfraujoch observational time base are 0.90×10^{15} molec cm^{-2} in January 1986 and 2.42×10^{15} molec cm^{-2} in December 2004. This corresponds to an increase of a factor of nearly 2.7 over this 19-year period (Zander et al., 2005). This factor is only a few percent larger than (i.e., not significantly different from) that determined from the Australian archived air (Langenfelds et al., 1996), AGAGE, and NOAA measurements.

There has been a substantial slowdown in the rates of accumulation of HCFC-141b (CH_3CCl_2F) and HCFC-142b (CH_3CClF_2), particularly in the last two years. The global mean mixing ratio of HCFC-142b has increased to about 15 ppt in mid-2004, compared with about 12 ppt in mid-2000, with an annual average growth rate of 0.6 ± 0.1 ppt/yr (4%/yr, 2003-2004). This is approximately half of the previously reported growth rate of 1.1 ppt/yr averaged from 1999-2002, based on data from both AGAGE and NOAA/ESRL measurements (O'Doherty et al., 2004). The growth rate of HCFC-141b has also slowed from an annual average rate of about 1.6 ppt/yr in 1999-2000 to 0.6 ± 0.1 ppt/yr (4%/yr) in 2003-2004, resulting in a global mean surface mole fraction of 17.3 ± 0.2 ppt in mid-2004. Northern Hemisphere mean mole fractions were approximately 2.5 ppt and 1.4 ppt higher than in the Southern Hemisphere, for HCFC-141b and 142b respectively, in mid-2004.

Figure 1-2 shows that the slowdown in the growth rates of all three gases in the atmosphere was not anticipated in the projections made in the Ab scenario in *WMO 2002*. The observed growth rates for 2000-2004 were 4.9, 1.1, and 0.6 ppt/yr for HCFC-22, HCFC-141b, and HCFC-142b, respectively, versus projected growth rates of 6.6, 2.6, and 1.6 ppt/yr.

Figure 1-3 shows monthly mean baseline mixing ratios (and occasional pollution events) for HCFC-123 ($CHCl_2CF_3$) measured at Cape Grim from 1998 through 2004 (Krummel et al., 2004). Its mixing ratio in 2004 is 0.064 ppt. A strong annual cycle is evident because of the annual cycle in hydroxyl and the short atmospheric lifetime (1.3 years) of HCFC-123. Overall the atmospheric mixing ratios have been increasing over the seven-year period at approximately 6 ± 1%/yr. These are the only reported measurements of HCFC-123 since a value of 0.03 ppt for 1996 by Oram (1999). Despite its small mixing ratio, there is considerable interest in this gas because as a refrigerant it is operated at sub-ambient temperatures and leakage is therefore exceptionally small. Moreover what does get into the atmosphere is rapidly destroyed. Equally important it has a very low Ozone Depletion Potential (ODP).
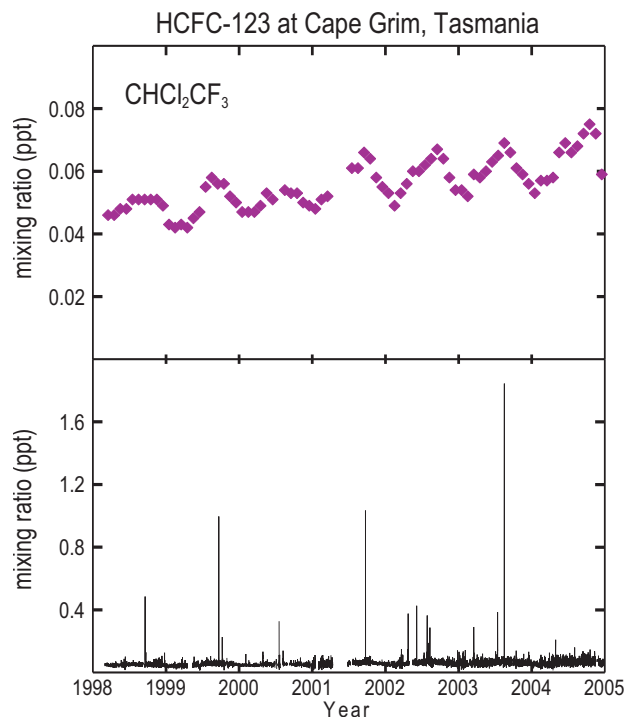

Figure 1-3. Monthly mean baseline mixing ratios (ppt) of HCFC-123 measured at Cape Grim, Tasmania (upper panel) (Krummel et al., 2004). The lower panel shows the continuous series of the measurements with the pollution events included.

Measurements of HCFC-124 ($CHClFCF_3$), which were first reported in *WMO 2002* (Montzka and Fraser et al., 2003), have been updated from AGAGE measurements at the two AGAGE stations at Mace Head, Ireland, and Cape Grim, Tasmania (Prinn et al., 2000). Trends and annual global means are reported in Table 1-2. The increase of HCFC-124 has been slowing rapidly since 1998 (see also *WMO 2002*). No new measurements of HCFC-21 ($CHCl_2F$) have been reported since *WMO 2002*. The atmospheric histories of several HCFCs have been reconstructed from analyses of air trapped in firn, and show that concentrations at the start of the 20th century were less than 2% of current mixing ratios (Sturrock et al., 2002).

1.2.1.3 HALONS

From the introduction of halons in the early 1960s, halon use grew steadily worldwide until the Montreal Protocol required an end to their consumption in developed countries by the end of 2003; however, production in developed countries was allowed for essential uses and to supply the needs of developing countries. Global production of halon-1211 ($CBrClF_2$) and halon-1301 ($CBrF_3$) peaked in 1988 at 43 Gg/yr and 13 Gg/yr, respectively

(UNEP, 2003). In developing countries, halon-1211 production began in the 1980s and showed a growth curve similar to that in developed countries until Multilateral Fund projects began to reverse that trend in the 1990s (UNEP, 2003). A third halon, halon-2402 ($CBrF_2CBrF_2$), was used predominantly in the former Soviet Union. No information on the production of halon-2402 before 1986 has been found. Fraser et al. (1999) developed emission projections for halon-2402 based on atmospheric measurements. They reported that the emissions grew steadily in the 1970s and 1980s, peaking in the 1988-1991 time frame at 1.7 Gg/yr. They found these results to be qualitatively consistent with the peak production of 28,000 ODP tonnes reported by the Russian Federation under Article VII of the Montreal Protocol (or assuming all production was halon-2402 and an ODP of 6, a peak production of approximately 4.650 Gg/yr).

Figure 1-4 shows the comparisons of the global mean mole fractions for halon-1211 and halon-1301 from the twelve times per day measurements by AGAGE (green lines) and the multiple samples per month analyzed by NOAA/ESRL (red lines). Also shown are the values derived from measurements of the air that has been archived several times per year in Australia and analyzed at the University of East Anglia (UEA) (blue lines; Oram et al., 1995; Fraser et al., 1999).

Observations from NOAA/ESRL, AGAGE, and UEA since 2000 suggest that the rate of increase of halon-1211 has continued to slow down, although halon-1211 mixing ratios continue to increase in the global atmosphere. The ground-based sampling network measurements of halon-1211 show that the global tropospheric mixing ratio of halon-1211 in 2004 was approximately 4.4 ppt, with a calibration uncertainty of approximately 0.3 ppt (Table 1-2). The mean rate of increase from 2000 to 2004 was 0.06 ± 0.01 ppt/yr (1.4%/yr). This is significantly lower than the rate of increase in 1999-2000, which was 0.12 ppt/yr (*WMO 2002*, Montzka and Fraser et al., 2003).

For halon-1301, the AGAGE, UEA, and NOAA/ESRL measurements show a large disparity in mixing ratio and rate of change during 2000-2004. The NOAA data show a negligible change (0.01 ± 0.01 ppt/yr), whereas AGAGE and UEA show an average rate of increase of 0.05 ± 0.01 ppt/yr (1.8%/yr). This discrepancy was not present in the pre-2000 measurements, perhaps because AGAGE measurements only began in 1998. Thus it is currently unclear whether there has been a significant slowdown in the growth rate compared with that reported in *WMO 2002* of 0.06 ppt/yr for 1999-2000 (Montzka and Fraser et al., 2003). Because of this, the observations do not provide as strong a constraint on the emissions as they do for the CFCs, HCFCs, and halon-1211.
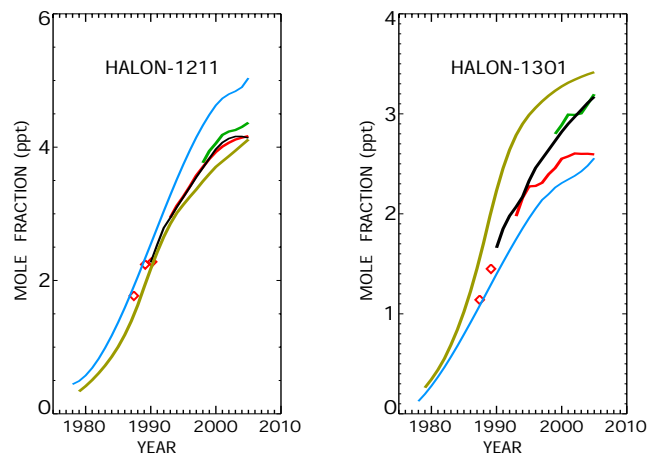

Figure 1-4. Annual global mean mole fractions for halon-1211 and halon-1301 derived from measurements at multiple sites in the AGAGE (green lines) and NOAA/ESRL (red diamonds, an update to Butler et al., 1998; red lines, from Montzka et al., 1999) networks. Also shown are annual global means calculated from measurements of archived air sampled at Cape Grim, Australia (blue lines, updated from Fraser et al., 1999) using the 12-box model. These measurements are compared against tropospheric annual means for the beginning of the years 1990 to 2005 given in Table 1-14 (scenario Ab) of *WMO 2002* (black lines). The greenish gold lines for halon-1211 and halon-1301 have been calculated from the UNEP Halons Technical Options Committee emission scenarios (UNEP, 2003) (modified for halon-1211, see text) using a 12-box model.

The measurements of the Australian air archive by UEA indicate that halon-2402 has remained approximately constant over the 2000-2004 period, and a fourth halon, 1202 (CBr_2F_2), which is not controlled under the Montreal Protocol, has declined by approximately 14%. The projections for this period given in *WMO 2002* were that halon-2402 would have declined slowly and halon-1202 would have declined by about 40%. Because the atmospheric lifetime of halon-1202 is approximately three years (Fraser et al., 1999), some residual production of halon-1202 is indicated, perhaps from over-bromination during the small remaining production of halon-1211.

All four halons have been measured in firn air from Dome C (75°S, Antarctica), Devon Island (75°N, Canada), and Greenland (75°N) (Reeves et al., 2005). At the base of the firn, the halon concentrations are below detection (<0.001 ppt), confirming that these species are entirely anthropogenic. The global halon mole fractions derived from these firn air samples are consistent with those

obtained from an analysis of the Cape Grim air archive (Fraser et al., 1999; Reeves et al., 2005).

By 2000, total tropospheric bromine from halons was about 8 ppt, having approximately doubled over the previous 10 years (Figure 1-5). The measurements show clear signs that the atmospheric accumulation of total halon bromine is slowing. However the Ab scenario in *WMO 2002* (Montzka and Fraser et al., 2003) projected that it should stop growing by approximately 2006, because of reductions in halon-1211 starting in 2003 (the black line in Figure 1-4). The *WMO 2002* Ab scenario provides a reasonable fit to the halon-1211 observations (Figure 1-4) but there is little evidence that halon-1211 stopped increasing in the 2000-2004 period. Therefore it seems likely that the total halon bromine maximum will be delayed by a year or two.

1.2.1.4 CARBON TETRACHLORIDE (CCl_4)

The major use for CCl_4 during the 1980s was believed to be as a feedstock for the production of the CFCs (Simmonds et al., 1988). Therefore as production of the CFCs was substantially reduced during the 1990s because of the Montreal Protocol, atmospheric mixing ratios of CCl_4 decreased (Figure 1-6). Global surface mixing ratios of CCl_4 are shown to have reached a maximum of about 106 ± 1 ppt in late 1990 and they have declined subsequently at a steady rate of 1.0 ± 0.1 ppt/yr (about 1%/yr) as a result of reduced emissions (Figure 1-6). Calibration differences between the different reporting groups since 1995 are 3-4%. The annual global mean in 2004 was 92-96 ppt (group average is 94.6 ppt) depending on which group made the measurements. For this gas in particular, a comparison of the measurements at the common measurement site in Samoa confirms that the NOAA/AGAGE difference is due to calibration and not due to the effects of differing site locations used to produce global means. Significant emissions of CCl_4 are still occurring and these sustain the interhemispheric difference of 1.4 ± 0.3 ppt, which has been relatively constant since 1995.

In *WMO 2002* (Montzka and Fraser et al., 2003), the estimated atmospheric lifetime of carbon tetrachloride was reduced to 26 years because of ocean losses (Yvon-Lewis and Butler, 2002). More recently, soil losses measured in North America have led to an estimated lifetime contribution from soil losses globally of 90 years, with an uncertainty range of 50 to 418 years (Happell and Roche, 2003; see also Borch et al., 2003). Combining this lifetime contribution with those due to ocean losses (94 years, with a range of 82 to 191 years) and an atmospheric lifetime from the 1998 WMO Assessment (35 years, with a
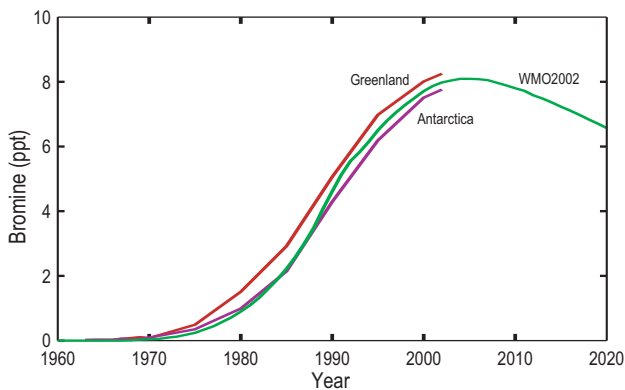

Figure 1-5. Tropospheric bromine from four halons (1211, 1301, 2402, 1202) at high northern (red) and high southern (purple) latitudes, based on model-derived emissions that best-fit the firn air data from Greenland and Antarctica and the air archive data from Cape Grim, Tasmania (Reeves et al., 2005). Those estimates are compared with model estimates (green) for the Southern Hemisphere (Fraser et al., 1999), using the Ab halon emission scenario prepared for *WMO 2002* (Montzka and Fraser et al., 2003).

range of 21 to 43 years; WMO, 1999) led Happell and Roche (2003) to infer an overall lifetime for carbon tetrachloride of 20 years. However, based on the discussion in the emissions section (Section 1.3.2.4), it was decided not to change the recommended overall lifetime from the *WMO 2002* value of 26 years at this time.

1.2.1.5 METHYL CHLOROFORM (CH_3CCl_3)

Because of Montreal Protocol restrictions, there has been a steady decline from an all-time high in methyl chloroform concentrations of more than 130 ppt in 1992 (Figure 1-6). The decline was due to a rapid decline in the emissions during the 1990s (McCulloch and Midgley, 2001) that resulted from the combination of an efficient replacement of methyl chloroform as an industrial solvent and its relatively short atmospheric lifetime of 5 years. The global mean surface mixing ratio of methyl chloroform has steadily decreased to 22.6 ± 1.0 ppt averaged over 2004 from 46.4 ppt in 2000 (averages of the AGAGE, NOAA, and UCI values given in Table 1-2). The decline since 1998 (Montzka et al., 2000) has occurred at an approximately exponential rate consistent with relatively small emissions. Furthermore, elevated concentrations have practically ceased to exist during pollution events at background sites such as Mace Head (Ireland), although
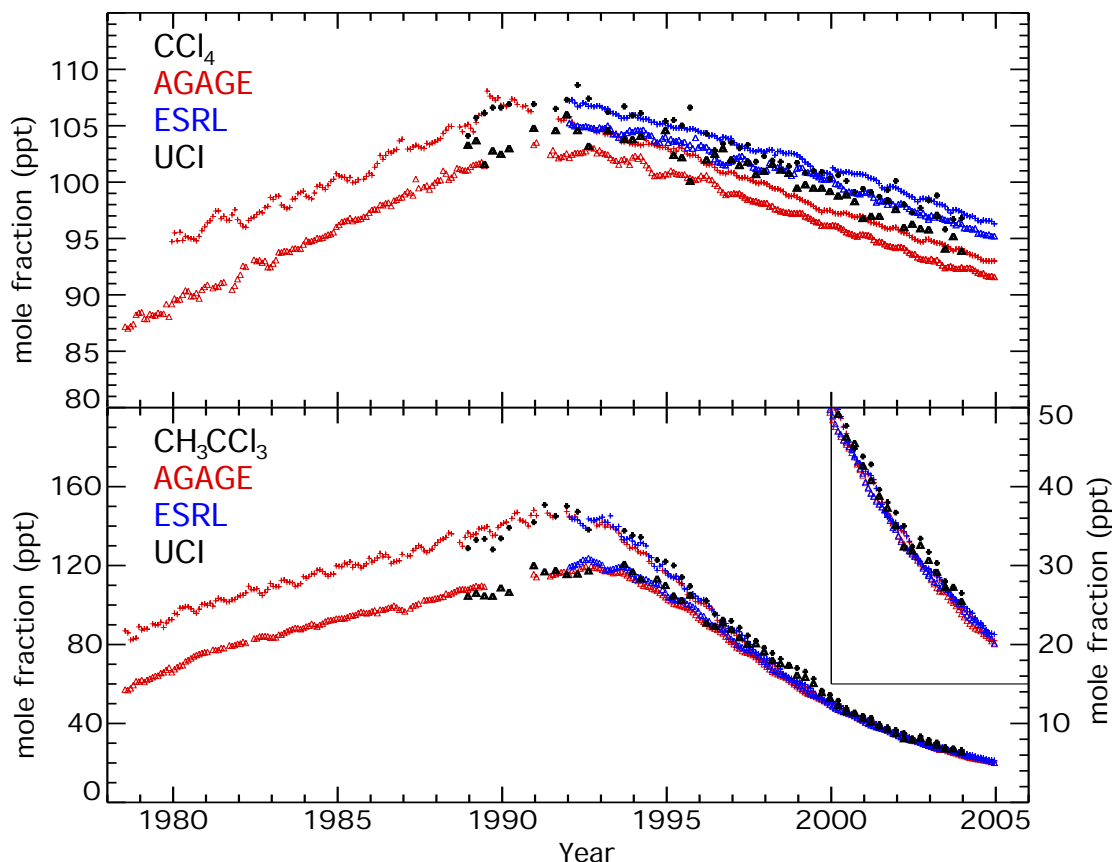
Figure 1-6. Hemispheric monthly mean of CH_3CCl_3 and CCl_4 (crosses for Northern Hemisphere and triangles for Southern Hemisphere) from the AGAGE stations (Prinn et al., 2000, 2005), the NOAA/ESRL network (Thompson et al., 2004; Montzka et al., 1999 updated), and UCI (D.R. Blake et al., 1996; N.J. Blake et al., 2001). Recent measurements for methyl chloroform are depicted in magnified form in the insert, using the scale on the right-hand side of the panel.

other European remote sites have reported distinct methyl chloroform excursions (Gros et al., 2003).

Background concentrations of CH_3CCl_3 from both hemispheres have been converging steadily from an interhemispheric gradient of more than 10% to an essentially constant annual mean difference of $2.1 \pm 0.4\%$ (corresponding to an uncertainty of ± 0.1 ppt) since 1999. In fact, during the warm season, Northern Hemispheric background concentrations can even be lower than in the Southern Hemisphere at the same time, due to the different hemispheric hydroxyl radical (OH) abundances. Calibration scales between the networks of NOAA/ESRL and AGAGE used to differ by several percent (*WMO 2002*, Montzka and Fraser et al., 2003), but since the newest scale updates by AGAGE (SIO-98) and NOAA (Hall et al., 2002) came into force, an excellent agreement exists. At stations with concurrent measurements from both net-

works, only small mean offsets of $0.4 \pm 1.8\%$ (1 sigma) are observed (AGAGE-NOAA) between 2000 and 2005.

1.2.1.6 METHYL CHLORIDE (CH_3Cl)

Methyl chloride (CH_3Cl) is the most abundant chlorine-containing compound in the atmosphere, with globally averaged concentrations of about 550 ppt. Before *WMO 2002*, there had been an imbalanced budget and large missing source, but in *WMO 2002* tropical and subtropical plants were proposed as potential sources to fill the gap. Recently, abiotic release of CH_3Cl by senescent or dead leaves has been proposed as a new significant source in the tropics and subtropics. The short- and long-term trends of atmospheric CH_3Cl, and source/sink estimates for biomass burning, oceans, rice paddies, OH reaction, and loss to polar oceans have been updated.

Atmospheric Distribution and Trends

Observations from NOAA/ESRL (since 1995) and AGAGE (since 1998) are consistent with the global average concentration ($\sim$550 $\pm$ 30 ppt) and the latitudinal variation (higher concentrations at the lower latitudes) reported in *WMO 2002* (Simmonds et al., 2004; Yoshida et al., 2004). These observations also suggest interannual variability for CH_3Cl, with significant enhanced concentrations during 1998 and a subsequent steady decrease until 2001, a trend that may be explained by large-scale forest fires in Indonesia and Canada during 1997-1998 (Simmonds et al., 2004; see also Table 1-2).

Aydin et al. (2004) and Trudinger et al. (2004) independently produced atmospheric histories of CH_3Cl for the 20th century based on Antarctic firn air measurements. These two studies both revealed an increase of about 10% in the 50 years prior to 1990 for atmospheric CH_3Cl mixing ratios over Antarctica, with a rather steady level after 1980 ($\sim$480-530 ppt). These tendencies are similar to the finding of Butler et al. (1999) in *WMO 2002*. The firn reconstruction of Kaspers et al. (2004), however, showed higher concentrations and a decreasing trend of 1.2 ppt/yr between 1975 and 2001; the difference from the results of the above studies remains unexplained. The ice core measurements during the past 300 years reported by Aydin et al. (2004) suggested a cyclic natural variability on the order of 110 years, which is in phase with the 20th-century rise inferred from firn air measurements.

Sources

Table 1-3 lists the revised estimates of source and sink strengths for atmospheric methyl chloride. Tropical forests remain a major source in the global atmospheric budget. High concentrations of atmospheric CH_3Cl have been observed in the tropical rainforests in Southeast Asia (up to 1500 ppt; Yokouchi et al., 2000) and above the canopy of tropical rainforests in South America (up to 809 ppt; Moore et al., 2005), supporting the significance of tropical forests as a potentially large CH_3Cl source. However, this source's strength and geographical distribution are still highly uncertain, mostly due to the large diversity of tropical vegetation.

Hamilton et al. (2003) reported abiotic release of CH_3Cl by senescent or dead plant material, both foliar and woody, and that these emissions rose dramatically when temperature increased. They estimated the global annual CH_3Cl emission from the weathering of leaf litter, between 30°N and 30°S, to be 30-2500 Gg/yr, possibly exceeding the source from live tropical vegetation.

For biomass burning, Andreae and Merlet (2001) provided a revised inventory (650 $\pm$ 325 Gg/yr) based on evaluation and integration of the available biomass-burning emission data. The value is closer to the lower limit of the estimate range (655-1125 Gg/yr) reported in *WMO 2002*, suggesting that biomass burning emissions may have been overestimated in *WMO 2002*. Three-dimensional (3-D) model studies (Lee-Taylor et al., 2001; Yoshida et al., 2004) have also shown that a smaller burning source is more consistent with observations.

The oceanic source estimate, which once had been understood as the major CH_3Cl source, has been revised downward again. On the basis of measurements of the solubility of CH_3Cl in seawater, Moore (2000) reported a global annual flux from warm waters ranging from 465 to 495 Gg/yr. Recalculation of the oceanic CH_3Cl flux with the empirical relationship between saturation and SST by Yoshida et al. (2004) gave a net flux of 350 Gg/yr, which requires an oceanic emission of 380-500 Gg/yr to compensate for the oceanic uptake of 30-150 Gg/yr (discussed below). These values are at the lower end of the *WMO 2002* estimate range (325-1300 Gg/yr).

Large CH_3Cl emission from some salt marshes has been attributed to the plants growing in these regions (Rhew et al., 2002; but see also Cox et al., 2004), and the emissions are probably influenced by the high concentrations of available chloride ions (Cl^-). In addition to white-rot fungal sources, ectomycorrhizal fungi recently have been found to emit CH_3Cl (0.003-65 μg g $dry^{-1}d^{-1}$; Redeker et al., 2004), but this source's global emission strength has not been estimated. Moore et al. (2005) suggested the possibility that some of the emission from woodrot fungi might compete with microbial uptake in the soil (see below). Thus, uncertainties for the fungal emissions of CH_3Cl have been added. Finally, the emissions from rice paddies have been revised downward from 5.0 to 2.4-4.9 Gg/yr using a new emission algorithm (Lee-Taylor and Redeker, 2005).

Sinks

The largest sink of CH_3Cl from the atmosphere is the reaction with the OH radical. The rate constant of the CH_3Cl + OH reaction was re-evaluated to be 2.4 $\times$ 10^{-12} $e^{1250/T}$ or 3.6 $\times$ 10^{-14} cm^3 $molec^{-1}$ s^{-1} at 298 K (Sander et al., 2003). The annual loss of CH_3Cl due to reaction with OH, calculated with detailed OH distributions, was 3800-4100 Gg/yr (Lee-Taylor et al., 2001; Yoshida et al., 2004), which exceeds the best estimate from *WMO 2002* of 3180 Gg/yr.

Soils are another important sink for CH_3Cl (Khalil and Rasmussen, 2000), and several bacterial strains capable of growth on CH_3Cl have been isolated recently from a variety of soils (McDonald et al., 2002; Miller et al., 2004). In addition to the ubiquitous bacteria capable of growing

Table 1-3. Estimated source and sink strengths for atmospheric methyl chloride from observations and three-dimensional model studies.

Source or Sink Type	Source or Sink Estimate[a] (Gg/yr)	3-D Model Studies Lee-Taylor et al. (2001)[b]	Yoshida et al. (2004)[c]
Sources			
Tropical and subtropical plants	820-8200[d]	2380	2900
Tropical senescent or dead leaves	30-2500[e]		
Biomass burning	325-1125[d,f]	733	611
Oceans	380-500[g,h]	477[i]	508
Salt marshes	65-440[d]	170	170
Fungi	43-470[d]	128	-
Wetlands	48[j]	48	48
Rice paddies	2.4-4.9[k]	-	-
Fossil fuel burning	5-205[d]	162	162
Waste incineration	15-75[d]		
Industrial processes	10[c]		
Subtotal	*(1743-13,578)*	*(4098)*	*(4399)*
Sinks			
OH⁻ reaction	3800-4100[h,k]	3850	3994
Loss to stratosphere	100-300[d]		-
Cl reaction	180-550[d]	-	-
Soil	100-1600[d]	256	256
Loss to cold waters (polar oceans)	93-145[g]	-	149
Subtotal	*(4273-6695)*	*(4106)*	*(4399)*

[a] Best estimates that appeared in the 2002 WMO Assessment table (WMO, 2003) are not given here, due to the difficulty of reasonable selection.
[b] Mean value of their best estimates is given.
[c] Model mean is given.
[d] WMO, 2003.
[e] Hamilton et al., 2003.
[f] Andreae and Merlet, 2001.
[g] Moore, 2000.
[h] Yoshida et al., 2004.
[i] Net ocean flux is given.
[j] Varner et al., 1999; no range was given.
[k] Lee-Taylor and Redeker, 2005.

aerobically on CH₃Cl, the potential importance of anoxic biodegradation as a CH₃Cl sink was shown by Freedman et al. (2004), but its global strength has not been quantified.

The oceanic uptake to cold waters (i.e., polar oceans) was re-examined using the measured solubility of CH₃Cl (Moore, 2000), and the estimate has been revised upward from 37-113 Gg/yr in *WMO 2002* to 93-145 Gg/yr. Studies by Tokarczyk et al. (2003a, b) using a stable-isotope incubation technique indicated that microbial activity plays an important role in CH₃Cl degradation in coastal seawater (Bedford Basin, Nova Scotia) as well as in the Southern Ocean. Thus, CH₃Cl-degrading bacteria are found in both terrestrial and marine environments. A common set of genes and proteins is found in certain ter-

restrial and marine methyl halide-oxidizing bacteria (Schafer et al., 2005). McDonald et al. (2002) suggested that these bacteria may play an important role in mitigating ozone depletion resulting from CH₃Cl.

There is no update for the other sinks, such as the reaction with Cl⁻ and loss to the stratosphere.

Atmospheric Budget

With high CH₃Cl emission from plants and dead leaves in the tropics and subtropics, global sinks of 4300-6700 Gg/yr could be balanced by known sources (Table 1-3), although uncertainties in emissions are so large that the possibility of missing sources or sinks cannot be denied.

By adding tropical terrestrial biogenic sources of 2400-2900 Gg/yr, model simulations of atmospheric CH_3Cl showed general agreement with the observations (Lee-Taylor et al., 2001; Yoshida et al., 2004).

An isotopic study (Gola et al., 2005) shows that the atmospheric isotopic ratio of CH_3Cl is not well explained by known sources and sinks unless the flux from senescent and dead leaves is quite large (1800-2500 Gg/yr). The values have large uncertainties, however, due to high variability of the stable carbon isotope ratios of biomass burning emission and tropical plants, as well as limited information on the isotope ratio of the oceanic source. In addition, no measurements of CH_3Cl emission from senescent and dead leaves have been made in the field.

Our understanding of the budget of CH_3Cl has been revised based upon the considerations discussed above, but it is still difficult to assess how atmospheric CH_3Cl levels might be affected by changes in global climate and land-use patterns, mostly due to large uncertainties in the strengths and geographical distribution of tropical terrestrial sources.

1.2.1.7   METHYL BROMIDE (CH₃Br)

Methyl bromide is the most abundant brominated gas regulated by the Montreal Protocol. Additional observational and modeling studies of methyl bromide have been published since 2002 Assessment (WMO, 2003). Recent atmospheric measurements have become available, as have additional results from the analysis of firn air. Methyl bromide also was measured in ice core air bubbles for the first time. New techniques have become available for the analysis and quantification of sources and sinks, and progress has been made in refining estimates of methyl bromide fluxes from the natural environment.

Recent Atmospheric Trends

Since the previous Assessment (WMO, 2003), three different groups have published multiyear observational records for CH_3Br at different surface sites (Yokouchi et al., 2002; Montzka et al., 2003; Simmonds et al., 2004). The updated studies indicate a global mean mixing ratio for CH_3Br of 9.2 ppt in the three years before 1999, which was the first year industrial production declined as a result of the Montreal Protocol. The observations also show that the tropospheric mixing ratio of CH_3Br started declining in 1999, with the largest decline observed in the Northern Hemisphere (Figure 1-7). By mid-2004, the global tropospheric mixing ratio of CH_3Br had declined by approximately 1.3 ppt (14%) from the amount observed in the

years before anthropogenic production began decreasing (9.2 ppt in 1996-1997). Reported industrial production of methyl bromide for emissive uses decreased by 50% during this same period (UNEP, 2002a, updated). Methyl bromide is unique among ODS regulated by the Montreal Protocol because it is emitted in substantial quantities from natural processes. As a result, attributing the observed declines to reduced industrial production is less straightforward than for other ODS. The coincidence of the observed decline with reduced anthropogenic production (as a result of Montreal Protocol), and the observation that the largest declines were observed in the NH argue that the atmospheric decline is primarily the result of reduced anthropogenic emissions. The decline observed through 2004 was somewhat larger than projected by scenario Ab (see black curve in Figure 1-4) from *WMO 2002* (Montzka and Fraser et al., 2003).

The enhanced decline observed for CH_3Br from the mid-1990s to mid-2004 could imply that its atmospheric abundance is more sensitive to changes in anthropogenic production than suggested in the best-estimate budget in *WMO 2002* (Montzka and Fraser et al., 2003), or that non-anthropogenic sources or sinks of CH_3Br changed systematically and simultaneously. For example, declines in CH_3Br mixing ratios from 1998 to 2001 may have been accelerated as the atmosphere recovered from high biomass burning levels in 1998 (Simmonds et al., 2004), although the influence of burning on CH_3Br trends over longer periods (1996-2004) is not well defined.

Interlaboratory differences for the absolute calibration of methyl bromide in the atmosphere are smaller than they were in *WMO 2002*. The range of results from the three laboratories reporting recent atmospheric data is ±2%.

Preindustrial Mixing Ratios

Methyl bromide was measured in air trapped in ice cores for the first time (Saltzman et al., 2004). The results from Siple Dome (81°S, 149°W) suggest that ambient air mixing ratios of CH_3Br over Antarctica during 1700-1900 were 5-6 ppt, or substantially lower than the 8 ppt observed during the 1990s (Figure 1-8). Independent measurements of CH_3Br in firn air at Law Dome suggest mixing ratios over Antarctica of 5.5 ppt in the 1930s (Trudinger et al., 2004). These firn air results are consistent with those obtained previously from numerous sites across Antarctica: South Pole, Siple Dome, Dome Concordia, and Dronning Maud Land (Butler et al., 1999; Sturges et al., 2001). Despite the variations in snow temperature, humidity, marine influence, and snow accumulation rates at these different Antarctic sites, similar atmospheric his-
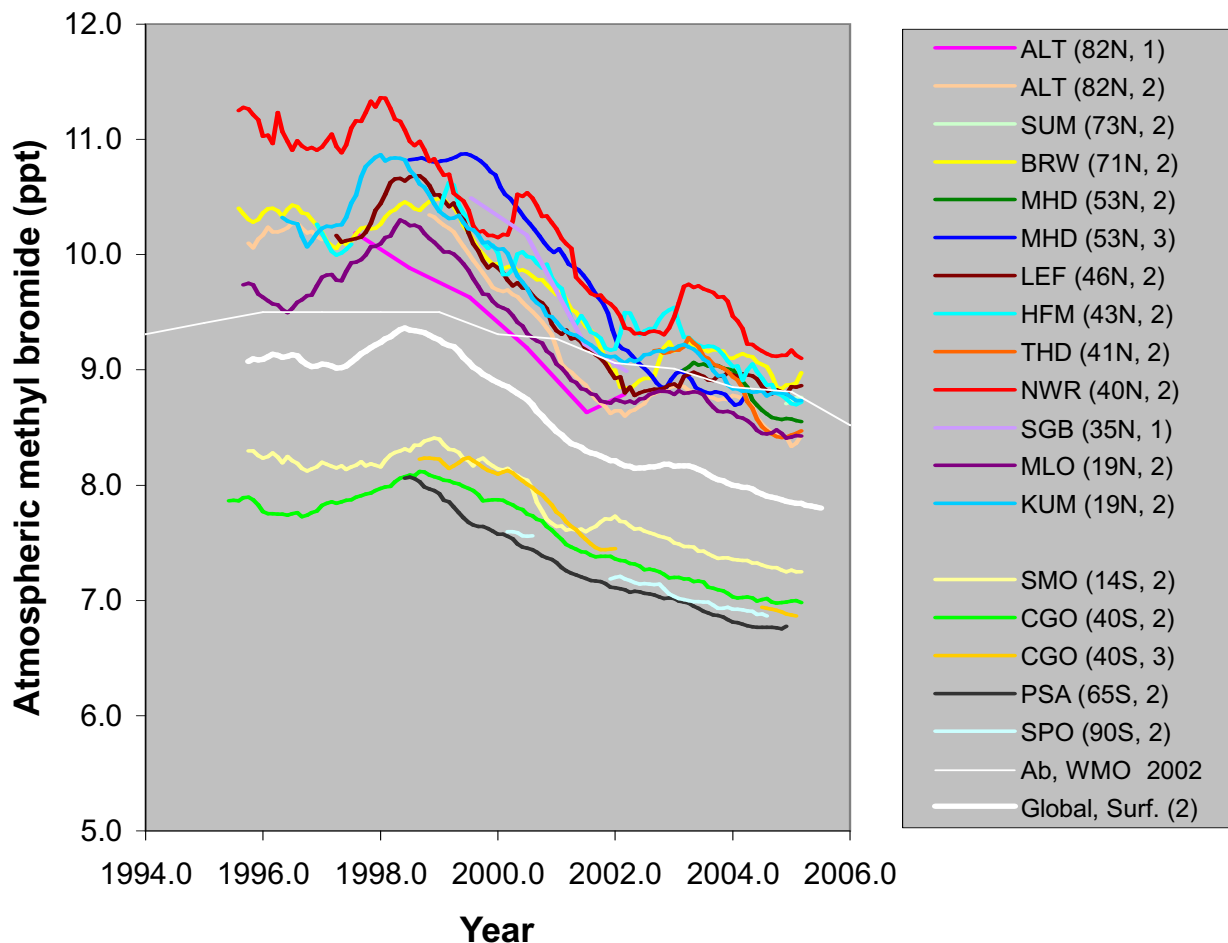
Figure 1-7. Measured mixing ratios of methyl bromide at different surface sites in the Northern and Southern Hemispheres. Most results are displayed as 12-month running means to highlight the observed long-term mixing ratio changes (larger seasonal variations that are observed at some sites are minimized here as a result). Results from the National Institute for Environmental Studies (NIES) are displayed as annual means connected by lines. Sampling latitudes and the data source are indicated in parentheses next to the site acronym: from NIES (1; Yokouchi et al., 2002), NOAA/ESRL (2; Montzka et al., 2003), and AGAGE (3; Simmonds et al., 2004). Sites are listed in the legend with the highest NH latitudes first: ALT (Alert, 82.5°N); SUM (Summit, 72.6°N), BRW (Barrow, 71.3°N), MHD (Mace Head, 53.3°N), LEF (Wisconsin, 45.9°N), HFM (Harvard Forest, 42.5°N), THD (Trinidad Head, 41.0°N), NWR (Niwot Ridge, 40.0°N), SGB (Sagami Bay, 35.0°N), MLO (Mauna Loa, 19.5°N), KUM (Kumukahi, 19.5°N), SMO (American Samoa, 14.2°S), CGO (Cape Grim, 40.4°S), PSA, (Palmer, 64.9°S), and SPO (South Pole, 90.0°S). A global mean derived from most of the NOAA/ESRL (2) data is shown as the thick white line; the thin white line is the global surface mixing ratio of CH_3Br from scenario Ab of *WMO 2002* (Montzka and Fraser et al., 2003).

tories have been derived for CH_3Br from firn and ice-core results from samples at all these locations. This consistency argues against processes that significantly influence CH_3Br mixing ratios during extended periods in contact with Antarctic snow and ice. In the Northern Hemisphere, however, this is not true; firn air results from different sites in Greenland show unusual variations that can be explained only by invoking in situ production of CH_3Br (Butler et al., 1999; Sturges et al., 2001).

Although consistent histories have been inferred from firn air samples collected at South Pole and Law Dome, the nature of the firn at Law Dome allows the derivation of a history with finer time resolution. For example, the results from Law Dome imply that the 20th-century mixing ratio increases for CH_3Br in the high-latitude Southern Hemisphere occurred mostly from 1950 to 1980 (Trudinger et al., 2004), not gradually over the entire century (Butler et al., 1999).
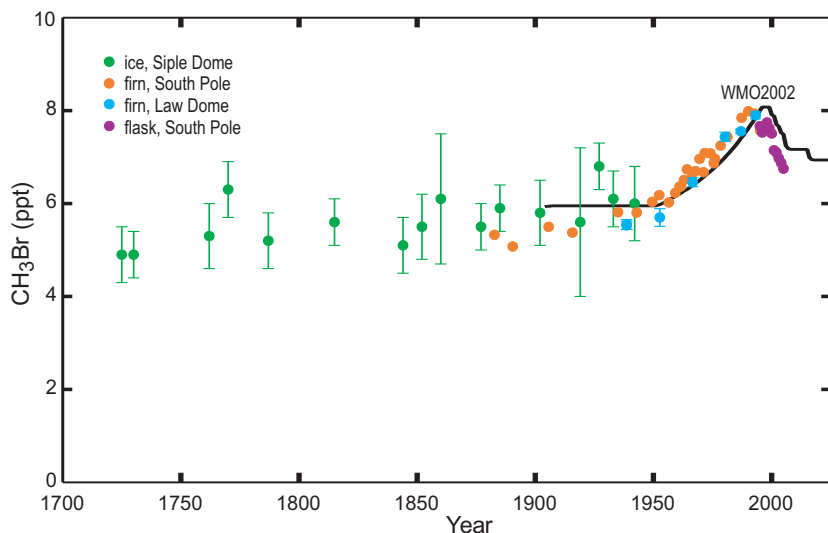
Figure 1-8. The history of methyl bromide abundance in the southern polar atmosphere, as measured in air samples from Antarctic ice and firn and from flasks collected at the South Pole (orange symbols, Butler et al. (1999) profiles dated with the Trudinger et al. (2004) firn diffusion model; blue symbols, Trudinger et al., 2004; green symbols, Saltzman et al., 2004; purple symbols, Montzka et al., 2003; http://www.cmdl.noaa.gov/noah/) compared with calculated Southern Hemisphere CH_3Br levels based on the Ab emission scenario in *WMO 2002* (black line) (Montzka and Fraser et al., 2003).

Updated Information on Nonindustrial Sources and Sinks

Work has continued since *WMO 2002* on identifying and quantifying the contribution of non-industrial fluxes of methyl bromide to and from the atmosphere. While progress has been made in improving our understanding of these fluxes, best estimates of their magnitudes remain essentially unchanged from Table 1-9 in the previous Assessment (Montzka and Fraser et al., 2003).

Regarding the oceans, previously it was learned that aqueous concentrations and saturations of methyl bromide in the temperate open ocean depend upon sea surface temperature (Groszko and Moore, 1998; King et al., 2000). Additional studies have attempted to refine this relationship (King et al., 2002), though it is clear that in some waters, additional unidentified factors influence methyl bromide saturation levels (Sturrock et al., 2003; Tokarczyk and Moore, 2006). These studies have confirmed that the ocean on average is a net sink of atmospheric methyl bromide. The role of biology in driving seasonal changes in flux through both production and degradation of methyl bromide has been further confirmed and quantified in temperate (Yvon-Lewis et al., 2002), polar (Tokarczyk et al., 2003b; Yvon-Lewis et al., 2004), and coastal (Sturrock et al., 2003) waters. The findings support the conclusions of *WMO 2002* regarding the lifetime of methyl bromide with respect to oceanic losses (1.9 (1.1-3.9) years).

The global contribution of plant emissions to the atmospheric burden of methyl bromide remains poorly quantified, given the plethora of species not yet studied. Improvements in quantifying this source may be possible with the identification of a gene that encodes an enzyme capable of producing methyl halides from aqueous chloride, bromide, and iodide ions (Rhew et al., 2003a). This finding may allow a genetic basis for understanding and predicting methyl halide production by plants. Other studies relating to plants have led to a slightly reduced estimate of emissions from rice paddies (Lee-Taylor and Redeker, 2005).

Uptake by soils has been studied further since the previous Ozone Assessment (WMO, 2003). A laboratory study of methyl bromide uptake by boreal soils found uptake rates similar to those measured in the past (Rhew et al., 2003b). This work was the first to allow the quantification of both uptake and emission fluxes through use of isotopically labeled methyl halides. Field measurements continue to show that terrestrial ecosystems can act both as a source and sink of CH_3Br. While net emission has been observed in coastal grasslands and wetlands in Tasmania, Australia, net uptake was observed at similar sites with exposed soil or leaf litter (Cox et al., 2004). A study of CH_3Br losses to a temperate forest soil over the 1999 growing season revealed a loss that was apparently an order of magnitude less than previous uptake estimates for this soil type (Varner et al., 2003). Also, a multiyear study in freshwater peatlands showed a close balance between emissions and uptake (White et al., 2005), in contrast with earlier studies that suggested large net sources from these ecosystems. Discrepancies between these recent studies and prior estimates may be caused by competing production and consumption mechanisms at individual field sites. Emissions from fungi, for example, may affect the net CH_3Br flux measured at different sites

(Varner et al., 2003; Redeker et al., 2004). Such discrepancies underscore the potential for isotopic studies to provide improved estimates of gross CH_3Br fluxes.

Ambient air measurements in a coastal region confirm previous findings from smaller-scale experiments that methyl bromide can be emitted from coastal areas (Sturrock et al., 2003; Cox et al., 2005). Enhanced mixing ratios were also observed at multiple sites on the west coast of California, though these measurements may have been influenced by agricultural activities in the region (Low et al., 2003). Unusual enhancements of CH_3Br have been observed during spring in the Arctic, however, that do not appear to be explained by surface-based emissions or other known sources (Wingenter et al., 2003). The authors proposed a photochemical mechanism by which CH_3Br may be produced in the background atmosphere in substantial amounts, though analogous reactions have been shown to be quite slow and unlikely.

Estimates of global carbon monoxide (CO) emissions from fires and their interannual variability have been derived based upon satellite data (Duncan et al., 2003). These estimates are similar in magnitude to those described in Andreae and Merlet (2001), who applied burning-specific emission factors to all major pyrogenic processes (grassland and forest fires, the burning of biofuels and agricultural residues, and the making and burning of charcoal) to derive a global emission for methyl bromide of 29 Gg CH_3Br/yr. Though this newer source estimate is slightly larger than the 20 (10-40) Gg CH_3Br/yr quoted in the previous Assessment for biomass burning (Montzka and Fraser et al., 2003), it falls well within the uncertainties of the older estimate.

On the Imbalance of CH_3Br Sources and Sinks and the Contribution of Industrially Derived CH_3Br

Despite the recent work on identifying and quantifying sources and sinks, best estimates of the magnitudes of sources cannot sustain measured mixing ratios during the past 25 years given the best estimates of loss (WMO, 2003). The firn air and ice bubble air data imply that this discrepancy existed before CH_3Br was produced industrially (Reeves, 2003; Saltzman et al., 2004). Though observational evidence for a significant CH_3Br source in the tropics is currently lacking, modeling studies have suggested that such a source could diminish the discrepancy in a way that is reasonably consistent with observations (Lee-Taylor et al., 1998; Warwick et al., 2006). Others (Reeves, 2003) have noted that the discrepancy could also be reduced if the CH_3Br lifetime were longer than 0.7 year (0.5-0.9 year) (WMO, 1999; WMO, 2003).

The firn air and ice bubble air results also suggest an atmospheric increase in the Southern Hemisphere during the 20th century that is larger than expected from increases in emissions of anthropogenically produced CH_3Br alone (Reeves, 2003; Saltzman et al., 2004). The increase can be explained if emissions from anthropogenic activities accounted for a larger fraction of the total flux than presumed in the "best-estimate" budget (1992 fumigation emissions of 41 Gg/yr in 1992 relative to a total flux of 204 Gg/yr; Montzka and Fraser et al., 2003), or if other emissions had also increased over this time, such as biomass burning. The large uncertainties in CH_3Br fluxes from biomass burning over time prevent deriving tight constraints on the CH_3Br fluxes from industrially derived production from the 20th century firn air and ice bubble results (Saltzman et al., 2004).

Previous Assessments have suggested that anthropogenic CH_3Br emissions in 1992 of 41 Gg/yr derived from industrial production accounted for 20 (10-40)% of the total annual flux at that time (this range encompasses a total flux estimated by total sources or sinks; WMO, 2003). Alone, the 20th-century increase in atmospheric CH_3Br inferred from firn air and ice bubble air, or the large decline observed in ambient air since 1999, do not tightly constrain this fraction additionally. Both the recent observed decline and the 20th-century increase inferred for atmospheric methyl bromide were larger than expected, however, given our understanding of the CH_3Br budget and declines in reported production (UNEP, 2002a; Yokouchi et al., 2002; Montzka et al., 2003; Reeves, 2003; Saltzman et al., 2004; Trudinger et al., 2004). Because CH_3Br emitted from fumigation changed more than any other known flux during both periods, the results suggest a contribution from fumigation-related emissions in the middle to upper half of the range quoted in the past, or 30 (20-40)%. This suggests that fumigation-related emissions could have a stronger influence on atmospheric methyl bromide mixing ratios than estimated in past Assessments, though uncertainties in the variability of natural emission rates and loss, and in the magnitude of methyl bromide banked in recent years, influence our understanding of this sensitivity.

The higher contribution of anthropogenic CH_3Br to the total flux may be explained in part by a mean release fraction of CH_3Br after application to soils for agriculture fumigation purposes that is greater than 50%. In past WMO Ozone Assessments, a mean release fraction of 50% had been suggested for this application; the Methyl Bromide Technical Options Committee (MBTOC), however, suggests a mean release fraction of 70% (40-87%; UNEP, 2002a). Such a larger fraction would imply emissions from all types of fumigation of 51 Gg instead of 41 Gg in 1992; this additional emission would partially reduce the imbalance between known sources and sinks. A rela-

tively larger contribution of fumigation-related emissions could also be explained if the total atmospheric lifetime of CH_3Br were longer than 0.7 year (Yokouchi et al., 2002; Reeves, 2003).

1.2.2 Lifetimes

1.2.2.1 HALOCARBON LIFETIME UPDATES AND VARIABILITY

After being emitted, most environmentally important trace gases, including methane and other organic compounds, carbon monoxide, nitrogen oxides, and sulfur gases, are removed from the atmosphere by oxidation. The strengths of the tropospheric sinks are essentially determined by the concentrations of oxidants, in particular the highly reactive hydroxyl radical (OH) that dominates the removal of many gases, including methane (CH_4), other hydrocarbons, CO, and natural and anthropogenic hydrohalocarbons. For that reason, global OH levels are often taken as a proxy for the oxidizing efficiency of the atmosphere. Through the OH feedback, even changes in the tropospheric emissions of gases that are too short lived to reach the stratosphere can affect the stratosphere when they influence tropospheric OH. The most important such gases are CO and nitrogen oxides. Lifetimes of many ozone-depleting substances are also determined by photolysis rates in the stratosphere. Hence, lifetimes of these gases can depend on the intensity of the Brewer-Dobson circulation as well. Changes in the oxidizing power of the atmosphere could have large impacts on air pollution, aerosol formation, greenhouse radiative forcing, and stratospheric ozone depletion. The quantification of possible recent changes in tropospheric OH continues to be an active and controversial area of research. The evidence for such changes is based primarily on inverse models of CH_3CCl_3 emissions and tropospheric observations that have deduced OH variations on the order of ±10% in recent decades but no systematic long-term trends (Bousquet et al., 2005; Prinn et al., 2005). In the future, the Intergovernmental Panel on Climate Change/Technology and Economic Assessment Panel (IPCC/TEAP Chapter 2; Velders and Madronich et al., 2005) concludes that tropospheric OH in the 21st century may change by −18% to +5%, depending on the choices of emission scenarios.

The atmospheric lifetimes for the vast majority of the gases listed in Table 1-4 are unchanged from *WMO 2002*. The list of gases and lifetimes in this Table is not limited only to gases with atmospheric lifetimes longer than 6 months, because it was decided to put all the lifetimes needed for Chapters 1 and 2 of this Assessment in a single table. This section describes the basis for changes that were made either due to new laboratory experiments or due to including additional gases. The best estimate lifetime for methyl chloride (CH_3Cl) was reduced due to the discovery of additional sinks. Analysis by Tokarczyk et al. (2003a, b) of the partial atmospheric lifetime with respect to ocean removal for CH_3Cl (4.1 years) reduces the total lifetime to 1.0 years.

The atmospheric lifetime for methyl chloroform has been left at 5.0 years, the same as in *WMO 2002* (Montzka and Fraser et al., 2003), because the suggestion by Prinn et al. (2005) for a lifetime of 4.9 years and a tropospheric lifetime due to reaction with OH of 6.0 years (6.1 years used in this Assessment) was not deemed to represent a significant change.

Although the atmospheric lifetime of the hydrofluoroether CHF_2OCF_3 (HFE-125) is unchanged at 136 years, the much longer atmospheric lifetime (1800 years) implied by the theoretical analysis of Wu et al. (2004) suggests that further study is needed for this compound.

The atmospheric lifetime of trifluoromethylsulfurpentafluoride (SF_5CF_3) was modified to a range of 650-950 years to better account for the findings in Takahashi et al. (2002). It did not seem warranted to use a single lifetime of 800 years. However, it should be noted that laboratory data by Chim et al. (2003) and Limão-Vieira et al. (2004) both imply an atmospheric lifetime closer to 1000 years for SF_5CF_3.

A number of additional gases have been included in Table 1-4 based on new laboratory data for their reaction rates with OH. These include: CFH_2CH_2OH, $CHF_2CF_2OCHF_2$, $CF_3CHFCF_2OCH_2CF_2CF_3$, $CF_3OC(O)H$, $C_2F_5OC(O)H$, $CF_3CHFCF_2CH_2OH$, $C_2F_5C(O)CF(CF_3)_2$, and n-$C_3F_7OC(O)H$. Some other compounds were not included because only room temperature reaction data were available.

Also included are several compounds that were otherwise included in the Global Warming Potential (GWP) analysis in *WMO 2002*: c-C_3F_6 (τ = 1000 years), NF_3 (740 years), $(CF_3)_2CHOCHF_2$ (3.1 years), and $(CF_2)_4CH(OH)$ (0.85 year).

1.2.2.2 UNCERTAINTIES IN OZONE-DESTROYING HALOCARBON LIFETIMES

In order to estimate the remaining banks (and their uncertainties) of CFCs and other ozone destroying halocarbons, it is useful to have the best possible estimates of the uncertainties in their lifetimes. For this purpose, the model-based stratospheric lifetime estimates from the 1998 Assessment (Table 1-4 in WMO, 1999) are combined with values derived from stratospheric measurements

Table 1-4. Trace gas lifetimes for selected halocarbons and perfluorinated gases. For completeness, estimates for local lifetimes for some very short-lived (lifetime (τ) < 0.5 year) species are included (in italics). As discussed in Chapter 2, the atmospheric lifetimes for these species (defined as the ratio of burden to emission) (Prather and Ehhalt et al., 2001; Montzka et al., 2003) depend on the location and time of emission. Thus, these local lifetimes should not be used in semi-empirical ODP, GWP, or EESC calculations for these gases.

Industrial Designation or Common Name	Chemical Formula	Lifetime (years)	Notes
Halogen-substituted methanes			
HFC-41	CH_3F	2.4	1
HFC-32	CH_2F_2	4.9	1
HFC-23	CHF_3	270	1
FC-14 (Carbon tetrafluoride)	CF_4	50 000	2
Methyl chloride	CH_3Cl	1.0	1, 3
Dichloromethane	CH_2Cl_2	*0.38*	15, 16
Chloroform	$CHCl_3$	*0.41*	15, 16
Carbon tetrachloride	CCl_4	26	5
HCFC-31	CH_2ClF	1.3	4
HCFC-22	$CHClF_2$	12.0	1, 6
HCFC-21	$CHCl_2F$	1.7	1, 6
CFC-13	$CClF_3$	640	2
CFC-12	CCl_2F_2	100	2, 7
CFC-11	CCl_3F	45	2, 7
Methyl bromide	CH_3Br	0.7	3
Dibromomethane	CH_2Br_2	*0.33*	8, 15, 16
Bromoform	$CHBr_3$	*0.07*	8, 15, 16, 19
Bromodifluoromethane	$CHBrF_2$	5.8	4
Bromochloromethane	CH_2BrCl	*0.41*	8, 15, 16
Bromodichloromethane	$CHBrCl_2$	*0.19*	7, 15, 16
Dibromochloromethane	$CHBr_2Cl$	*0.21*	7, 15, 16
Halon-1301	$CBrF_3$	65	2, 7
Halon-1211	$CBrClF_2$	16	9
Halon-1202	CBr_2F_2	2.9	17
Methyl iodide	CH_3I	*0.02*	7, 15, 16, 20
Diiodomethane	CH_2I_2	*Minutes*	7, 15, 16
Chloroiodomethane	CH_2ClI	*Hours*	7, 15, 16
Trifluoroiodomethane	CF_3I	*0.01*	2, 15
Halogen-substituted ethenes			
Trichloroethene	C_2HCl_3	*0.01*	15
Perchloroethene	C_2Cl_4	*0.27*	15
Halogen-substituted ethanes			
HFC-161	CH_3CH_2F	*0.21*	2, 15
HFC-152	CH_2FCH_2F	0.60	2, 15
HFC-152a	CH_3CHF_2	1.4	1, 6
HFC-143	CH_2FCHF_2	3.5	1

Table 1-4, continued.

Industrial Designation or Common Name	Chemical Formula	Lifetime (years)	Notes
HFC-143a	CH_3CF_3	52	1
HFC-134	CHF_2CHF_2	9.6	1
HFC-134a	CH_2FCF_3	14.0	1, 6
HFC-125	CHF_2CF_3	29	1, 6
FC-116 (Perfluoroethane)	CF_3CF_3	10 000	2
Chloroethane	CH_3CH_2Cl	*0.08*	15
1,2 Dichloroethane	CH_2ClCH_2Cl	*0.19*	10, 15
Methyl chloroform	CH_3CCl_3	5.0	9
HCFC-142b	CH_3CClF_2	17.9	1, 6
HCFC-141b	CH_3CCl_2F	9.3	1, 6
HCFC-123	$CHCl_2CF_3$	1.3	6, 11
HCFC-124	$CHClFCF_3$	5.8	6, 11
CFC-113	CCl_2FCClF_2	85	2
CFC-113a	CCl_3CF_3	NA	NA
CFC-114	$CClF_2CClF_2$	300	2
CFC-115	$CClF_2CF_3$	1700	2
Halon-2402	$CBrF_2CBrF_2$	20	17
Iodoethane	C_2H_5I	*0.01*	7, 15, 16, 20
Halogen-substituted propanes			
HFC-281ea	CH_3CHFCH_3	*0.06*	15
HFC-263fb	$CH_3CH_2CF_3$	1.6	2
HFC-245ca	$CH_2FCF_2CHF_2$	6.2	1
HFC-245ea	$CHF_2CHFCHF_2$	4.0	2
HFC-245eb	$CH_2FCHFCF_3$	4.0	12
HFC-245fa	$CHF_2CH_2CF_3$	7.6	1
HFC-236cb	$CH_2FCF_2CF_3$	13.6	1
HFC-236ea	CHF_2CHFCF_3	10.7	1
HFC-236fa	$CF_3CH_2CF_3$	240	1
HFC-227ea	CF_3CHFCF_3	34.2	1
FC-218 (Perfluoropropane)	$CF_3CF_2CF_3$	2600	2
n-Propyl chloride	$CH_3CH_2CH_2Cl$	*0.06*	13, 15
HCFC-243cc	$CH_3CF_2CCl_2F$	26.4	4
HCFC-225ca	$CHCl_2CF_2CF_3$	1.9	11
HCFC-225cb	$CHClFCF_2CClF_2$	5.8	11
n-Propyl bromide (n-PB)	$CH_3CH_2CH_2Br$	*0.03*	15, 16
n-Propyl iodide	$CH_3CH_2CH_2I$	*0.001*	7, 15, 16, 20
Isopropyl iodide	CH_3CHICH_3	*0.003*	7, 15, 20
Halogen-substituted higher alkanes			
HFC-365mfc	$CH_3CF_2CH_2CF_3$	8.6	1, 14
HFC-356mcf	$CH_2FCH_2CF_2CF_3$	1.2	1, 14
HFC-356mff	$CF_3CH_2CH_2CF_3$	8.1	1, 14
HFC-338pcc	$CHF_2CF_2CF_2CHF_2$	12.3	1, 14

Table 1-4, continued.

Industrial Designation or Common Name	Chemical Formula	Lifetime (years)	Notes
FC-C318 (Perfluorocyclobutane)	$c\text{-}C_4F_8$	3200	1
FC-31-10 (Perfluorobutane)	C_4F_{10}	2600	2
HFC-43-10mee	$CF_3CHFCHFCF_2CF_3$	15.9	1
HFC-458mfcf	$CF_3CH_2CF_2CH_2CF_3$	23.2	1
FC-41-12 (Perfluoropentane)	C_5F_{12}	4100	2
Perfluorodecalin	$C_{10}F_{18}$	2000	29
HFC-55-10mcff	$CF_3CF_2CH_2CH_2CF_2CF_3$	7.7	2
FC-51-14 (Perfluorohexane)	C_6F_{14}	3200	2
Perfluorocyclopropane	$c\text{-}C_3F_6$	>1000	2
Fluorinated alcohols and ketones			
	CF_3CH_2OH	*0.41*	15
	$CF_3CF_2CH_2OH$	*0.39*	15, 23
	$(CF_3)_2CHOH$	2.0	4
	$CF_3(CF_2)_3CH_2OH$	*0.45*	23
	CFH_2CH_2OH	*0.04*	27
	$CF_3CHFCF_2CH_2OH$	*0.34*	22
	$C_2F_5C(O)CF(CF_3)_2$	*0.04*	21
Fluorinated ethers			
HFE-152a	CH_3OCHF_2	1.6	1
HFE-143a	CH_3OCF_3	4.3	1
HFE-134	CHF_2OCHF_2	26	1
HFE-125	CHF_2OCF_3	136	1
HFE-227ea	$CF_3OCHFCF_3$	11	2
HCFE-235da2	$CHF_2OCHClCF_3$	2.6	2
HFE-236ea2	$CHF_2OCHFCF_3$	5.8	2
HFE-236fa	$CF_3OCH_2CF_3$	3.7	2
HFE-245fa1	$CHF_2CH_2OCF_3$	2.2	2
HFE-245fa2	$CHF_2OCH_2CF_3$	4.9	1
HFE-245cb2	$CH_3OCF_2CF_3$	5.1	4
HFE-254cb2	$CH_3OCF_2CHF_2$	2.6	4
HFE-263fb2	$CH_3OCH_2CF_3$	*0.1*	2
HFE-329mcc2	$CF_3CF_2OCF_2CHF_2$	6.8	2
HFE-338mcf2	$CF_3CF_2OCH_2CF_3$	4.3	2
HFE-347mcc3	$CH_3OCF_2CF_2CF_3$	5.2	4
HFE-347mcf2	$CF_3CF_2OCH_2CHF_2$	2.8	2
HFE-347pf3	$CHF_2OCH_2CF_2CF_3$	5.9	4
HFE-347sy2	$CF_3CF(OCH_3)CF_3$	3.7	4
HFE-356mec3	$CH_3OCF_2CHFCF_3$	0.94	2
HFE-356mff2	$CF_3CH_2OCH_2CF_3$	*0.4*	15
HFE-356pcc3	$CH_3OCF_2CF_2CHF_2$	0.93	2
HFE-356pcf3	$CHF_2OCH_2CF_2CHF_2$	3.6	4
HFE-356pcf2	$CHF_2CH_2OCF_2CHF_2$	2.0	2
HFE-365mcf3	$CH_3OCH_2CF_2CF_3$	*0.11*	2, 15

Table 1-4, continued.

Industrial Designation or Common Name	Chemical Formula	Lifetime (years)	Notes
HFE-374pc2 [a]	$CH_3CH_2OCF_2CHF_2$	5.0	2
	$CHF_2CF_2OCHF_2$	26.5	24
	$CF_3CHFCF_2OCH_2CF_2CF_3$	9.1	24
	$(CF_3)_2CHOCHF_2$	3.1	2
	$CF_3CH(OCF_3)CHF_2$	3.1	2
	$(CF_3)_2CFOCH_3$	3.4	2
	$CF_3OC(O)H$	3.6	25
	$C_2F_5OC(O)H$	3.6	26
	$n-C_3F_7OC(O)H$	2.6	26
HFE-7100 (HFE-44-9)	$CH_3OC_4F_9$	5.0	2
HFE-7200 (HFE-56-9)	$C_2H_5OC_4F_9$	0.77	2
HFE-43-10pccc124 [b]	$CHF_2OCF_2OCF_2CF_2OCHF_2$	6.3	2
HFE-236ca12 (HG-10)	$CHF_2OCF_2OCHF_2$	12.1	2
HFE-338pcc13 (HG-01)	$CHF_2OCF_2CF_2OCHF_2$	6.2	2

Other fluorinated species

Trifluoromethylsulfur-pentafluoride	SF_5CF_3	650-950	18
Sulfur hexafluoride	SF_6	3200	2
Nitrogen trifluoride	NF_3	740	2

Notes:

1. Global lifetime estimated from a process lifetime with respect to tropospheric OH calculated relative to 6.1 years for CH_3CCl_3, assuming an average temperature of 272 K (Spivakovsky et al., 2000; Prather and Ehhalt et al., 2001); OH rate constants from Sander et al. (2006); and stratospheric loss lifetimes inferred from IPCC (2001).
2. Prather and Ehhalt et al. (2001) and Ramaswamy et al. (2001).
3. See Section 1.2.1.6 for further discussion related to methyl halide global lifetimes. Includes estimate of ocean sink from Tokarczyk et al. (2003a, b).
4. Lifetime calculated as in Note 1 except that no estimate of a stratospheric loss lifetime was available to include in the lifetime estimate listed. Hence this is an upper bound to the global lifetime estimate.
5. Based on *WMO 2002*, including oceanic loss term with 94-year partial lifetime observed in saturation data and ascribed to an unidentified process (Yvon-Lewis and Butler, 2002) but also accounting for soils sink with 90-year partial lifetime (Happell and Roche, 2003). However, see Section 1.3.2.4 for additional considerations based on atmospheric measurements.
6. Including oceanic loss term from Yvon-Lewis and Butler (2002). The contribution of oceanic loss to the lifetime of HCFC-21, HCFC-22, HCFC-123, HCFC-124, HCFC-141b, HFC-125, and HFC-152a is small; for HFC-134a and HCFC-142b it is negligibly small at the reported precision.
7. WMO (1999).
8. Lifetimes listed include local tropospheric photolysis lifetimes from Table 2-9 in Kurylo and Rodríguez et al. (1999). Consideration of only tropospheric OH loss results in local lifetimes of 0.34 years for CH_2Br_2, 0.21 years for $CHBr_3$, and 0.37 years for CH_2BrCl.
9. See Section 1.4 text for discussion.
10. OH rate constant from Qiu et al. (1992).
11. Lifetime calculated as in Note 1, but with stratospheric loss from Naik et al. (2000).
12. Lifetime calculated as in Note 1, but with OH rate constant and stratospheric loss from Naik et al. (2000).
13. Markert and Nielsen (1992).
14. OH rate constant from DeMore and Bayes (1999).
15. The values estimated correspond to local lifetimes in the free troposphere from Chapter 2 (this Assessment). For species that react with OH, the process lifetime due to OH reaction is calculated using the rate constant at 275 K (for lifetimes greater than 10 days) or 300 K (for lifetimes less than 10 days) and OH concentration of 1×10^6 molec cm^{-3}. These should not be used in estimating ODP, GWP, or EESC because the atmospheric burden for these short-lived gases ($\tau < 0.5$ year) depends on the location and time of emissions.
16. See Chapter 2.
17. From the 2-D model calculation in Fraser et al. (1999).
18. Takahashi et al. (2002), Chim et al. (2003), and Limão-Vieira et al. (2004). Range in lifetime depends on whether solar proton events reduce the lifetime.
19. Bayes et al. (2003).

Table 1-4, continued.

20.   Cotter et al. (2003).
21.   Taniguchi et al. (2003).
22.   Chen et al. (2003).
23.   Hurley et al. (2004) estimate the lifetimes of $F(CF_2)_nCH_2OH$, for n = 1-4, to be 0.45 year.
24.   Chen et al. (2005).
25.   Chen et al. (2004a).
26.   Chen et al. (2004b).
27.   Rajakumar et al. (2005).
28.   Li et al. (2006).
29.   Shine et al. (2005).

[a]   Referred to as HFE-374pcf2 in past Assessments.
[b]   Referred to as H-Galden 1040x in past Assessments.

by Volk et al. (1997, Table 5). This provides lifetime uncertainties that are almost entirely independent of the estimates that can be produced by using the atmospheric measurements from the ground-based networks combined with emissions estimated from industrial production figures. The uncertainties are obtained by taking the root mean square sum of the variances from the model-based estimates and the variances given by Volk et al. The results are lifetime uncertainty ranges of 35-57 years for CFC-11, 79-113 years for CFC-12, and 66-114 years for CFC-113. However, it was indicated in Section 1.2.1.1 that CFC-113 is decreasing in the atmosphere at a rate of 1%/yr, which implies a maximum lifetime of approximately 100 years. A range of 66-100 years is then derived for CFC-113. The stratospheric lifetime uncertainty range for CCl_4 calculated in the same way is 28-46 years. It may be noted that the recommended lifetimes in the previous section do not lie exactly in the middle of these uncertainty ranges. That is because, except where new measurements had been made, there was no justification for changing the values used in *WMO 2002*.

For the major HCFCs, the lifetime uncertainty ranges are obtained by combining the uncertainty in the hydroxyl value of 14% given by Prinn et al. (2001) with the uncertainties in the reaction rates between the HCFCs and hydroxyl from Sander et al. (2006). This gives lifetime uncertainties of ±17% for HCFC-22, ±20% for HCFC-141b, and ±24% for HCFC-142b.

1.2.3   Total Atmospheric Chlorine and Bromine

1.2.3.1   TOTAL ORGANIC CHLORINE IN THE TROPOSPHERE

Total organic chlorine (CCl_y) from long-lived source gases continued to slowly decrease in the troposphere during 2001-2004 (Montzka et al., 2003;

O'Doherty et al., 2004) (Figure 1-9 and Table 1-5). In mid-2004 tropospheric CCl_y was approximately 3.44 parts per billion (ppb), or about 0.25 ppb Cl (nearly 7%), below the peak observed in 1992-1994. The rate of decline in CCl_y from 2003 to 2004 (−20 ppt Cl/yr or −0.59%/yr) was slightly less than in previous years (−23 ppt Cl/yr or −0.64%/yr), owing to the reduced influence of methyl chloroform. In 2004, mixing ratio changes for methyl chloroform still contributed substantially to the decrease in CCl_y (−13.5 ppt Cl/yr), though this contribution was nearly matched by the decline observed in the aggregate of CFCs plus CCl_4 (−12.7 ppt Cl/yr). In 2004, the CFCs accounted for 62% of CCl_y in long-lived gases in the lower atmosphere; this fraction has increased slightly over the past decade as Cl from shorter-lived gases has diminished more rapidly than Cl from CFCs.

Increases in CCl_y from HCFCs slowed during 2000-2004. CCl_y from the three major HCFCs increased at a rate of nearly 6 ppt Cl/yr during 2004, or almost half the rate of annual increase measured in 1996 (Table 1-5). HCFCs accounted for 214 ppt of CCl_y in mid-2004, or about 6%.

1.2.3.2   TOTAL CHLORINE IN THE STRATOSPHERE AND HYDROGEN CHLORIDE (HCl)

Stratospheric chlorine time series are different from tropospheric time series in many respects. Stratospheric chlorine levels lag tropospheric levels, due to the time it takes for the trends to propagate. During the propagation of tropospheric trends into the stratosphere, mixing leads to a distribution of transit times in any air parcel in the stratosphere, which is described by the concept of "age of the air." This mixing will inevitably make long-term trends in stratospheric time series less sharp, if they are driven by tropospheric trends (see, e.g., Waugh et al., 2001, and Engel et al., 2002). The peak in the tropospheric chlorine is thus expected to occur later in the stratosphere and be broader and have somewhat lower mixing ratios in its
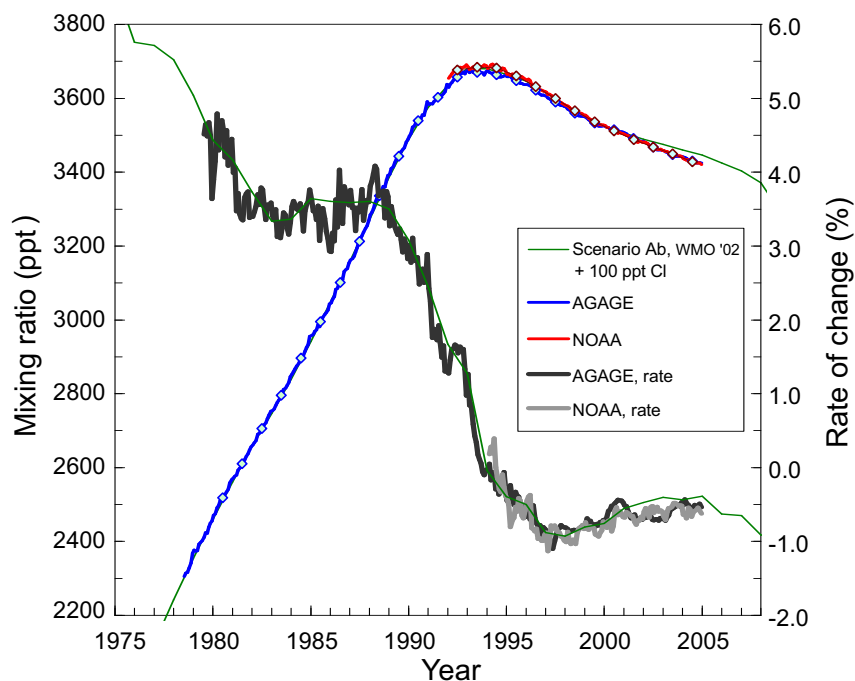
Figure 1-9. The tropospheric abundance of organic chlorine (CCl$_y$) from the NOAA/ESRL and AGAGE global measurement networks (updates of Montzka et al., 1999, and O'Doherty et al., 2004) and its rate of change over time. Quantities are based upon independently measured mixing ratios of CFC-11, CFC-12, CFC-113, HCFC-22, HCFC-141b, HCFC-142b, methyl chloroform, and carbon tetrachloride. Results for CFC-114 and CFC-115 from Prinn et al. (2000) are used in both compilations. An additional constant 550 ppt was added for CH$_3$Cl and 100 ppt was added for short-lived gases such as CH$_2$Cl$_2$, CHCl$_3$, C$_2$Cl$_4$, and COCl$_2$. Rates of change are determined from 12-month differences and are plotted with respect to the right-hand axis. Observations are compared with the projections from *WMO 2002* (green line).

Table 1-5. Contributions of halocarbons to total chlorine (Cl) in the troposphere. An average of AGAGE and NOAA/ESRL global means was used to derive these mid-year mixing ratios. Rates of change were calculated as the difference between the indicated year and the previous year. Uncertainties in rates of change (1 standard deviation) are estimated from the difference in rates derived from observations by the different global networks, NOAA/ESRL and AGAGE. The uncertainty in total Cl is approximately 25 ppt Cl (1 standard deviation) throughout the period 1996-2004 (based on the sum of differences in global tropospheric means derived for individual gases between the AGAGE and NOAA/ESRL networks).

	Total Cl (ppt Cl)			Contribution to Total Cl (%)			Rate of Change in Total Cl (ppt Cl/yr)		
	1996	2000	2004	1996	2000	2004	1996	2000	2004
Aggregated CFCs	2160	2156	2126	59%	61%	62%	5.8 (3.4)	−1.4 (2.0)	−8.9 (0.4)
CH$_3$Cl [a]	550	550	550	15%	16%	16%	0.0 [b]	0.0 [b]	0.0 [b]
CCl$_4$	407	393	378	11%	11%	11%	−4.2 (0.6)	−3.6 (0.3)	−3.8 (0.7)
Aggregated HCFCs	141	180	214	4%	5%	6%	10.3 (0.5)	9.2 (0.8)	5.9 (1.0)
CH$_3$CCl$_3$	274	137	66	8%	4%	2%	−39.7 (0.2)	−26.8 (1.0)	−13.5 (0.4)
CH$_2$Cl$_2$, CHCl$_3$, etc. [c]	100	100	100	3%	3%	3%	0.0 [b]	0.0 [b]	0.0 [b]
Halon-1211	3.5	4.0	4.2	0%	0%	0%	0.2	0.1	0.0
Total Cl	3636	3521	3437				−28 (3.5)	−23 (2.4)	−20 (1.4)
							−0.76%	−0.64%	−0.59%

[a] CH$_3$Cl assumed to be 550, consistent with the previous Assessment (Montzka and Fraser et al., 2003).
[b] Growth rate assumed to be zero here, though some very short-lived gases have been declining over the past decade (see Chapter 2).
[c] CH$_2$Cl$_2$, CHCl$_3$, etc., also includes the very short-lived gases C$_2$Cl$_4$, C$_2$HCl$_3$, and CH$_2$ClCH$_2$Cl, and an additional 50 ppt to account for Cl from COCl$_2$ (see Chapter 2 for additional discussion of the contribution of short-lived gases to total Cl).

maximum (about 150 ppt lower; see Engel et al., 2002). Figure 1-10 shows an update of stratospheric chlorine trends for midlatitudes (44°N) calculated by Engel et al. (2002), based on tropospheric observations by NOAA/ ESRL up to the year 2005, mean profiles of mean age, and a parameterization of the width of the age spectrum. Based on these calculations, the maximum chlorine levels were expected in the lower stratosphere around 1995 and were expected to have reached altitudes above 30 km by about 2000. It is expected that total chlorine is now decreasing at all altitudes.

Total chlorine in the stratosphere could either be in the form of organic chlorine or inorganic chlorine. Figure 1-11 is constructed based on the profiles of organic and inorganic species derived from observations and modeling results (see figure caption for details). Nassar et al. (2006a) derived the total chlorine budget for 30°N-60°N, based mainly on observations by the ACE-FTS, yielding 3.65 ppb chlorine (with an estimated accuracy of ±0.13 ppb) in 2004. This value is slightly larger than the value of 3.54 ppb (with a precision of ±0.10 ppb) derived by Zander et al. (1996) for 1994 from ATMOS experiment

observations, when stratospheric chlorine levels were still increasing.

At high altitudes (above 50 km) the total chlorine budget is dominated by hydrogen chloride (HCl), which at this altitude may serve as a good proxy for total inorganic chlorine (Cl_y) and even total chlorine. The longest continuous time series of HCl from satellite observations is that of the Halogen Occultation Experiment (HALOE) (Russell et al., 1993; Anderson et al., 2000). For about 55 km altitude, Figure 1-12 compares the HCl measurements with model values of HCl that are derived from a total chlorine time series that has been convoluted with spectra of various widths, each having a mean age of 5.5 years. The total chlorine values are based on the NOAA/ESRL and AGAGE measurements including a 100 ppt contribution from very short-lived (VSL) source gases (full lines), whereas the dashed curve (from scenario Ab in *WMO 2002*) excludes a contribution from VSL compounds. These Cl_y time series have been reduced by a factor of 0.96, which represents model estimates of the HCl/Cl_y ratio at 55 km, in order to arrive at the model curves for HCl shown in Figure 1-12.
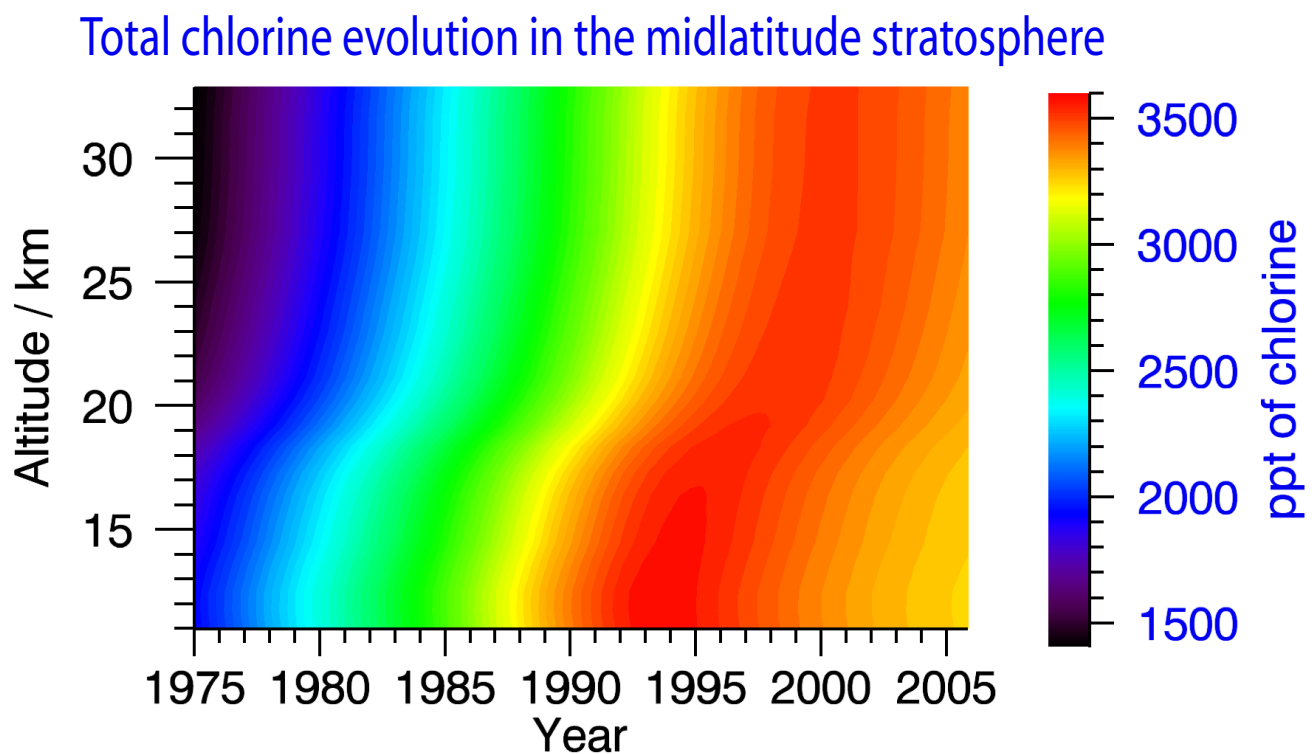

Figure 1-10. Total chlorine calculated based on the vertical distribution of mean age (derived from observations of the age tracers sulfur hexafluoride (SF_6) and carbon dioxide (CO_2)) and assumptions on the width of the age spectrum. Tropospheric data by NOAA/ESRL are used as the basis of the calculation (updated from Engel et al., 2002). No chlorine contribution from very short-lived (VSL) species is included in this calculation.
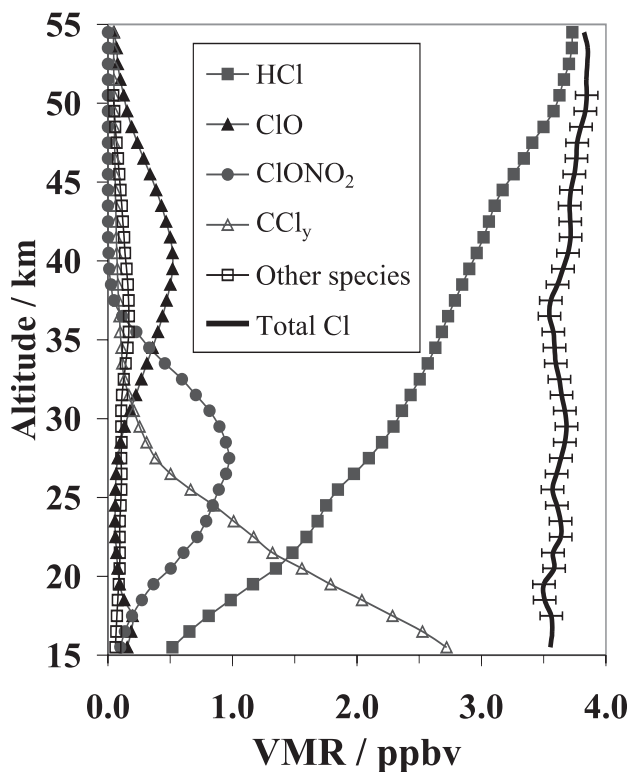
Figure 1-11. The northern midlatitude (30°N-60°N) stratospheric chlorine budget for 2004 expressed in volume mixing ratio (VMR) (Nassar et al., 2006a). It includes ACE-FTS measurements of HCl, chlorine nitrate (ClONO$_2$), chlorofluorocarbonyl (COClF), CH$_3$Cl, CCl$_4$, CFC-11, CFC-12, CFC-113, HCFC-22, and HCFC-142b, which are complemented by chlorine monoxide (ClO) observations from the Sub-Millimeter Receiver (SMR) on the Odin satellite (Berthet et al., 2005), hypochlorous acid (HOCl) measurements by the Michelson Interferometer for Passive Atmospheric Sounding (MIPAS) (von Clarmann et al., 2006), and phosgene (carbonyl chloride, COCl$_2$) observations from the balloon-borne MkIV (Toon et al., 2001). ACE-FTS measurements of HCFC-22 were extended above 25 km based on values from the Stratospheric Chemistry Transport Model-1 (Rummukainen, 1996; Coheur et al., 2003). CH$_3$CCl$_3$ and the minor contributors CFC-114, CFC-114a, CFC-115, HCFC-141b, and halon-1211 were based on SAGE III Ozone Loss and Validation Experiment (SOLVE) measured profiles (Schauffler et al., 2003) scaled to 2004. The sum of the chlorine contributions from these species gives the total chlorine profile, with error bars indicating the 1-sigma precision.

The linear trend in HALOE values from January 1999 to November 2005 is −26 ± 12 ppt/yr (one sigma), which is larger than, but not significantly different from, the trend in the total chlorine based on the organic record. The time of the peak in HCl is somewhat ill defined in the HALOE data. Rinsland et al. (2005) showed that the HCl change observed between ATMOS observations in 1985 and 1994 and ACE observations in 2004 are broadly consistent with the expectations due to the changes in total stratospheric chlorine (Figure 1-12). Overall, the time series of the lower mesospheric HCl (Cl$_y$) are qualitatively consistent with expectations from ground-based measurements after considering lag times (~5-6 years) (Waugh et al., 2001; Waugh and Hall, 2002) associated with transport of tropospheric air to the lower mesosphere, although the fine-scale structure observed between 1997 and 2002 in the HALOE data remains unexplained.

There are considerable differences in the amount of upper stratospheric HCl measured by the four instruments. The systematic difference in HCl observations between MLS and HALOE is about 0.2-0.4 ppb (about 7-15%, HALOE lower), while ACE and MLS show better agreement (Froidevaux et al., 2006). Measurements of HCl by MLS and ACE both show values between 3.4 and 3.6 ppb in 2006 (Figure 1-12), which would imply a peak value for total chlorine of ~3.5 to 3.8 ppb, larger than can be supplied by the 12 long-lived source gases. The HALOE measurements of HCl are consistent with supply of chlorine from only long-lived source gases. The differences between the instruments are not currently understood, but it should be noted that the different measurements do agree within the stated accuracies, indicated by the error bars (±2 sigma) in Figure 1-12. Due to these differences in absolute values of these observations, it is at present not possible to state whether upper stratospheric inorganic chlorine is consistent with supply from only the 12 long-lived source gases, or it is large enough to allow for a chlorine contribution from short-lived gases of 0.05 to 0.1 ppb. This issue is discussed further in Section 2.5.2 of Chapter 2, which focuses on possible contributions from the very short-lived substances.

As is evident from Figure 1-11, column observations of HCl and chlorine nitrate (ClONO$_2$) can also be used to gain insight regarding the total inorganic chlorine in the stratosphere. Recent high spectral resolution infrared ground-based observations have also provided evidence that the total loading of stratospheric chlorine has reached its maximum, with tentative evidence, at the 1-sigma level, of the onset of a long-term decline. For example, observations from the Network for the Detection of Atmospheric Composition Change (NDACC) from the 3 stations with measurements spanning up to 24 years have
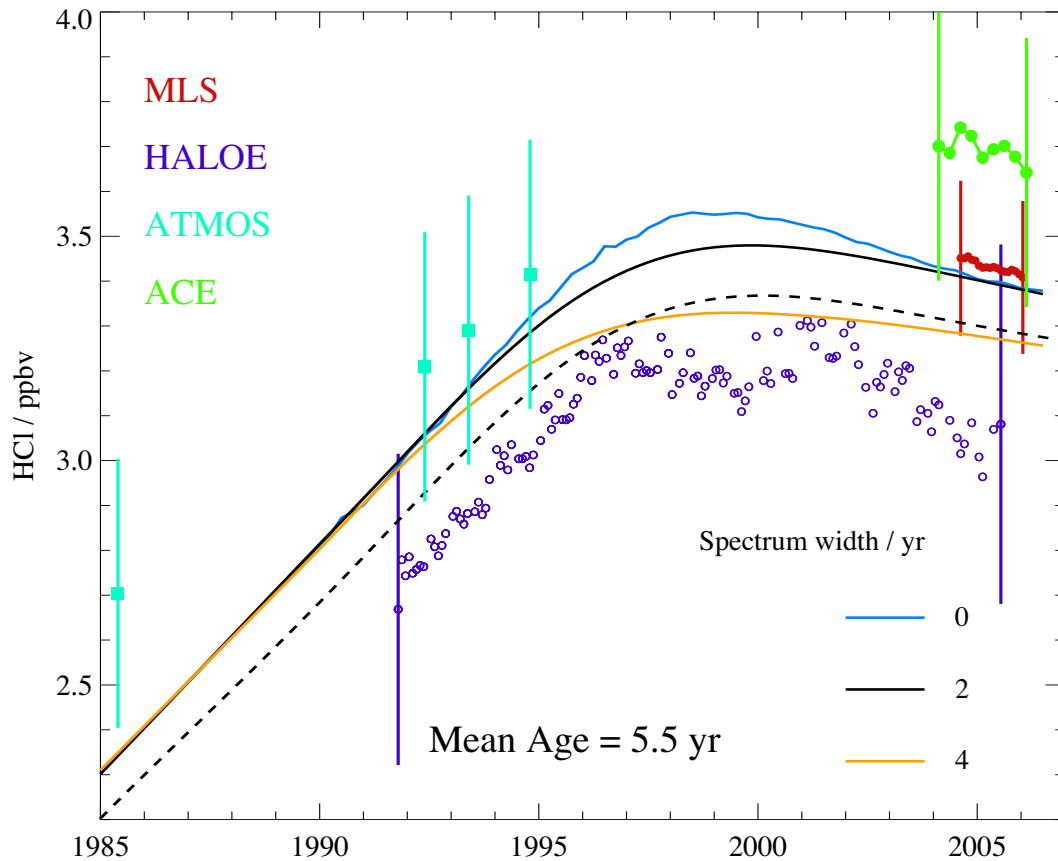
Figure 1-12. HCl monthly averages for 60°S-60°N at 0.46 hPa from MLS (red dots; Froidevaux et al., 2006 updated) and HALOE (purple circles; Anderson et al., 2000 updated), along with quarterly averages from ACE (in green; Nassar et al., 2006a updated) and ATMOS version 3 data averages (cyan squares; Irion et al., 2002; Rinsland et al., 2005) for 50-60 km; error bars are 2-sigma estimates of accuracy. Solid curves use total chlorine time series from tropospheric data (including 100 ppt from very short-lived (VSL) chlorinated substances) and a mean age assumption of 5.5 years, with various age spectrum widths, as indicated; a factor of 0.96 is applied to get HCl. The dashed black curve shows expected HCl based on the *WMO 2002* scenario Ab (no contributions from VSL compounds) and a mean age of 5.5 years, with a spectrum width of 2 years.

provided evidence for stabilization in total chlorine loading, with a broad peak starting at the end of the 1990s, following a rapid buildup during the 1980s (Rinsland et al., 2003). Figure 1-13 provides an update to the NDACC time series from the Jungfraujoch station measurements extending through 2004 from monthly mean time series. It indicates that the total stratospheric inorganic chlorine loading (Cl_y) has decreased slowly ($-0.7 \pm 0.3\%$/yr, 1σ) since it peaked in late 1996, at the limit of being statistically significant at the 2σ level (an update of Mahieu et al., 2004). Multiplying this percentage by a stratospheric Cl_y burden of 3.6 ppb suggests a trend in Cl_y of -25 ± 11 ppt/yr. The column measurements are in good agreement with model calculations by a two-dimensional (2-D) model

run at the University of Leeds (orange trace in Figure 1-13, described in Rinsland et al., 2003).

Solomon et al. (2006) have reported a steeper downtrend for stratospheric chlorine monoxide (ClO) from 1996 to 2005 of $-1.5 \pm 0.2\%$/yr, based on remotely sensed millimeter wave measurements. They calculate however that this downtrend contains an enhancement of about -0.5%/yr, relative to Cl_y trends, because of increases in upper stratospheric methane that have been measured by HALOE. Their observations, which extend from 1984 to present, are broadly consistent with the rise in total chlorine due to human activities and recent declines due to the Montreal Protocol.
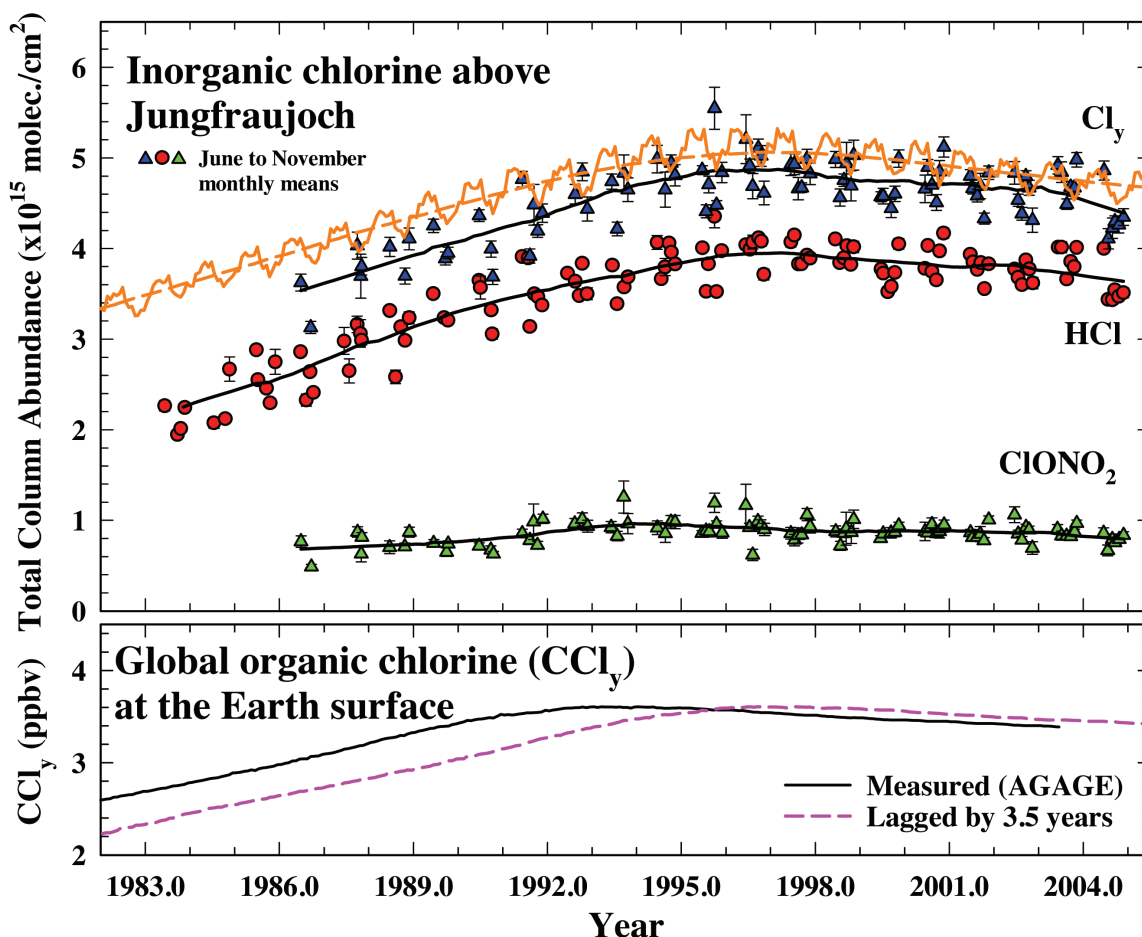
Figure 1-13. Top: Time series of monthly mean total column HCl (red circles) and ClONO$_2$ (green triangles), as derived from the Jungfraujoch (46.5°N) observational database; Cl$_y$ (blue triangles) results from the summation of the corresponding HCl and ClONO$_2$ data points. To avoid the influence of the significant variability affecting measurements in winter- and springtime, these time series have been limited to the June to November months. Nonparametric least-square fits to these datasets are reproduced as thick black curves; they help to appraise the two-decade mean evolution of HCl, ClONO$_2$, and Cl$_y$. Also shown is the sum of the HCl and ClONO$_2$ columns calculated by the University of Leeds 2-D model (top orange curve). Bottom: Evolution of total surface organic chlorine derived from measurements performed by the AGAGE network. For better comparison with the Jungfraujoch data, the tropospheric chlorine trend is also shown with a 3.5-year time shift (magenta line). Updated from Mahieu et al. (2004).

1.2.3.3 ORGANIC BROMINE IN THE TROPOSPHERE FROM METHYL BROMIDE AND HALONS

Because bromine is an efficient catalyst for depleting stratospheric ozone, the Montreal Protocol set limits on anthropogenic production and consumption of the most abundant and long-lived brominated gases in the atmosphere: methyl bromide and the halons. Increased anthropogenic production and use of these gases led to increasing amounts of bromine (Br) in the atmosphere during the second half of the 20th century. Enhanced human-related emissions of methyl bromide and halons likely dominated changes in atmospheric bromine concentrations over the past 50 years. By the late 1990s, about half of the Br in the stratosphere was derived from anthropogenic activities (Montzka and Fraser et al., 2003).

Natural processes deliver bromine to the stratosphere in the form of methyl bromide and short-lived bromocarbons or oxidation products of these gases. Long-term changes in atmospheric Br arising from natural processes likely were smaller than the changes in anthropogenically-derived Br during the 20th century. The background level of stratospheric Br accounted for by short-lived bromocarbons is an area of active research (Chapter 2).

New measurements of methyl bromide have been reported (see Section 1.2.1.7) since the previous Ozone Assessment (WMO, 2003) and they allow trends in total bromine from regulated gases to be assessed. The results (Figure 1-14) indicate that the global tropospheric burden of Br from the sum of methyl bromide and halons peaked in 1998 and has declined since (Montzka et al., 2003). By mid-2004, tropospheric Br was 0.6 to 0.9 ppt below the peak; the mean decline from 1998 to 2004 was between −0.1 and −0.15 ppt Br/yr (a range is given here to reflect differences in recent trends for halon data from different networks and the possibility that mean tropospheric CH_3Br mixing ratios trends are 7% less than observed at Earth's surface). The decline is solely the result of a decrease in global mixing ratios of methyl bromide, which declined at a mean rate of −0.24 ppt/yr from 1999 to 2004, or somewhat faster than expected. Mixing ratios of halon-1301 and halon-1211 still increased slowly from 1999 to 2004; the mean increase in Br from these gases over this period was between 0.08 and 0.12 ppt/yr. Continued increases in the halons are consistent with the existence of substantial banks of halons that are released at a slow rate to the atmosphere.

The decline observed for bromine from regulated gases is significant relative to changes in chlorine, considering that the efficiency for Br to deplete stratospheric ozone is 60 times greater than Cl on a per-atom basis (see Chapter 2 and Chapter 8 for an updated discussion of this efficiency factor, alpha). A decline of −0.1 to −0.15 ppt Br/yr, multiplied by 60, corresponds to a rate of −6 to −9 ppt Cl equivalents/yr, or more than one-third of the rate of decline in atmospheric chlorine over this same period (−20 ppt Cl/yr; Table 1-5).

As was the case for Cl, initial declines in atmospheric Br have been achieved through reduced production and emission of a short-lived gas even while the long-lived gases continued to slowly increase.

1.2.4 Effective Equivalent Chlorine and Equivalent Effective Stratospheric Chlorine

Effective equivalent chlorine (EECl) and equivalent effective stratospheric chlorine (EESC) provide a rough means of gauging the influence of measured changes in both chlorinated and brominated halocarbons on the ozone-depleting halogen abundance in the future stratosphere (see
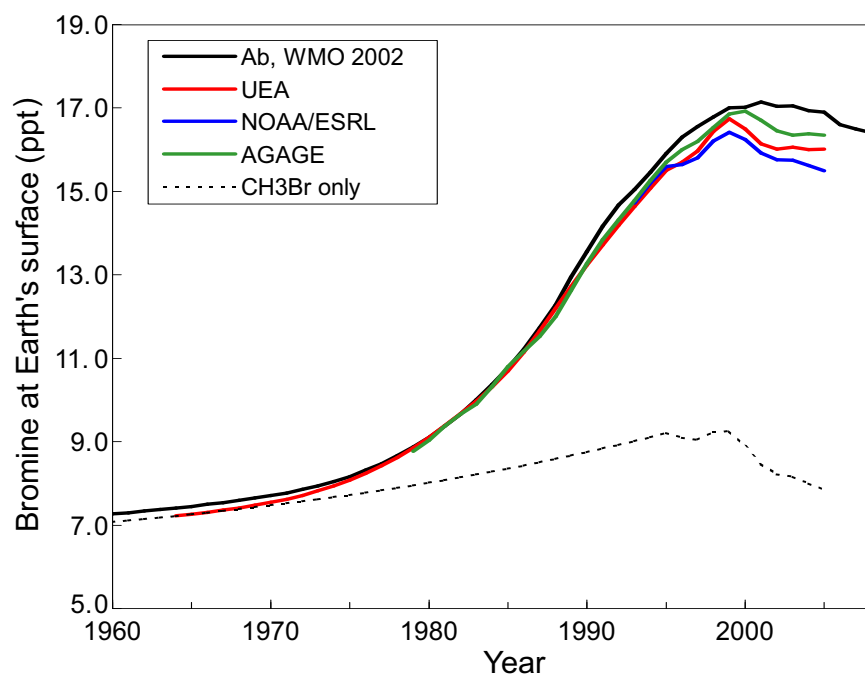

Figure 1-14. Trends in the abundance of Br from brominated gases regulated by the Montreal Protocol on Substances that Deplete the Ozone Layer (halon-1211, halon-1301, halon-2402 and methyl bromide) as projected in the *WMO 2002* Ab scenario (black line) and as measured by different stations (red, green, and blue lines). Although independent global surface means are derived for halon-1211 and halon-1301 by different laboratories, the same is not true for methyl bromide and halon-2402. For these gases, the source of data included in the compilation of total Br for all labs was solely NOAA/ESRL (methyl bromide) and UEA (halon-2402). The global surface estimates are made with samples collected from single sites (AGAGE prior to the mid-1990s and UEA) or multiple sites (AGAGE after the mid-1990s and NOAA/ESRL).

descriptive box on EECl and EESC in Chapter 8). EECl and EESC are derived from ground-based observations of trace gas mixing ratios. As currently formulated, EECl and EESC do not include contributions from very short-lived halogen source gases. Weighting factors are applied to measured mixing ratios to account for the variable rates at which these gases undergo degradation in the stratosphere and liberate halogen atoms for interaction with ozone. Mixing ratios of bromine are multiplied by a factor alpha (α), which reflects the enhanced per-atom efficiency for bromine to catalyze the destruction of stratospheric ozone, relative to chlorine (60 is used here). Finally, a lag time is applied in estimating EESC to account for the time it takes air to be transported from the surface to regions in the stratosphere. A lag of 3 years is used to approximate transport

times and halogen burdens in the midlatitude lower stratosphere (Daniel et al., 1995); longer lag times are more appropriate for the polar stratosphere and the upper stratosphere (Andrews et al., 2001; Newman et al., 2006). No time lag is applied when deriving EECl, so that dates quoted for EECl correspond to sampling dates. Further details on uncertainties and limitations of these quantities are discussed in Chapter 8 of this Assessment, as well as in Chapter 1 of the previous Assessment (WMO, 2003).

Decreases in EECl and EESC continued during 2000-2004, owing to continued declines in tropospheric mixing ratios of most regulated ozone-depleting source gases (Figure 1-15). By 2005, EECl was 277 ppt, or 8-9% below the peak observed in the 1992-1994 time period. This decline represents about 20% of the decline
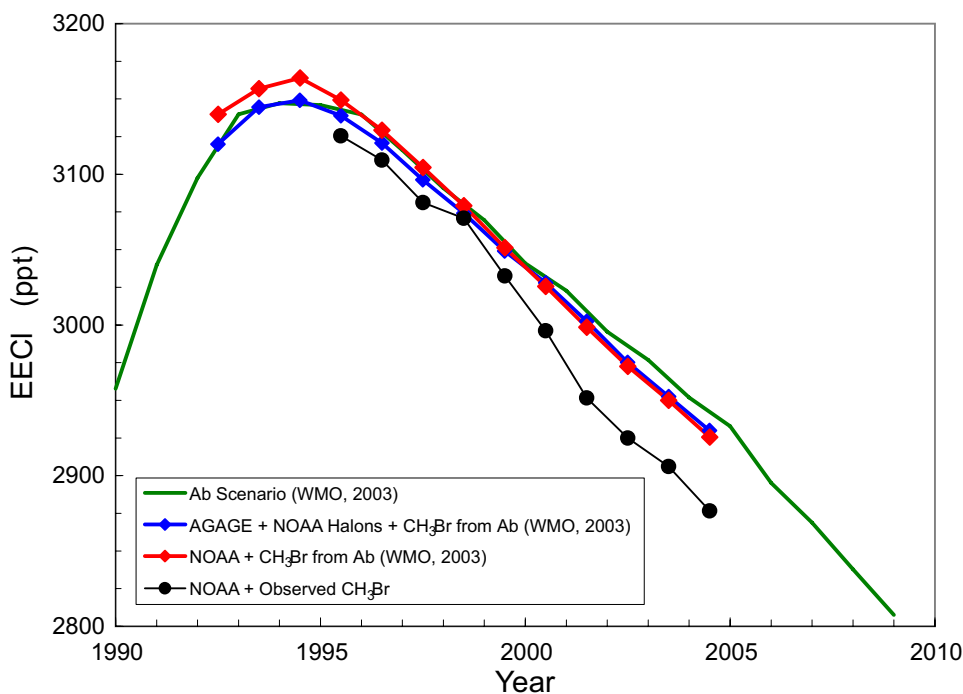

Figure 1-15. EECl calculated from observations of the most abundant long-lived chlorinated gases (CFC-11, -12, -113, CH_3CCl_3, CCl_4, HCFC-22, -141b, and -142b) and the longest-lived brominated gases (halon-1211 and halon-1301). Results for CH_3Br are also included either as projected in the *WMO 2002* Ab scenario (WMO, 2003) (in data represented by blue, red, and green symbols and lines) or as observed in the NOAA/ESRL network along with observational data for all other gases (black points and line). Results from global measurements programs AGAGE (blue diamonds and line; O'Doherty et al., 2004) and NOAA/ESRL (red diamonds and line; Montzka et al., 2003) are compared with scenario Ab from the 2002 WMO Assessment report (Montzka and Fraser et al., 2003) (green line). In the calculations presented here, all bromine atoms are multiplied by a factor of 60, owing to evidence suggesting that Br atoms are 60 times more effective at destroying stratospheric ozone (see discussion in Chapter 8). Fractional release factors used here are taken from Table 8-1, and all release factors have been normalized to 0.8 for CFC-11, despite reports that absolute release factors may be substantially smaller for the middle stratosphere (Schauffler et al., 2003). Using a smaller absolute release factor would affect all absolute mixing ratios and growth rates reported here, but would not affect relative quantities or integrated EESC calculated for future scenarios in Chapter 8.

needed for atmospheric EESC to return to 1980 levels (Figure 1-16). The mean rate of decline during 2000-2004 was similar to that observed during 1996-2000 but was faster than projected in scenario Ab of *WMO 2002* (Montzka and Fraser et al., 2003). This discrepancy arises primarily from a more rapid decline in CH_3Br, though slower-than-projected increases in measured mixing ratios of HCFCs and halon-1301, and a more rapid decline than projected for CH_3CCl_3, also contributed (Figure 1-15). Note that discussions related to trends in observationally derived EECl and EESC did not include CH_3Br in the recent WMO 1998 and 2002 reports, because of a lack of CH_3Br measurements for recent years that have since become available. Declines in shorter-lived gases (CH_3Br and CH_3CCl_3) continue to be the largest contributors to declining EECl. The early removal of shorter-lived gases means that later decreases in EECl and EESC will likely be dominated by the atmospheric decay of the longer-lived gases. Despite diminished mixing ratios of CH_3CCl_3, this gas remained the single largest contributor to decreasing EECl during 2000-2004 (-61 ppt EECl out of a decline from all gases

of -120 ppt EECl over this period). Declines in CH_3Br accounted for about one-third of the overall decline (-44 ppt EECl); the CFCs together accounted for less of the overall decline (-23 ppt EECl) as did CCl_4 (-13 ppt EECl). These decreases were offset somewhat by continued increases from HCFCs (+12 ppt EECl) and halons (+11 ppt EECl).

Calculations of EECl discussed here include the assumption that mixing ratios measured at the Earth's surface provide an accurate estimate of the amount of Cl and Br from halocarbons entering the stratosphere. For source gases whose tropospheric loss rates are similar to rates of vertical mixing within the troposphere, surface-based observations may overestimate the amount and trend of Cl and Br reaching the stratosphere. Such influences may affect CH_3Br more than other gases considered in the calculation of EECl here, because it has the shortest lifetime with respect to atmospheric photochemical loss in the troposphere (~1.7 years). Vertical gradients on the order of 0-15% have been observed for CH_3Br between the lower and upper troposphere (Schauffler et al., 1999).

1.2.5 Fluorine in the Stratosphere

1.2.5.1 TOTAL STRATOSPHERIC FLUORINE AND HYDROGEN FLUORIDE (HF) AT 55 KM

The majority of the fluorine in today's atmosphere is derived from anthropogenic activities, as there are no known significant natural fluorine sources (Zander et al., 1994). Stratospheric fluorine is unimportant for stratospheric ozone depletion in comparison to chlorine and bromine, but, because it is mainly due to CFCs, HCFCs, and HFCs, it provides an important consistency check on the anthropogenic chlorine input. An inventory of total fluorine (F_{TOT}) in the stratosphere, including both organic and inorganic species, from 82°N to 82°S over the period of February 2004-January 2005 inclusive has been reported by Nassar et al. (2006b), based primarily on ACE-FTS measurements. Stratospheric F_{TOT} values were 2.50-2.59 ppb at all latitudes with a precision of ±0.04-0.07 ppb. The highest value of mean F_{TOT} occurred in the tropics, which is qualitatively consistent with increasing stratospheric fluorine and the mean stratospheric circulation pattern. Figure 1-17 shows the stratospheric F_{TOT} budget for 30°N-60°N in 2004.

The main source of stratospheric HF is photodissociation of chlorofluorocarbons (CFCs), and it is therefore an effective tracer of fluorine input to the stratosphere. As altitude increases, the organic fluorine compounds decom-
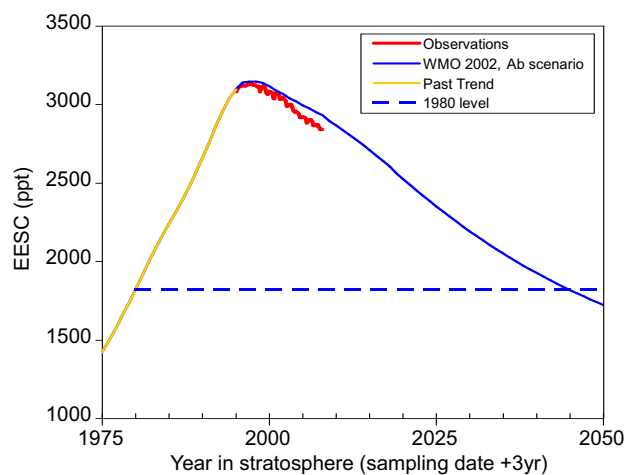

Figure 1-16. Observed and projected changes in EESC relative to the 1980 level. The 1980 level is chosen to represent the atmospheric EESC burden before the ozone hole was observed. Here, EESC is derived from observations of all gases included in the *WMO 2002* Ab scenario (Montzka and Fraser et al., 2003). The observed decline in EESC of 277 ppt EESC from its peak in the 1990s is 20% of the difference between the peak and 1980 EESC levels. Dates are meant to be relevant for the midlatitude stratosphere and are derived by adding 3 years to the date at which samples were collected at the surface (to account for the time it takes for air at Earth's surface to reach the midlatitude stratosphere).
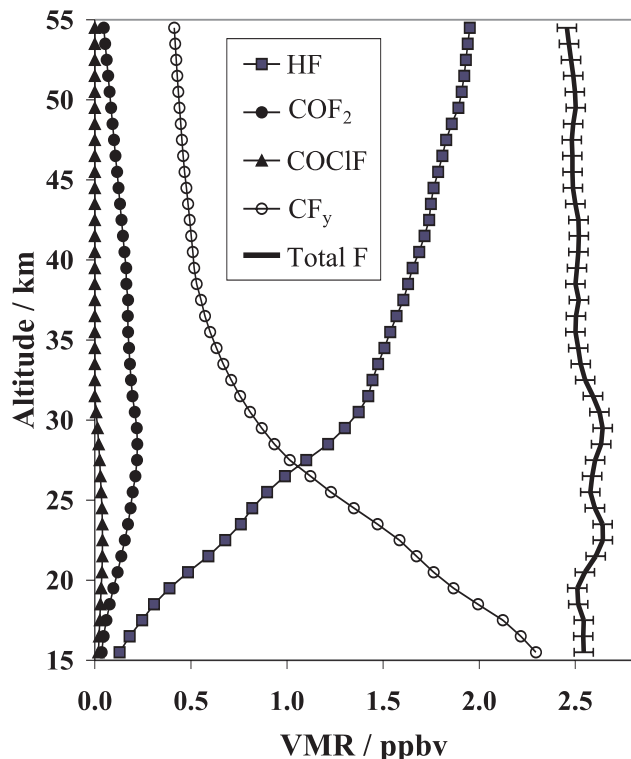
Figure 1-17. The northern midlatitude (30°N-60°N) stratospheric fluorine budget for 2004 expressed in volume mixing ratio (VMR) (Nassar et al., 2006b), which includes hydrogen fluoride (HF), carbonyl fluoride (COF$_2$), chlorofluorocarbonyl (COClF), carbon tetrafluoride (CF$_4$), CFC-11, CFC-12, CFC-113, HCFC-22, and HCFC-142b measured by the ACE-FTS, along with estimates of 15 minor organic fluorine species (including CFCs, HCFCs, hydrofluorocarbons (HFCs), fluorocarbons (FCs), and halons) based on predicted values in the previous WMO Assessment (WMO, 2003). ACE-FTS measurements of COF$_2$ were extended above 40 km based on the model of Kaye et al. (1991). SF$_6$ is not shown, but its contribution has been accounted for. The sum of the fluorine contributions from these species gives the total fluorine profile, with error bars indicating the 1-sigma precision of 0.05 ppb.

pose due to photolysis and chemistry, forming inorganic compounds. At 55 km altitude, HF comprises ~93% of the total inorganic fluorine (F$_y$) at high latitudes and ~86% near the equator, based on National Center for Atmospheric Research (NCAR) two-dimensional model results (Brasseur et al., 1990). The HALOE instrument has provided temporal and spatial information on the near-global distribution of HF since October 1991. The accuracy for a single HF profile at 55 km is ~14% and the precision is

better than 0.05 ppb (Russell et al., 1996). Figure 1-18 shows the time series of HALOE-observed near-global HF, HALOE-derived F$_y$ using latitude-dependent HF/F$_y$ ratios between 86 and 93%, (updated from Anderson et al., 2000), and the *WMO 2002* scenario Ab convolved with an age spectrum with a mean age of six years and a width of three years (Waugh et al., 2001). The HALOE-derived F$_y$ at 55 km was increasing at an approximately constant rate until about 1996, and at a slower rate thereafter. Overall, these changes in the F$_y$ record are strongly consistent with expectations from ground-based measurements after considering lag times (~6 years) associated with transport of tropospheric air to the lower mesosphere (Waugh et al., 2001; Waugh and Hall, 2002). This lag time is also consistent with the lag time derived for Cl$_y$ in Section 1.2.4.

1.2.5.2 TOTAL AND STRATOSPHERIC COLUMN INORGANIC FLUORINE

Of the three species relevant for column inorganic chlorine measurements (HF, COF$_2$, and COClF), COClF cannot be monitored by FTIR measurements from the ground but F$_y$* = HF + 2COF$_2$ is an excellent surrogate of the total F$_y$ burden in the stratosphere (Zander et al., 1994). Monthly mean total column time series of HF, COF$_2$, and
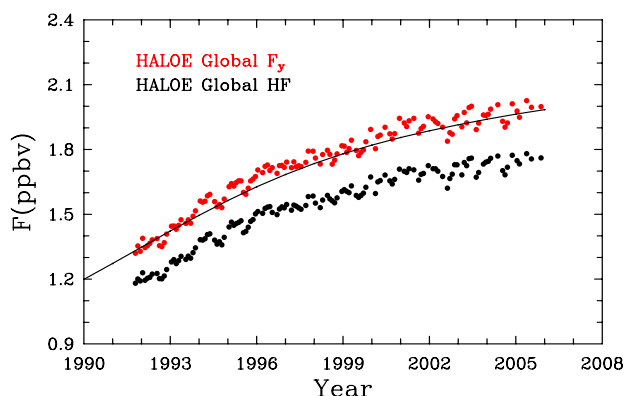

Figure 1-18. Time series of HALOE-observed near-global HF (black dots) and HALOE-derived total inorganic fluorine (F$_y$) at 55 km (red dots). The total F$_y$ was derived from HALOE by applying 86-93% HF/F$_y$ ratios to the observed HF. The estimated precision (±1 sigma) of the near-global HF and F$_y$ averages is on the order of the size of the data points. The black solid line through the F$_y$ data points is the WMO 2002 baseline scenario (Ab) convolved with a spectrum with mean of 6 years and width 3 years. Updated from Anderson et al. (2000).

F_y^* derived from the Jungfraujoch observational database are shown in Figure 1-19. The F_y^* curve indicates a temporal slowing in 1999, mainly resulting from the COF_2 behavior. Overall, there has been a slowing down of the F_y^* accumulation, with a mean rate of increase of (1.3 ± 1.2)%/yr (1 sigma) determined over the 2000-2004 time period. This has essentially resulted from the phasing out of important fluorine-containing source gases (CCl_2F_2 (CFC-12), CCl_3F (CFC-11), and CCl_2FCClF_2 (CFC-114)), which at present has only been partially compensated for by increases in substitute products such as $CHClF_2$ (HCFC-22) and CH_2FCF_3 (HFC-134a) (Anderson et al., 2000; Anderson and Russell, 2004). The sum of the HF and 2 times COF_2 contributions as deduced from 2-D model runs for 47°N (Chipperfield et al., 1997) are also reproduced on Figure 1-19 (upper trace). These calculations account for the evolution of the relevant source gas concentrations characterized by past measurements and by the Ab baseline scenario (WMO, 2003). However, it is important to mention that, so far, the Chipperfield et al. 2-D model runs have not properly reproduced the partitioning among the two main fluorine reservoirs (with an overestimation of the COF_2 contribution to F_y). A possible cause for the latter discrepancy would be a new pathway for destroying COF_2.

A 27-year time series record of daily mean stratospheric HF columns has also been derived by Rinsland et al. (2002) from analysis of infrared solar spectra recorded from the U.S. National Solar Observatory on Kitt Peak (31.9°N, 111.6°W, 2.09 km altitude). The long-term HF evolution is modeled by assuming a seasonal cycle combined with a polynomial expression that solves for coefficients to determine linear and quadratic coefficients for the 14-50 km column as a function of time. The measurements show a continued buildup of the stratospheric HF column, with a spring maximum and an autumn minimum superimposed on significant short-term variability. The latter variations are presumably due to latitudinal trans-
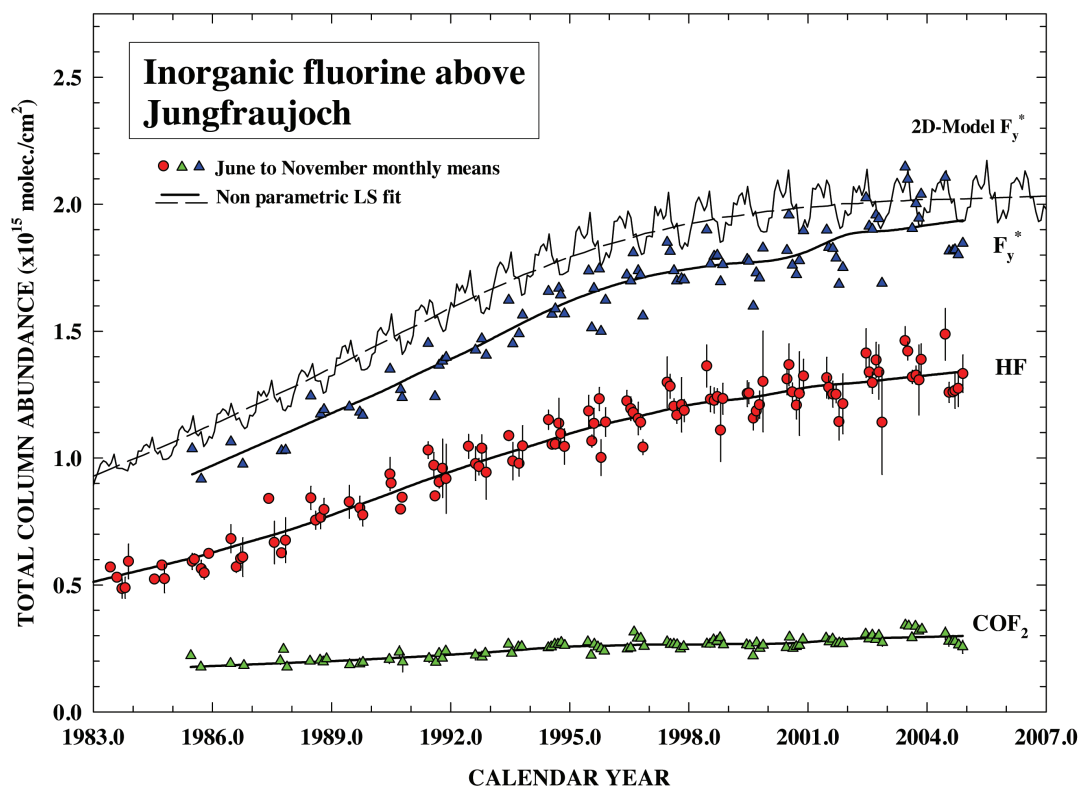

Figure 1-19. Time series of monthly mean total column HF (red circles) and COF_2 (green triangles), as derived from the Jungfraujoch (46.5°N) observational database; F_y^* (blue triangles) results from the summation of the corresponding HF and 2 times COF_2 data points. To avoid the influence of the significant variability affecting measurements in winter- and springtime, these time series have been limited to the June to November months. Nonparametric least-square fits to these datasets are reproduced as thick black solid and dashed curves; they help to appraise the two-decade mean evolution of HF, COF_2, and F_y^*. Also shown is column F_y^* above the Jungfraujoch station calculated with a two-dimensional model (top black curve) (Chipperfield et al., 1997).

port of lower stratospheric air above the Kitt Peak station. The updated results also indicate a rapid buildup in fluorine loading in the middle atmosphere, and that the rate of increase has slowed during recent years.

1.3 EMISSIONS ESTIMATED FROM THE HALO-CARBON MEASUREMENTS

1.3.1 Regional Emissions and Inverse Modeling

In the last few years, inverse modeling of ground-based measurements has been increasingly used to assess emissions of trace gases on regional to continental scales. This approach provides a tool for the validation of emissions and a real-world check for compliance with international agreements. For the Montreal Protocol, in particular, these regional studies have a potential to be used as a tool to test the consistency of different phase-out schemes within the developed and the developing regions of the world. In this section, an assessment of regional emissions, which are estimated by inverse modeling, will be given, together with an attempt to account for uncertainties due to systematic and random errors. A global integration is then attempted to check for compliance with worldwide emissions derived from trends, although the significance of this analysis is limited by large uncertainties in the summed regional emissions.

For the estimation of regional emissions by inverse modeling of ground-based measurements, the same basic principles are generally followed. Observations at one or more locations within the region of interest are separated by statistical or meteorological methods into periods that are influenced by emissions and those that are representative of background conditions. Afterwards the regional emissions are estimated by two principal approaches. In the first method, emissions are calculated by comparing concentrations of the gas with unknown sources with concurrent data on a gas for which a regional emission inventory is available (tracer-ratio method). In the second method, the recent travel histories of the air masses arriving at the observation site are combined with the measured concentrations. The recent history of the air can be deduced using a range of methods including single or multiple back trajectories, or Lagrangian particle dispersion models (LPDM). Results of such inverse modeling-derived emission estimates for ozone-depleting trace gases for different regions of the globe are summarized in Table 1-6.

For Europe, emissions of CFCs have been estimated for the period of 1995-2000 by a combination of measurements from Mace Head (Ireland) and calculations using a sophisticated LPDM model (Numerical Atmospheric Dispersion Modeling Environment, NAME) (Manning et al., 2003). Resulting European emissions in this period were 8.5-9.6 Gg/yr and 13.5-15.2 Gg/yr for CFC-11 and CFC-12, respectively. Interestingly, consumption-based emissions (UNEP, 2002b) show considerably higher values for CFC-11 (18.5-23.0 Gg/yr), whereas values for CFC-12 (9.6-25.0 Gg/yr) were in the same range. Recent European HCFC emissions were estimated to be highest for HCFC-22 (38-41 Gg/yr) and approximately 10 Gg/yr or less for HCFCs 141b and 142b (O'Doherty et al., 2004).

For CH_3CCl_3, a combined analysis of 4 years of data from Jungfraujoch (Switzerland) and Mace Head (Ireland) provided estimates of European emissions in the years 2000-2003 between 0.3 and 3.4 Gg/yr (Reimann et al., 2005), which contrasts with estimated European emissions of over 20 Gg/yr in 2000 from a short-term aircraft campaign over Germany (Krol et al., 2003). On the basis of the much larger time period covered by the study of Reimann et al. (2005), it is assumed that average emissions in Europe after 2000 were in the range of a few Gg/yr and that the higher results of more than 20 Gg/yr were probably due to short-term emissions not being representative for longer time periods.

In contrast to these observations, consumption-based emission estimates for CH_3CCl_3 in Europe were declared to be smaller than 0.1 Gg/yr after 1997. The observed ongoing emissions could have been caused, in part, by consumers banking CH_3CCl_3 in anticipation of the restrictions of the Montreal Protocol. This hypothesis is supported by the drastic decline in consumption-based estimates between 1995 and 1996 (McCulloch and Midgley, 2001), which is not represented by observation-based estimates. Additional sources of CH_3CCl_3 not covered by industry or Montreal Protocol consumption data could include hazardous waste sites, illegal imports, and small releases during HCFC production. Although these ongoing emissions are not significant for stratospheric ozone depletion, they point to the possibility of noncompliance with the Montreal Protocol (see Section 1.3.2.5 for further discussion). For Eastern and South Eastern Europe (Ukraine, Bulgaria, Romania, Turkey, and Greece), indications exist that emissions of CH_3CCl_3 and CFC-113 were still occurring at a non-negligible level in August 2001 (Gros et al., 2003).

In the United States, several studies haven been performed in the last decade. Between 1996 and 2003, ongoing emissions have been detected for CFC-11 and CFC-12. Whereas sources of CFC-11 have not changed much over the period, estimated emissions of CFC-12 have declined unambiguously (Barnes et al., 2003; Hurst et al., 2006; Li et al., 2005; Millet and Goldstein, 2004). This

Table 1-6. Annual emissions derived from regional models and from networks (Gg/yr).

	Europe (EU-15)	United States	Australia	Japan	Asia (including Japan)	Russia	Global Total from Regional Models	Global Total Emissions (Section 1.3.2)
CFC-11	8.5-9.6[1]	6.6[7] 7.3[4]	0.2[8]	1.4[9]	30.1[10]	1.2[11]	49	90
CFC-12	13.5-15.2[1]	13.4[7] 16.4[4]	0.5[8]	2.2[9]	39.4[10]	64[11]	135	122
CFC-113	NA	0.6[4] 1.4[6]	ND	NA	NA	0.8[11]	(1.8)	10
CCl_4	NA	<0.6[4]	ND	1.2[9]	21.5[10]	0.6[11]	(22)	70
CH_3CCl_3	0.3-3.4[2] 24[3]	2.2[5] 3.6[7] 4.4[6]	ND	2.0[9]	14.2[10]	0.4[11]	22-46	See Section 1.3.2.5

NA: not available; ND: not detected; values in parenthesis: data coverage is too weak to derive a global figure. Global emission estimates are an average from 2001-2003.

[1] 1995-2000 (Manning et al., 2003).
[2] 2000-2003 (Reimann et al., 2005).
[3] 2000 (Krol et al., 2003).
[4] 1999-2002 (Li et al., 2005); for the total emissions from the U.S., combined emissions from (Li et al., 2005) and (Barnes et al., 2003) were used, except for CCl_4, where emissions from California alone were extrapolated to the U.S. using a population figure of 273 million.
[5] 2001-2002 (Li et al., 2005).
[6] 2001-2002 (Millet and Goldstein, 2004).
[7] 2003 (Hurst et al., 2006) (only estimating U.S. emissions, related to 273 million inhabitants).
[8] 1998-2000 (Dunse et al., 2005).
[9] 2002 (Yokouchi et al., 2005).
[10] 2001 (Palmer et al., 2003).
[11] 2001 (Hurst et al., 2004).

behavior can be rationalized by different emission functions for these substances in the U.S. Whereas CFC-11 emissions are primarily originating from in-use foams with small but continuing emissions from a large reservoir, CFC-12 emissions from its use in refrigeration and air conditioning occur over a shorter time span and CFC-12 is being replaced by non-ozone depleting substances. United States emissions of CFC-113 between 1996 and 2002 were small and those of CCl_4 have essentially been no longer detectable in the regional studies. On the other hand, CH_3CCl_3 emissions were estimated to be between 2.2-4.4 Gg/yr, which is comparable to values in Europe on an emissions per capita basis.

In Australia and Japan, emissions of the most important ozone-depleting substances were estimated to be of the order of a few Gg/yr in the last few years (Dunse et al., 2005; Yokouchi et al., 2005). Noteworthy is that CH_3CCl_3 emissions were no longer detectable in Australia after 1998, but continuing emissions of 1.7 Gg/yr were estimated in Japan in 2000-2003. For the developing countries in Asia available emission inventories are of limited quality. This is unfortunate because production and usage was still allowed within the Montreal Protocol in many of these countries (e.g., China and India). An aircraft campaign studying the outflow of the Asian subcontinent (Transport and Chemical Evolution over the Pacific, TRACE-P) resulted in estimates of the emissions of several countries within the region in 2001 (Blake et al., 2003; Palmer et al., 2003). For East Asia (China, Japan, and Korea), emissions of 21.5 Gg/yr for CCl_4, 14.2 Gg/yr for CH_3CCl_3 (with a considerable share from sources around Shanghai), 30.1 Gg/yr for CFC-11, and 39.4 Gg/yr for CFC-12 were found. In addition, halon-1211 emissions were 0.2 Gg/yr from Southeast Asia and 2.3 Gg/yr from South China, primarily originating from the Shanghai region.

Emission estimates for Russia are also based on insufficient coverage. This is an important issue because of large uncertainties in the production and banks of ozone-depleting substances for this country. A campaign along

the Trans-Siberian railway (Trans-Siberian Observations Into the Chemistry of the Atmosphere, TROICA-7) indicated only very small emissions of 1.2 Gg/yr for CFC-11, which contrasted with high estimates of 64 Gg/yr for CFC-12 (Hurst et al., 2004). The latter possibly originated from releases due to leakage from excessively large banks or from unaccounted production. On the other hand, emissions of CCl_4 and CH_3CCl_3 were small, in accordance with expectations.

Summation of the regional emission estimates for CFCs, CH_3CCl_3, and CCl_4 (Table 1-6) provides a consistency check on the global emissions that have been calculated from the combination of the background trends in their concentrations and their atmospheric lifetimes (Section 1.3.2). This comparison is however hampered by several likely sources of random and systematic errors. The largest source of potential error is the result of the substantial gaps in the spatial and temporal coverage in the existing regional studies. Whereas in Europe, the U.S., and Australia continuous measurements are being routinely exploited for deriving regional emissions, capabilities for doing this in regions with a substantial potential for large uncounted emissions (e.g., Southeast Asia) are still to be developed. Furthermore, the emission estimates described contain uncertainties resulting from the meteorological information or from the emission inventories that are often used as a priori information. In addition, errors can arise from inadequate calibration or sampling (e.g., contamination) as well as insufficient measurement precision. The quantification of these errors is far from straightforward.

A comparison between several of the reported regional emission estimates provides a possible range of uncertainty for an individual estimate. For methyl chloroform three independent studies were performed in the United States within the period of 2001-2003 and ranging from the East Coast to the West Coast (Hurst et al., 2006; Li et al., 2005; Millet and Goldstein, 2004). The three emission estimates for the U.S. ranged from 2.2-4.4 Gg/yr, giving a standard deviation around the mean of 33%. Larger uncertainties were found in a study on European methyl chloroform emissions (Reimann et al., 2005), which was based on two measurement sites and three techniques of analysis. The spread of the emission estimates for Western Europe ranged from 0.33 to 3 times the geometric annual means. The larger uncertainties for Europe than for the U.S. possibly originate from traditional differences in industrial activities between the European countries.

The substantial range of uncertainty in the regional emissions indicated by the European estimates for CH_3CCl_3

may have been significantly affected by the generally small remaining emissions detected in these recent observations. In fact a substantially smaller spread in the estimates from the Mace Head observations for 1995-2000 is reported in Reimann et al. (2005). Moreover Simmonds et al. (2006), using continuous observations at Mace Head, report a spread in the annual estimates of Western European emissions of dichloromethane, trichloroethene, and tetrachloroethene, for all of which the current emissions are more than ten times those of CH_3CCl_3, of a factor of three in the worst case. Therefore when pollution events may be easily separated from baseline observations, a factor of three in the inferred regional emission uncertainty is probably to be expected. This factor is likely to increase significantly when the pollution events are small. In addition, for some large areas of the world (e.g., Asia), where estimates are dependent on only a few short-term campaigns, the uncertainties are also likely to be considerably larger.

A first indicative comparison between global and the summed regional emission estimates is attempted (Table 1-6). For CFC-11, only about 54% of the estimated global emissions are found in the summed regional emissions, with the partitioning between CFC-11 and CFC-12 from Russia especially appearing to be suspect. For CFC-12 a good consistency is obtained, with the principal contributions coming from Russia and China. For CFC-113 regional emissions are consistently low, with most studies not being able to identify detectable emissions. For CCl_4 the only detectable current emissions were from China, but the amount was only a relatively small fraction (31%) of the inferred global emissions for a 26-year lifetime. Unfortunately only limited data are available from regions such as Korea and India, which might be responsible for significant emissions. There are indications that India in particular is still a source of CCl_4 emitted from solvent use and from process agent applications. For example, air from India observed at a background site in the Indian Ocean has been found to contain elevated concentrations of CCl_4 (Lobert and Harris, 2002). Furthermore, a study in Mumbai (India) found concentrations of CCl_4 that were noticeably above the background (Srivastava et al., 2006). For CH_3CCl_3, indications of Indian emissions have also been found during campaigns, although their extent could not be quantified (Lobert and Harris, 2002; Srivastava et al., 2006).

In summary, however, the present spatial and temporal coverage, especially in developing regions (e.g., Southeast Asia), is still too inhomogeneous to provide quantifiably useful comparisons of the summed regional emissions with the global emissions derived from trends in observed concentrations.

1.3.2 Global Emissions

This section describes time series of global emissions inferred from the measurements by the ground-based sampling networks (see Section 1.2.1). For the AGAGE measurements, the estimates are based on an inverse procedure using the AGAGE two-dimensional model (12 boxes: 4 in the lower troposphere, 4 in the upper troposphere, and 4 in the stratosphere), with transport parameters tuned to simulate the observed latitudinal gradients for the CFCs (Cunnold et al., 1994; 1997). There are five AGAGE sites with long time series of measurements (e.g., for the CFCs) using electron capture detectors, but there are only two AGAGE sites (Mace Head, Ireland, and Cape Grim, Tasmania) employing mass spectrometer detectors that have provided shorter time series of measurements of gases such as the HCFCs and the HFCs.

For the derivation of global emission rates from the NOAA/ESRL measurements, the estimation procedure starts from their reported tropospheric mean mole fractions. Those tropospheric means are derived from weighting (usually by latitude) high-frequency results at 5 sites, or low-frequency flask measurements at 8-10 remote sites (Montzka et al., 1999). The stratospheric contents are derived from the tropospheric means by ratioing the values to the AGAGE tropospheric means and multiplying by the stratospheric contents calculated in the 12-box model that was tuned to the AGAGE measurements.

Measurements of the halocarbons in the Australian archived air samples have been used to extend the time series back to 1978 for a number of the gases (e.g., Langenfelds et al., 1996; Fraser et al., 1996). In this case, the 12-box model, and other two-dimensional models (Oram et al., 1995; Fraser et al., 1999), have been used to infer global means and global emission rates from measurements at this one location.

For most of these long-lived gases, the largest sources of uncertainty in the emission estimates are the species lifetimes. Smaller uncertainties arise from absolute calibration uncertainties (except for halon-1301, for which the calibration uncertainties are quite large) and from inadequacies in simulating atmospheric transport. The effects of measurement errors are substantially reduced by reporting emissions averaged over three-year periods. The effects of these errors may be seen in Figures 1-20 and 1-21 in differences, if any, between the emission estimates derived from the AGAGE and the NOAA/ESRL measurements. The upper and lower envelopes of the error bars in these two figures for the AGAGE-based estimates, corresponding to the shortest and the longest lifetimes respectively, were calculated using the 12-box model using those lifetimes. Note that the trends in the emission esti-

mates in %/yr are not very sensitive to the lifetime uncertainties. Errors in the representativeness of the measurement sites for deriving global means also adds uncertainty to derived emissions, but during periods when emissions and atmospheric gradients are small (CFCs and CH_3CCl_3 currently), these uncertainties are dramatically reduced.

1.3.2.1 CFCs

Figure 1-20 illustrates the global emission estimates derived from the combination of AGAGE and NOAA/ESRL measurements for three different years for the CFCs. It shows that, as suggested by the latitudinal gradient information in Section 1.2.1.1, emissions of CFC-11 and CFC-12 are continuing but at lower levels than in 2000 (Table 1-7). Moreover, the emissions are about 25% of those (in 1986) before the Montreal Protocol was enacted. On the basis of the regional emission estimates summarized in Section 1.3.1, it would appear that most of the remaining emissions are coming from Asia and Russia. It should be noted that the estimates for CFC-11 emissions in 2003 are very sensitive to its lifetime. Emissions of CFC-113 have now almost ceased (now 3% of 1986 values) and the regional emission estimates, at the few sites where measurements have been made, support the current, low global emissions. Except for CFC-11, the decays of the CFC emissions from 2000 to 2003 derived from global observations are not significantly different from those predicted by the Ab (most likely) scenario from *WMO 2002*. For CFC-11, a significantly faster decline in the emissions was projected in that scenario relative to those given in Figure 1-20. The emissions from the Ab scenario are not shown in Figure 1-20 because those emissions were calculated from the Ab scenario mixing ratios using a one-box model, whereas the emissions in Figure 1-20 were calculated using a 12-box model. The differences between emissions calculated by the 12-box model and the 1-box model are illustrated in Figure 8-1 of Chapter 8. It can therefore be misleading to compare emissions calculated by the two different models. The faster decline in the CFC-11 emissions in 2000-2004 than projected in *WMO 2002* is therefore inferred from the more rapid decline in the observed mixing ratios (see Section 1.2.1.1) versus those projected in the Ab scenario.

An important objective of this report is to estimate the remaining banks, which will be responsible for the emissions of ozone-destroying halocarbons over the next few years. Total emissions up to the present time can be estimated from the ground-based measurements. These are shown in Table 1-7. An assumption about how these emissions were distributed in time prior to the start of observations in 1978 is needed. However, because the
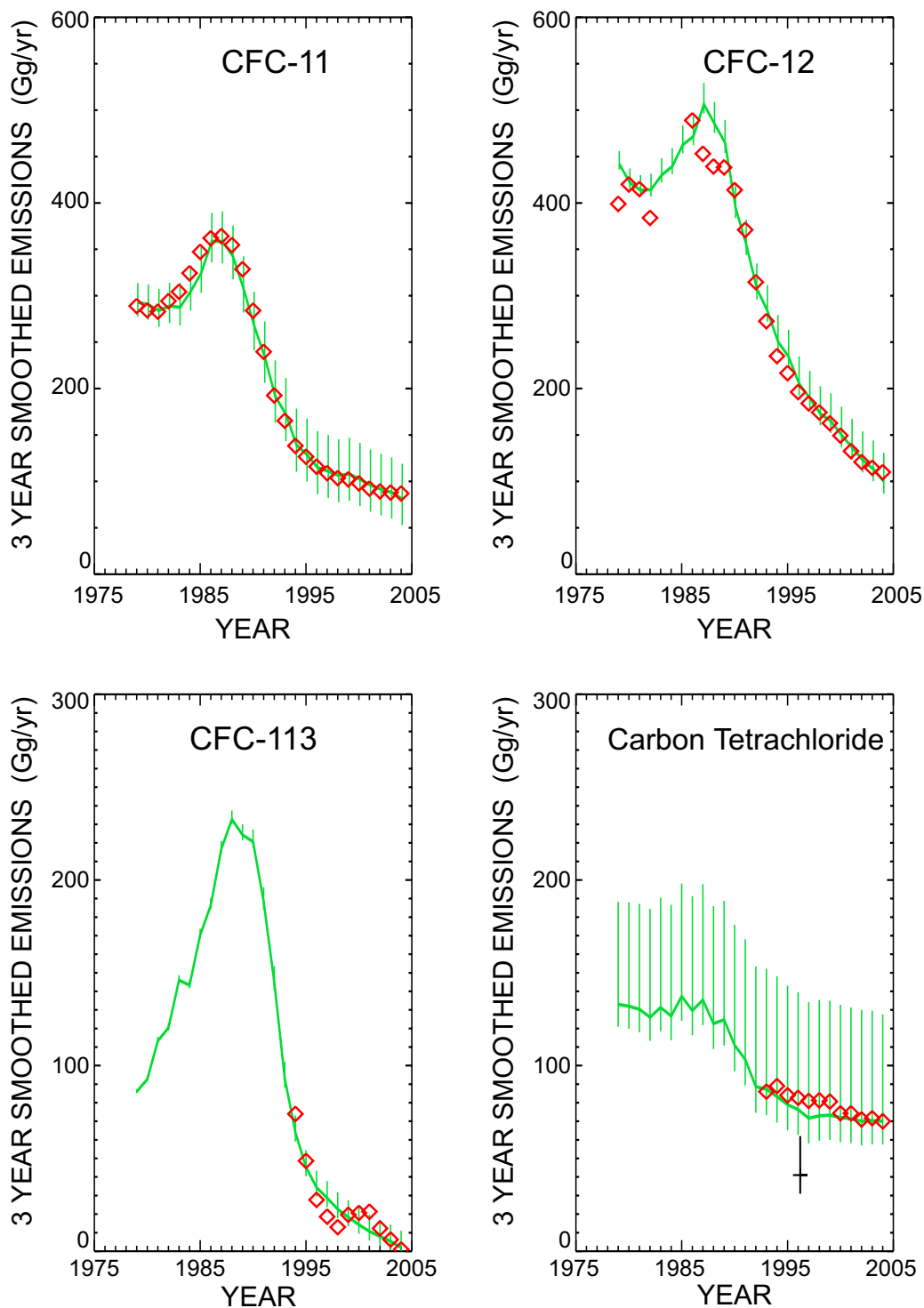
Figure 1-20. Annual global emissions for CFC-11, CFC-12, CFC-113, and carbon tetrachloride, smoothed over three-year intervals, calculated by inverting measurements, using the 12-box model, from the AGAGE (green lines) and NOAA/ESRL (red diamonds) ground-based networks (as in Cunnold et al., 1997). The calculations used equilibrium lifetimes of 45, 100, 85, and 26 years for CFC-11, CFC-12, CFC-113, and carbon tetra-chloride, respectively. The green error bars indicate the uncertainties in the estimates due to the uncertainties in the species lifetimes (see Table 1-7). The TEAP (UNEP, 1998) estimate of the CCl$_4$ emissions in 1996 is indicated in black.
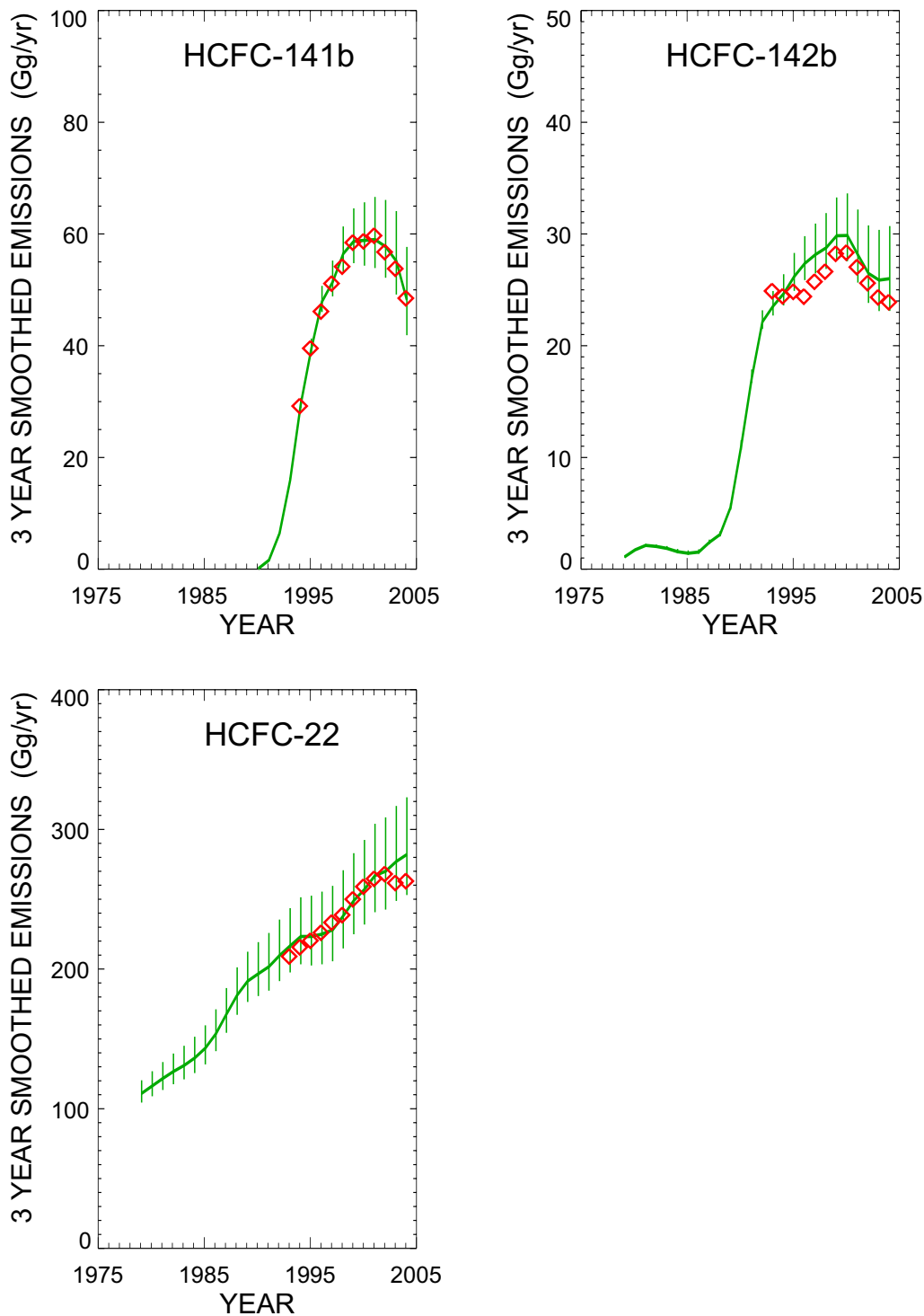
Figure 1-21. Annual global emissions for HCFC-141b, HCFC-142b, and HCFC-22, smoothed over three-year intervals, calculated by inverting the measurements (see Figure 1-2) from the AGAGE (green lines starting from 1995) and NOAA/ESRL (red diamonds) ground-based networks and measurements of the air archived in Australia (green lines before 1995) with a 12-box model (as in, and updated from, O'Doherty et al., 2004). The calculations were based on equilibrium lifetimes of 9.3, 17.9, and 12.0 years for HCFC-141b, HCFC-142b, and HCFC-22, respectively. The green error bars indicate the effects of uncertainties in the life-times listed in Table 1-7.

Table 1-7. Global emission estimates. Emissions are in Gg/yr, smoothed over 3-year intervals and given to 3 significant figures, and are derived using a 12-box model from a combination of AGAGE and NOAA/ESRL measurements. The total emissions are based solely on AGAGE measurements and they include emission estimates for 2004. The lifetimes and their uncertainties are from Sections 1.2.2.1 and 1.2.2.2. Uncertainty ranges, instead of standard deviations, are given because the central values typically do not lie in the centers of the uncertainty ranges, primarily because the estimated emissions are typically proportional to the inverses of the lifetimes.

Species	Release Estimates (Gg/yr)			Rate of Change (2000-2003) (%/yr)	Total Emissions (1920-2004) (Gg)	Lifetime Used (yr)	Lifetime Uncertainty Range (yr)	2003 Emission Estimate Range	Total Emissions Uncertainty Range	
	1986	2000	2003						Gg	%
CFC-11	360	100	88	−4.3	9,450	45	57-35	60-126	8,700-10,460	18
CFC-12	472	150	114	−9.1	14,300	100	113-79	101-144	14,000-15,000	7.5
CFC-113	186	18	6	−33.3	3,170	85	100-66	1-15	3,080-3,340	8.4
CCl_4	130	73	71	−0.9	6,620	26	30-16	58-131	6,060-8,590	34
HCFC-22	154	258	270	+1.5	6,040	12	14.0-10.0	242-310	5,530-6,760	20
HCFC-141b	0	58.8	54.4	−2.6	589	9.3	11.2-7.4	48.4-63.5	548-651	17
HCFC-142b	1.5	29.1	25.1	−4.9	407	17.9	22.2-13.6	22.3-29.6	380-450	17
HFC-134a	0	76	104	+10.4	721	14	16.4-11.6	99-111	696-757	8.4

largest emissions occurred after 1979, and they have been in the atmosphere for a shorter time, this introduces uncertainties that are small compared with the effects of atmospheric lifetime uncertainties that are shown in Table 1-7. The remaining banks may be estimated by subtracting the accumulated production from the numbers in Table 1-7. Chapter 8 provides both those numbers and estimates of the banks. The effects of using the 12-box model used here to estimate the emissions that have already occurred may be compared against the one-box model results given in Chapter 8.

Table 1-7 also provides estimates of the total emissions integrated from the beginning of production to 2004. It may be noted that these total emission estimates and their one sigma uncertainty limits, when combined with total production numbers that are known fairly accurately (e.g., from UNEP 2005), can be used to constrain the expectations of future emissions (e.g., the current global banks of unreleased gases).

1.3.2.2 HCFCs

Figure 1-21 shows HCFC emission estimates derived from applying the 12-box model to the AGAGE and NOAA/ESRL ground-based network measurements. The two sets of estimates differ because of absolute calibration differences (e.g., 4-5% for HCFC-142b, less for HCFC-141b and HCFC-22) and some other minor differences in the most recent measurements. The emissions of

HCFC-141b (54.4 Gg/yr in 2003) and HCFC-142b (25.1 Gg/yr in 2003) are calculated to have decreased from 2000 to 2004 by approximately 15% (10 and 4 Gg/yr for HCFC-141b and HCFC-142b, respectively) and this is seen by both networks. These emission estimates correspond to a recent decrease in the rates of growth in the atmospheric mole fractions compared with the growth rates reported in *WMO 2002* (Figure 1-2, Montzka and Fraser et al., 2003). HCFC-22 emissions have been increasing fairly slowly or not at all from 2000 to 2004 (e.g., at less than 2%/yr for AGAGE and less than 1%/yr for NOAA/ESRL). This is down from increases of approximately 3%/yr from 1994 to 2000. Note that the ranges of uncertainty, in percent, on the 2003 emissions of the HCFCs and HFC-134a (Table 1-7) are less than for those other gases in Table 1-7 that have much longer emission histories.

The recent decreases in the emissions of HCFC-141b and HCFC-142b, and the fact that the measured mole fractions in 2000-2004 are less than projected (see Section 1.2.1.2) in the best-guess scenario in *WMO 2002*, may mean that emissions are occurring more slowly than expected and the future emissions from the banks will be larger and occur over a longer time than originally anticipated.

1.3.2.3 HALONS

Difficulties in reconciling the halon measurements with emission estimates derived from production and the

remaining banks of halon-containing fire extinguishing equipment (e.g., the estimates shown on page 75 of IPCC/TEAP 2005) were previously pointed out by Fraser et al. (1999). Currently the remaining very small world-wide production of these halons is insignificant in relation to the size of the global halon bank. For halon-1301, the estimates are from the United Nations Environment Programme/Halons Technical Options Committee (UNEP, 2003) emission scenario. Those emissions have been run through the 12-box model to yield the gold curve in the halon-1301 panel of Figure 1-4 (which is similar to that in Figure 1-17 of *WMO 2002*). A smaller emission rate for halon-1301 has recently been suggested by the work of Verdonik and Robin (2004).

For halon-1211, there is less spread in the measurements and the mole fractions estimated from the emission banks do not differ as much as they do for halon-1301. The emission scenario used is that of TEAP (an update to the UNEP (1999) model, see *WMO 2002*, Section 1.6.1.5), which is similar to the UNEP (1999) model. It should be noted that this scenario contains lower emissions than those shown in IPCC/TEAP (2005, page 75), which were from UNEP (2003). An error in that model was recently discovered in accounting for the production by Article 5(1) countries in 1987-1993. The *WMO 2002* Ab scenario also provides a reasonable fit to the observations except that, although the observations indicate a slowing of the increases, there is little evidence that halon-1211 stopped increasing in the 2000-2004 period as the Ab model predicted.

1.3.2.4 CARBON TETRACHLORIDE

Table 1-7 and Figure 1-20 show the estimated emissions of carbon tetrachloride, for a lifetime of 26 years, determined from the measurements by the ground-based sampling networks combined with AGAGE 12-box model calculations. The emission uncertainty error bars are based on the combined uncertainties in the contributions of stratospheric, oceanic, and soil losses. A lifetime of 20 years increases the calculated emissions by approximately 26 Gg/yr, from 71 Gg/yr in 2003 to 97 Gg/yr. Simmonds et al. (1988 and 1998) argued that most of the CCl_4 emissions in the past were fugitive emissions from the carbon tetrachloride used in the manufacture of CFCs. For a lifetime of 20 years, not only would the CCl_4 emissions have to have been equivalent to approximately 16% of CFC production prior to 1994, versus approximately 9% based on International Trade Commission figures on CCl_4 production in the U.S. in 1979-1985 (Simmonds et al., 1988), but the proportion would have had to have increased to almost 60% after 1995 as a result of the substantial reduc-

tion in CFC manufacture (cf. *WMO 2002*, Montzka and Fraser et al., 2003, Figure 1-15). TEAP (UNEP, 1998) indicated that approximately 23 Gg/yr of carbon tetrachloride emissions could arise from uses other than in CFC manufacture; that report also estimated total emissions from industry data of 31 to 62 Gg in 1996, with a most likely value of 41 Gg (see Figure 1-20). Therefore it is difficult to reconcile the atmospheric observations with an atmospheric lifetime for CCl_4 of 20 years.

In addition, recent high-frequency atmospheric measurements (see Section 1.3.1) at a number of global locations have only detected approximately 22 Gg/yr in 2001, which came almost entirely from Eastern Asia. Therefore, even though emissions from India are unknown, it is difficult to account for the approximately 97 Gg/yr in 2003 (99 Gg/yr in 2001) required for consistency with a 20-year lifetime (or even the 71 Gg/yr in 2003 required for a lifetime of 26 years). Simmonds et al. (1998) showed that the observed latitudinal gradient from the AGAGE observations was reasonably well simulated by a lifetime of 42 years. Updated calculations suggest a gradient-based lifetime of approximately 35 years, unless a substantial fraction of the emissions are coming from the Southern Hemisphere.

Overall the budget of carbon tetrachloride remains poorly understood. Because the currently observed regional emissions, the TEAP emission estimate, and the measured interhemispheric gradient seem inconsistent with an overall lifetime of 20 years and because the uncertainty ranges for both the ocean and soil sinks allow for the possibility of only very small sinks, no change from the lifetime of 26 years given in *WMO 2002* is recommended at this time.

1.3.2.5 METHYL CHLOROFORM

Global production and sales of methyl chloroform from 1970 to 1995 were tabulated in a database from annually provided figures from the producing companies. According to McCulloch and Midgley (2001), the uncertainties were 2.1% on production and 4.2% on emissions. These uncertainties are smaller than for most other ozone-destroying gases because of the smaller number of companies that produced methyl chloroform and because of the generally short time (less than a year) between production and emission into the atmosphere. After 1995, emissions were derived from figures on production and consumption reported to the United Nations Environment Programme (UNEP, 2002b). Global emissions have been calculated to be 19.7 ± 2.3 Gg in 2000 and 12.9 Gg in 2002. This may be compared against maximum emissions of 718 Gg, which occurred in 1990 (McCulloch and Midgley, 2001).

McCulloch and Midgley also pointed out that there are discrepancies in the databases for 1994-1996. In particular, there is a production versus consumption discrepancy in the UNEP figures in 1995-1996. It was noted in Section 1.3.1 that regional emission estimates suggested an anomalous large disagreement for methyl chloroform emissions versus global emissions in 1996. Furthermore Prinn et al. (2005) suggested that, based on summing the recent regional emission estimates, the global emissions in the past ten years might be somewhat low. They pointed out that the regional emissions could be approximately accommodated (within the uncertainties of the measurements) by placing 5% of the global emissions in a slower release category, with emissions being divided equally over a 10-year interval. This would not have affected the production numbers. The slower releases would have increased the emissions in 2002 by 3.6 Gg to 16.5 Gg and from 93.5 Gg to 112.3 Gg in 1996. The revised global totals would not, however, account for the European emissions estimate of over 20 Gg in 2000 by Krol et al. (2003), which Prinn et al. (2005) did not include because of the much lower estimates from the European ground stations (see also Section 1.3.1). This discrepancy, and hence the global emissions since 2000, are not understood. These ongoing emissions are not, however, significant for stratospheric ozone depletion.

Historically, accurate methyl chloroform emissions data have been useful in the estimation of global OH abundance. Prinn et al. (2005) used the emission estimates just described to calculate the annual atmospheric loss rates for methyl chloroform that produce the best fit to the AGAGE observations. This resulted in a time series of annual globally averaged tropospheric OH concentrations from 1979 to 2003 and particularly low OH values (by 10%) in 1997/1998. Monte Carlo estimates of the uncertainties in the recent emissions of methyl chloroform produce uncertainties of only a few percent in these OH estimates. Wennberg et al. (2004) pointed out that the methyl chloroform that had entered the ocean could have been trapped in the polar region and, because of the very steep decline in the atmospheric concentrations in recent years, much of it could now be returning to the atmosphere. Prinn et al. (2005) estimated that these ocean fluxes could make annual contributions to the methyl chloroform budget that varied between 4 and 7 Gg/yr between 1995 and 2003. This increased the OH estimates by approximately 5% after 2000.

In order to derive methyl chloroform emissions using the ground-based networks' measurements, independent estimates of OH are required. Calculations of OH in chemical models yield a methyl chloroform lifetime approximately 10% less (Spivakovsky et al., 2000) than

the Prinn et al. value of 4.9 years, and other models produce larger differences (*WMO 2002*, Montzka and Fraser et al., 2003). Therefore because of the relatively small uncertainties in the emissions given by McCulloch and Midgley (2001), it is not generally very productive to estimate emissions from the measurements.

1.4 OTHER TRACE GASES

1.4.1 Carbon Dioxide (CO_2)

Carbon dioxide is the primary agent of anthropogenic climate change, accounting for 60% of the increase in direct radiative forcing since preindustrial times (IPCC, 2001). Climate change can affect the ozone budget, for example due to temperature changes in the polar vortices, and due to changes in atmospheric transport. Such changes may delay ozone recovery. In 2004, global annual average (surface) CO_2 was 377 ± 0.2 parts per million by volume (ppmv), as determined through the NOAA/ESRL global network.

The atmospheric growth rate of CO_2 has averaged about 0.5% per year over the nearly 50 years of in situ measurements (Keeling and Whorf, 2005). The observed atmospheric growth rate is explained by about one-half of CO_2 emissions from fossil fuel combustion and land use change being absorbed at the surface of the Earth. CO_2 can be taken up by either the ocean or terrestrial biosphere; there is considerable year-to-year variability in the uptake that, at the global scale, is closely related to the impact of El Niño on both ocean and land. Two tracers complementary to CO_2 are molecular oxygen (O_2) and $^{13}CO_2$. Both tracers allow for partitioning of total uptake into terrestrial and oceanic components, and both indicate that the majority of interannual variability is driven by terrestrial processes (Battle et al., 2000). Over the long term (> 500 years), however, it is likely that the oceans, as the largest carbon reservoir, will exert the strongest control on atmospheric CO_2.

Future levels of atmospheric CO_2 will be strongly determined by future fossil fuel emissions. Additionally, there are no guarantees that the current uptake rate of 50% will be maintained, because both the terrestrial and oceanic carbon cycles may change as a result of changing climate. Furthermore, the mechanisms by which carbon is absorbed at the surface, especially by the terrestrial biosphere, are not fully understood. Simulations in which simple models of the carbon cycle are coupled to climate models have shown positive feedbacks between temperature and CO_2 emissions in the 21st century, which can reduce or even eliminate net CO_2 uptake of anthropogenic emissions. In

one study (Cox et al., 2000), coupling resulted in an additional 1.5 K global temperature increase by 2100, compared with the uncoupled case. Although the magnitude of the feedbacks is uncertain, the direction is likely to be positive, and it is clear that the carbon cycle is a first-order uncertainty in prediction of future climate.

1.4.2 Methane (CH_4), Including Isotopic Data

Methane is important for its impact on climate both through its radiative properties and chemically as a major source of water vapor to the stratosphere and as a sink for Cl. In the troposphere, its oxidation products are controlling the chemistry. The global average CH_4 mixing ratio for 2004 at the surface was 1777 ± 0.6 ppb, determined from marine boundary layer sites in the NOAA/ESRL and other surface monitoring networks (GLOBALVIEW-CH_4, 2005). This compares with glacial values of about 400 ppb (Spahni et al., 2005) and 700 ppb in 1800 AD (MacFarling-Meure, 2004). The precise reasons for inter-glacial/glacial CH_4 variability as well as variability during the Holocene (Flückiger et al., 2002; Ruddiman, 2003) are not well known but may relate to large-scale moisture and temperature changes affecting wetland emissions. The rise to present-day values has resulted from increases in emissions related to fossil fuel extraction, biomass combustion, and agriculture, and current atmospheric mixing ratios are unprecedented in at least the last 650,000 years (Spahni et al., 2005). The global growth rate of methane has varied from about 14 ppb/yr in 1985 to near zero in 2000 but with significant interannual variability. Since 2000, the growth rate has averaged to 0 ± 4 ppb/yr. The decline in growth rate has been explained as an approach to steady state, with a constant total of global sources and constant sink strength (Dlugokencky et al.,1998). However, despite evidence for only small variations in the global total, individual sources like biomass burning (van der Werf et al., 2004) and emissions from the former Soviet Union (Dlugokencky et al., 2003) have seen substantial changes during this period (Simpson et al., 2002). Changes in the dominant CH_4 sink, the hydroxyl radical (OH), also affect atmospheric interannual variability and trends (Bousquet et al., 2005; Krol et al., 1998; Prinn et al., 2001).

The source budget of atmospheric methane is very diverse, with no dominant source (IPCC, 2001), making determination of the causes of atmospheric changes difficult. Major sources include boreal and tropical wetlands, leakage during coal and natural gas extraction, enteric fermentation, fires, and rice agriculture. Recent laboratory measurements (Keppler et al., 2004) have also shown living plants to be a source, but their global impact is currently unknown. "Bottom-up" inventories rely on spatial and temporal extrapolation of small-scale field measurements, leading to significant uncertainties in the total. On the other hand, "top-down" approaches inverting atmospheric data can accurately determine continental-scale totals, but cannot independently identify the different sources in a given region. Prediction of future atmospheric levels of CH_4 would require, at a minimum, a much better understanding of how different sources and sink variations have changed the atmospheric burden.

Measurements of the carbon (^{13}C) (Lowe et al., 1994; Quay et al., 1999; Miller et al., 2002) and hydrogen (^{2}H or "D") (Quay et al., 1999; Rice et al., 2001) isotopic ratio of atmospheric methane ($\delta^{13}C$ or δD) can be used to help quantify the contribution of different sources to the atmospheric growth rate. For $\delta^{13}C$, sources can be divided into microbial, biomass burning, and fossil fuel sources, which have distinct isotopic signatures. Isotopic and mixing ratio mass balances can be used to constrain the source distribution of these broad categories. One consistent result of carbon isotopic data is to infer a significantly stronger global biomass burning source than bottom-up estimates both in the modern (Quay et al., 1999; Miller et al., 2002) and paleo atmospheres, where recent results have shown much larger than expected combustion sources between 0 and 1200 AD (Ferretti et al., 2005), possibly due to human activity. Though there are currently only a few δD measurements, they, along with $^{14}CH_4$ measurements (which help constrain the fossil-fuel related source), will likely allow for better determination of atmospheric growth rate variations. New measurements of CH_4 from space (Frankenberg et al., 2005), with unprecedented spatial coverage, also afford an opportunity to improve our understanding of the CH_4 source distribution.

The broad range of CH_4 sources (roughly half anthropogenic, half non-anthropogenic) and the fact the source mixture has likely changed over the last century, imply great difficulty in prediction of future mixing ratios. Predictions range from 1575 to 3730 ppb, depending on emission scenario (IPCC, 2001). However, these predictions do not include the possibility of large source changes like destabilization of vast quantities of CH_4 hydrates in Arctic permafrost, which adds further uncertainty to predicted methane abundances at the end of the 21st century.

1.4.3 Nitrous Oxide (N_2O)

Nitrous oxide is the major source of nitrogen oxides (NO_x) in the stratosphere, with the latter contributing significantly to ozone depletion. In addition,

N_2O, which has a lifetime of about 120 years, is an important greenhouse gas targeted by the Kyoto Protocol. Its actual global concentration is close to 320 ppb. This constituent is emitted at the Earth surface by a large number of sources; major natural contributions are from the oceans and tropical forests, while most important anthropogenic emissions are from cultivated soils, cattle, and biomass burning (IPCC, 2001).

Several studies have dealt with the historical evolution of the N_2O atmospheric concentration. Nitrous oxide levels started to decrease in the early Holocene and reached minimum levels (less than 260 ppb) around 8,000 B.C., before exhibiting a slow increase to the preindustrial value of about 265 ppb. MacFarling-Meure (2004) has produced a 2,000-year record of atmospheric N_2O variations from measurements on air in ice from Law Dome, Antarctica. Notable features in the N_2O record are a preindustrial level of 260-275 ppb, a slowing of growth in the 1940s and 1950s, a 5 ppb lowering during the Little Ice Age (LIA: 1300-1850 A.D.), and a 10 ppb increase between 670 and 810 A.D. The origin of this latter increase is unknown and was not reflected in corresponding CH_4 or CO_2 changes.

N_2O isotopic composition studies of air from Greenland ice and Antarctic (South Pole) firn (1785-1990) show a decline in $\delta^{15}N$ (1.9 per mil) since preindustrial times, consistent with a 30% increase in total N_2O emissions that are primarily related to agricultural activities (Sowers et al., 2002). A similar decrease in $\delta^{15}N$ (1.8 per mil) since preindustrial times has been reported from analyses of Antarctic (Maud Dronning Land and Dome C) firn air (Röckmann et al., 2003). The corresponding latter data have been interpreted as due to an increasing soil source of N_2O with a time-dependent isotopic signature. A larger trend in $\delta^{15}N$ (2.8 per mil) of N_2O since preindustrial times has been reported in firn and ice air from Greenland and Antarctica (Berkner Island). The data are consistent with an increase in the use of fertilizers in agriculture (Bernard et al., 2006).

Since the 2002 WMO Assessment, measurements performed by the AGAGE and NOAA/ESRL networks have confirmed the steady increase of the N_2O atmospheric concentration observed over the last two decades: globally averaged surface mixing ratio amounted to 318-319 ppb in January 2005 (updated from Prinn et al., 2000; Conway et al., 2004). On the basis of flask samples collected regularly at 11 worldwide sites from 1981 to 1996 (Khalil et al., 2002), concentrations are higher on average by 0.7 ± 0.04 ppb in the Northern Hemisphere, and differences of concentrations over land and oceans indicate large land-based emissions. Annual rates of change of the N_2O concentrations have been monotonic but quite vari-

able, with a mean annual increase of 0.69 ± 0.02 ppb/yr (0.22%/yr) for 1985-1996 (Khalil et al., 2002) and 0.74 ± 0.02 ppb/yr (0.24%/yr) for 1986-2005 (updated from Prinn et al., 2000).

Remote Fourier transform infrared (FTIR) measurements performed at the NDACC site of Jungfraujoch have also shown a regular buildup of the N_2O atmospheric burden, with a linear fit to the monthly mean total column dataset indicating an annual increase of 1.06×10^{16} molec/cm^2, which corresponds to 0.26%/yr in 2003-2004 (Zander et al., 2005).

1.4.4 Hydrofluorocarbons (HFCs)

HFCs have rapidly replaced CFCs in refrigeration, foam blowing, and aerosol applications. For example, mobile air conditioning accounted for 60% of CFC-12 in 1990 and by 1994 had been replaced by HFC-134a in all but a few countries. HFC-134a (CH_2FCF_3) and HFC-23 (CHF_3) are the two most abundant hydrofluorocarbons in the atmosphere, and they are continuing to grow rapidly (Prinn et al., 2000; Sturrock et al., 2001; O'Doherty et al., 2004). Recently Culbertson et al. (2004) have also reported measurements of these two principal HFCs from the analyses of flask samples collected at Cape Meares, Oregon; Point Barrow, Alaska; and Palmer Station, Antarctica. Updated measurements of HFC-125 (CHF_2CF_3) and HFC-152a (CH_3CHF_2), which were first reported in the previous Assessment (WMO, 2003), also exist.

1.4.4.1 HFC-134a

HFC-134a has rapidly mostly replaced CFC-12 in several refrigeration and air-conditioning applications. As a consequence of increased emissions, the annual global mean concentration in mid-2004 was about 30 ppt, increasing at an annual average rate of approximately 3.9 ppt/yr (2000-2004) (O'Doherty et al., 2004; updates to Montzka et al., 1996) (Figure 1-22 (a)). Annual emissions have been increasing at approximately 10 Gg/yr from 2000 to 2004 (Figure 1-22 (b)). Because so little of the HFC-134a has yet been destroyed in the atmosphere, the error bars on the annual emission estimates in 2003 are just ±6 Gg/yr.

1.4.4.2 HFC-23

HFC-23 is primarily emitted as a byproduct of HCFC-22 production, with smaller amounts released from semiconductor etching and refrigeration and fire extinguisher losses (Oram et al., 1998). HFC-23 has been measured since 1978 in flask samples from Cape Grim (Oram
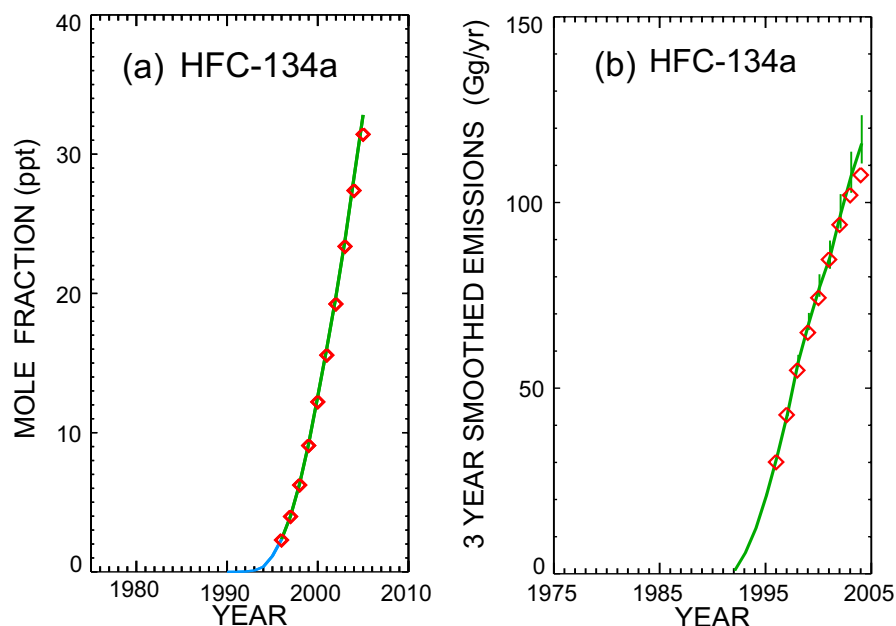
Figure 1-22. (a) Annual global mean mole fractions for HFC-134a derived from the AGAGE (green line) and NOAA/ESRL (red diamonds) networks of ground-based sites (O'Doherty et al., 2004; Montzka et al., 1996). The early measurements (before 1995, in blue) are based on analysis of the air archived in Australia (Oram et al., 1996). (b) Annual global emissions of HFC-134a smoothed over three-year intervals, calculated by inverting the measurements in (a) using the 12-box model. A lifetime of 14.0 years was used. The green error bars, which are very small, indicate the effect of a ±17% uncertainty in the lifetime.

et al., 1998) and, until 1997, approximately 10% larger values from Oregon (Culbertson et al., 2004). The mixing ratio at Cape Grim in 2004 was approximately 18 ppt and the average growth rate in 2001-2004 was approximately 0.7 ppt/yr (Figure 1-23). This rate of growth is significantly less than that (approximately 0.9 ppt/yr) in 1994-2001. The IPCC/TEAP report (Velders and Madronich et al., 2005, Figure 2.4) shows estimated emissions, on the basis of the Cape Grim measurements, of 13 Gg/yr in 2001 versus 6.4 Gg/yr in 1990.

1.4.4.3 HFC-143a, HFC-125, AND HFC-152a

Measurements of HFC-143a (CH_3CF_3) have been reported by Culbertson et al. (2004) for flask samples collected at Cape Meares, Oregon; Point Barrow, Alaska; and Palmer Station, Antarctica. Tropospheric mixing ratios in the Oregon samples increased from about 0.2 ppt in 1978 to about 2 ppt in 1997. Average annual concentrations during 1997 at Alaska and Antarctica were 1.7 and 1.3 ppt, respectively.

HFC-125 is mainly used in refrigeration, while the primary uses of HFC-152a are in foam-blowing and aerosol propellants. Measurements from Cape Grim (updated from Sturrock et al., 2001) and at Mace Head are shown in Figure 1-23. In 2000-2004, mixing ratios have been increasing approximately exponentially at 23%/yr (HFC-125) and 17%/yr (HFC-152a). In mid-2004, globally averaged values derived from these measurements were 3.1 ppt for both gases.

1.4.5 Perfluorocarbons, Sulfur Hexafluoride (SF_6), and SF_5CF_3

Perfluorocarbons (PFCs) and SF_6 are very powerful and long-lived greenhouse gases whose emissions contribute to national inventories of greenhouse gas emissions that are regulated under the Kyoto Protocol. Trifluoromethylsulfurpentafloride (SF_5CF_3) is a similar chemical species whose source is very uncertain and that is not included in the Kyoto Protocol.

1.4.5.1 CF_4 AND CF_3CF_3

Aoki and Makide (2004) have measured CF_4 (FC-14) levels of 80-81 ppt in Tokyo during August 2003. Long-term trend data (1978-1997) have been reported for CF_4 and CF_3CF_3 (FC-116) in the Cape Meares, Oregon, air archive, and in flask data from Point Barrow, Alaska, and Palmer Station, Antarctica (Khalil et al., 2003). The observed mixing ratios of CF_4 and CF_3CF_3 in 1997 at Cape Meares were 74 ppt and 2.9 ppt, respectively. These mixing ratios are consistent with the values given in *WMO 2002* (Montzka and Fraser et al., 2003). CF_4 increases have been determined from infrared high spectral resolution solar occultation Fourier transform spectrometer measurements between 3 and 50 hPa (~20 to 40 km altitude) and latitudes from 50°N to 50°S during 1985, 1992, 1993, 1994, and 2004. These space-based measurements show that the slowdown in the rate of CF_4 accumulation previously reported from surface measurements through
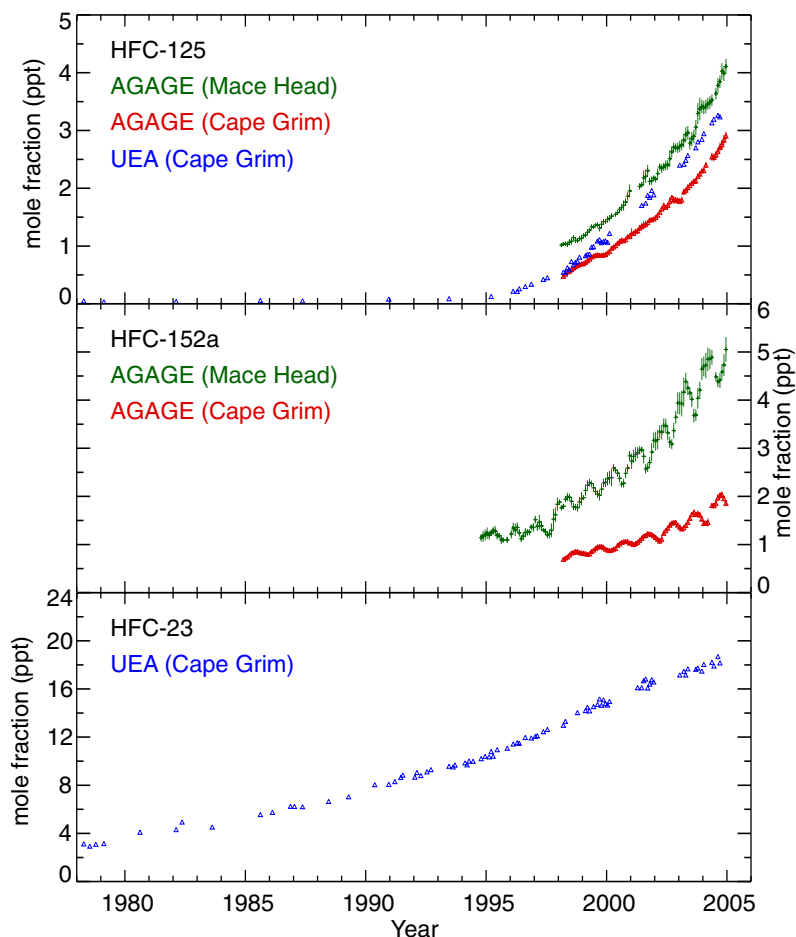
Figure 1-23. Monthly means (ppt) and standard deviations of the AGAGE measurements of HFC-125, HFC-152a, and HFC-23 at Mace Head, Ireland (green) and Cape Grim, Tasmania (red). Individual measurements of the Australian air archive for Cape Grim analyzed by Oram (1999) are shown in blue.

1997 has propagated to the stratosphere and is continuing (Rinsland et al., 2006).

Using historical estimated emissions rates of CF_4 for the aluminum industry and the semiconductor industry, Khalil et al. (2003) estimated that the aluminum industry and the semiconductor industry contributed 33 ppt and 1 ppt, respectively, to the 74 ppt observed in 1997. CF_3CF_3 is also emitted in aluminum processing. By assuming that the CF_3CF_3 and CF_4 emissions in 1997 associated with the aluminum industry maintained a constant ratio through the years, Khalil et al. concluded that the aluminum industry emissions are responsible for 2.4 ppt of the observed CF_3CF_3 concentration, with the balance assumed to be from the semiconductor industry.

Harnisch and Höhne (2002) have compared the estimates of global emissions of CF_4 and CF_3CF_3 from atmospheric observations (top-down) with a summation of emissions in national inventories (bottom-up). For CF_4, atmospheric measurements indicate global emissions of 16 Gg/yr (late 1980s) decreasing to 12 Gg/yr (late 1990s), compared with a decrease from 11 to 8 Gg/yr over the same period based on a summation of national inventories. Khalil et al. (2003) estimated a decrease from 16 to 10

Gg/yr, respectively, based on global aluminum production (using an industry-based, varying emission factor) together with a small (of order 10%) contribution from the semiconductor industry. Atmospheric measurements of CF_3CF_3 indicating constant global emissions of about 2 Gg/yr (late 1980s to late 1990s) compare well with 1.4-2.2 Gg/yr over the same period based on a summation of national inventories. An estimate of the annual emissions of CF_3CF_3 from Japan (0.19 Gg/yr, 2003) has been made, based on interspecies ratios (with HCFC-22) observed in aircraft profiles near Tokyo (Yokouchi et al., 2005).

1.4.5.2 $CF_3CF_2CF_3$ AND c-C_4F_8

Long-term trend data (1978-1997) have been reported for perfluoropropane ($CF_3CF_2CF_3$) in the Cape Meares, Oregon, air archive, and in flask data from Point Barrow, Alaska, and Palmer Station, Antarctica (Khalil et al., 2003; Culbertson et al., 2004). $CF_3CF_2CF_3$ mixing ratios at Cape Meares were <0.1 ppt in 1978, growing to >0.2 ppt in 1997, corresponding to global emissions of 0.04 Gg/yr in 1977-1982, rising to 0.48 Gg/yr in 1992-1997. An estimate of the annual emissions of $CF_3CF_2CF_3$

and perfluorocyclobutane (c-C_4F_8) from Japan (0.06 and 0.02 Gg/yr, respectively, 2003) has been made, based on interspecies ratios (with HCFC-22) observed in aircraft profiles near Tokyo (Yokouchi et al., 2005).

1.4.5.3 SF_6

Sulfur hexafluoride (SF_6), which is mostly used as an insulating fluid in transformers, has been measured by a number of laboratories at Cape Grim, Tasmania, since 1978 via a combination of in situ and flask measurements, including measurements on the Cape Grim air archive (Fraser et al., 2004) (Figure 1-24). The long-term growth rate of SF_6 as observed at Cape Grim has increased from 0.1 ppt/yr in the late 1970s to 0.24 ppt/yr in the mid-1990s. Since then the growth rate has remained relatively constant at 0.23 ± 0.02 ppt/yr, indicating relatively constant global emissions ($\pm10\%$) since 1995. The 2003 annual mean SF_6 concentration at Cape Grim was 5.0 ± 0.1 ppt (Fraser et al., 2004). The global average SF_6 mixing ratio in 2003 was 5.2 ppt, growing at 0.2 ppt/yr (Thompson et al., 2004).

The burden of SF_6 above the Jungfraujoch (Switzerland) has continued to accumulate during the past few years by 3.4×10^{12} molec cm^2/yr, which corresponds to an increase of 4.1%/yr in 2003-2004 (Zander et al., 2005). Corroboration of the regular accumulation of atmospheric SF_6 at other sites, namely, Kitt Peak (32°N) and Ny Ålesund (79°N), has been reported by Krieg et al. (2005). These authors have also shown that the temporal extrapolation of the best fit to the two decades-long Jungfraujoch database of SF_6 results in atmospheric SF_6 loadings in 2050 and 2100 that are significantly lower than those predicted by the most realistic emission scenarios (see Figure 1-21 in *WMO 2002*, Montzka and Fraser et al., 2003). Satellite observations of SF_6 show a globally-averaged upper tropospheric mixing ratio of 4.3 ppt and stratospheric value of 3.5 ppt in September 2002 (Burgess et al., 2004).

Harnisch and Höhne (2002) have compared the estimates of global emissions of SF_6 from atmospheric observations (top-down) with a summation of emissions in national inventories (bottom-up). The bottom-up estimates of emissions, which are critically dependent on the accuracy of assumed leak rates from electrical transformers, are $60 \pm 10\%$ of the top-down estimates. An estimate of the annual emissions of SF_6 from Japan (0.15 Gg/yr, 2003) has been made, based on interspecies ratios (with HCFC-22) observed in aircraft profiles near Tokyo, which compare favorably to the national emissions for 2001 (0.20 Gg/yr) (Yokouchi et al., 2005).

1.4.5.4 SF_5CF_3

Trifluoromethylsulfurpentafluoride (SF_5CF_3) has an exceptionally large radiative forcing efficiency and was reported to have an atmospheric mixing ratio of about 0.12 ppt in 1999 (Sturges et al., 2000). A potential source of this gas has recently been identified (Huang et al., 2005). Under spark discharge conditions, SF_6 does not react with PFCs, but does so with HFC-23 (CHF_3) and HFC-32 (CH_2F_2), which may be emitted from the surface of fluoropolymers in high-voltage equipment. The only other potential source that has been identified is a byproduct during the manufacture of certain fluorochemicals (Santoro, 2000).
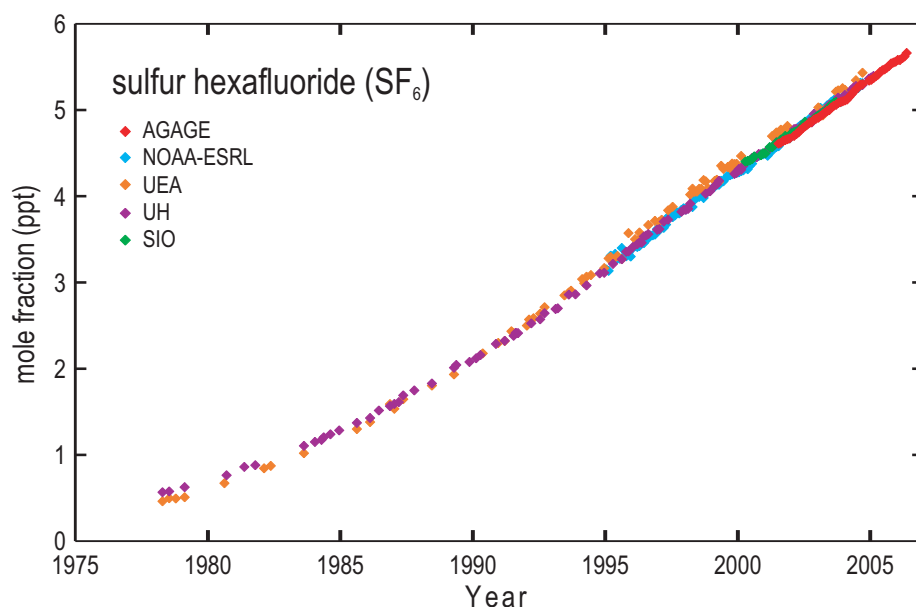

Figure 1-24. Ground-based measurements of sulfur hexafluoride at Cape Grim, Tasmania. The data are updates of the following time series: continuous AGAGE measurements (red; Fraser et al., 2004); NOAA/ESRL flask measurements (blue; Thompson et al., 2004); individual measurements of the Cape Grim air archive analyzed by Oram (orange; UEA, 1999) and by Maiss and Brenninkmeijer (purple, University of Heidelberg-UH, 1998); and Scripps Institution of Oceanography flask measurements by Vollmer and Weiss (green; SIO, 2002).

REFERENCES

Anderson, J., and J.M. Russell III, Long term changes of HCl and HF as observed by HALOE, in *Ozone Vol. I, Proceedings of the XX Quadrennial Ozone Symposium*, 1-8 June 2004, Kos, Greece, edited by C.S. Zerefos, 223-224, Int. Ozone Comm., Athens, Greece, 2004.

Anderson, J., J.M. Russell, S. Solomon, and L.E. Deaver, Halogen occultation experiment confirmation of stratospheric chlorine decreases in accordance with the Montreal protocol, *J. Geophys. Res., 105* (D4), 4483-4490, 2000.

Andreae, M.O., and P. Merlet, Emission of trace gases and aerosols from biomass burning, *Global Biogeochem. Cycles, 15* (4), 955-966, 2001.

Andrews, A.E., K.A. Boering, B.C. Daube, S.C. Wofsy, M. Loewenstein, H. Jost, J.R. Podolske, C.R. Webster, R.L. Herman, D.C. Scott, G.J. Flesch, E.J. Moyer, J.W. Elkins, G.S. Dutton, D.F. Hurst, F.L. Moore, E.A. Ray, P.A. Romashkin, and S.E. Strahan, Mean ages of stratospheric air derived from in situ observations of CO_2, CH_4, and N_2O, *J. Geophys. Res., 106* (D23), 32295-32314, 2001.

Aoki, N., and Y. Makide, Precise determination of the atmospheric CF_4 concentration by using natural Kr in the atmosphere as an internal reference in the pre-concentration/GC/MS analysis, *Chem. Lett., 33* (12), 1634-1635, 2004.

Aydin, M., E.S. Saltzman, W.J. De Bruyn, S.A. Montzka, J.H. Butler, and M. Battle, Atmospheric variability of methyl chloride during the last 300 years from an Antarctic ice core and firn air, *Geophys. Res. Lett., 31*, L02109, doi: 10.1029/2003GL018750, 2004.

Bacmeister, J.T., V. Kuell, D. Offermann, M. Riese, and J.W. Elkins, Intercomparison of satellite and aircraft observations of ozone, CFC-11, and NO_y using trajectory mapping, *J. Geophys. Res., 104* (D13), 16379-16390, 1999.

Barnes, D.H., S.C. Wofsy, B.P. Fehlau, E.W. Gottlieb, J.W. Elkins, G.S. Dutton, and S.A. Montzka, Urban/industrial pollution for the New York City - Washington, DC, corridor, 1996-1998: 2. A study of the efficacy of the Montreal Protocol and other regulatory measures, *J. Geophys. Res., 108* (D6), 4186, doi: 10.1029/2001JD001117, 2003.

Battle, M., M.L. Bender, P.P. Tans, J.W.C. White, J.T. Ellis, T. Conway, and R.J. Francey, Global carbon sinks and their variability inferred from atmospheric O_2 and delta ^{13}C, *Science, 287* (5462), 2467-2470, 2000.

Bayes, K.D., D.W. Toohey, R.R. Friedl, and S.P. Sander, Measurements of quantum yields of bromine atoms in the photolysis of bromoform from 266 to 324 nm, *J. Geophys. Res., 108* (D3), 4095, doi: 10.1029/2002JD002877, 2003.

Bernard, S., T.R. Röckmann, J. Kaiser, J.-M. Barnola, H. Fischer, T. Blunier, and J. Chappellaz, Constraints on N_2O budget changes since pre-industrial time from new firn air and ice core isotope measurements, *Atmos. Chem. Phys., 6*, 493-503, 2006.

Berthet, G., P. Ricaud, F. Lefèvre, E. Le Flochmoën, J. Urban, B. Barret, N. Lautié, E. Dupuy, J. De La Noë, and D. Murtagh, Nighttime chlorine monoxide observations by the Odin satellite and implications for the ClO/Cl_2O_2 equilibrium, *Geophys. Res. Lett., 32*, L11812, doi: 10.1029/2006GL022649, 2005.

Blake, D.R., T.-Y. Chen, T.W. Smith Jr., C.J.-L. Wang, O.W. Wingenter, N.J. Blake, F.S. Rowland, and E.W. Mayer, Three-dimensional distribution of non-methane hydrocarbons and halocarbons over the northwestern Pacific during the 1991 Pacific Exploratory Mission (PEM-West A), *J. Geophys. Res., 101* (D1), 1763-1778, 1996.

Blake, N.J., D.R. Blake, I.J. Simpson, J.P. Lopez, N.A.C. Johnston, A.L. Swanson, A.S. Katzenstein, S. Meinardi, B.C. Sive, J.J. Colman, E. Atlas, F. Flocke, S.A. Vay, M.A. Avery, and F.S. Rowland, Large-scale latitudinal and vertical distributions of NMHCs and selected halocarbons in the troposphere over the Pacific Ocean during the March-April 1999 Pacific Exploratory Mission (PEM-Tropics B), *J. Geophys. Res., 106* (D23), 32627-32644, 2001.

Blake, N.J., D.R. Blake, I.J. Simpson, S. Meinardi, A.L. Swanson, J.P. Lopez, A.S. Katzenstein, B. Barletta, T. Shirai, E. Atlas, G. Sachse, M. Avery, S. Vay, H.E. Fuelberg, C.M. Kiley, K. Kita, and F.S. Rowland, NMHCs and halocarbons in Asian continental outflow during the Transport and Chemical Evolution over the Pacific (TRACE-P) Field Campaign: Comparison with PEM-West B, *J. Geophys. Res., 108* (D20), 8806, doi: 10.1029/2002JD003367, 2003.

Borch, T., P. Ambus, F. Laturnus, B. Svensmark, and C. Gron, Biodegradation of chlorinated solvents in a water unsaturated topsoil, *Chemosphere, 51* (2), 143-152, 2003.

Bousquet, P., D.A. Hauglustaine, P. Peylin, C. Carouge, and P. Ciais, Two decades of OH variability as inferred by an inversion of atmospheric transport and chemistry of methyl chloroform, *Atmos. Chem. Phys., 5*, 2635-2656, 2005.

Brasseur, G., M.H. Hitchman, S. Walters, M. Dymek, E. Falise, and M. Pirre, An interactive chemical dynamic radiative two-dimensional model of the middle atmosphere, *J. Geophys. Res., 95* (D5), 5639-5655, 1990.

Burgess, A.B., R.G. Grainger, A. Dudhia, V.H. Payne, and V.L. Jay, MIPAS measurement of sulphur hexafluoride (SF_6), *Geophys. Res. Lett., 31* (5), L05112, doi: 10.1029/2003GL019143, 2004.

Butler, J.H., S.A. Montzka, A.D. Clarke, J.M. Lobert, and J.W. Elkins, Growth and distribution of halons in the atmosphere, *J. Geophys. Res., 103* (D1), 1503-1511, 1998.

Butler, J.H., M. Battle, M.L. Bender, S.A. Montzka, A.D. Clarke, E.S. Saltzman, C.M. Sucher, J.P. Severinghaus, and J.W. Elkins, A record of atmospheric halocarbons during the twentieth century from polar firn air, *Nature, 399* (6738), 749-755, 1999.

Chen, L., K. Tokuhashi, S. Kutsuna, A. Sekiya, Y. Yonei, and A. Yamamoto, Kinetic study of the gas-phase reaction of $CF_3CHFCF_2CH_2OH$ with OH radicals at 230-430 K, *Chem. Phys. Lett., 382* (3-4), 277-282, 2003.

Chen, L., S. Kutsuna, K. Tokuhashi, and A. Sekiya, Kinetics of the gas-phase reactions of $CF_3OC(O)H$ with OH radicals at 253-328 K, *Int. J. Chem. Kinet., 36* (6), 337-344, 2004a.

Chen, L., S. Kutsuna, K. Tokuhashi, and A. Sekiya, Kinetics study of the gas-phase reactions of $C_2F_5OC(O)H$ and n-$C_3F_7OC(O)H$ with OH radicals at 253-328 K, *Chem. Phys. Lett., 400* (4-6), 563-568, 2004b.

Chen, L., S. Kutsuna, K. Tokuhashi, and A. Sekiya, Kinetics study of the gas-phase reactions of $CHF_2CF_2OCHF_2$ and $CF_3CHFCF_2OCH_2CF_2CF_3$ with OH radicals at 253-328 K, *Chem. Phys. Lett., 403* (1-3), 180-184, 2005.

Chim, R.Y.L., R.A. Kennedy, and R.P. Tuckett, The vacuum-UV absorption spectrum of SF_5CF_3; implications for its lifetime in the earth's atmosphere, *Chem. Phys. Lett., 367* (5-6), 697-703, 2003.

Chipperfield, M.P., M. Burton, W. Bell, C.P. Walsh, T. Blumenstock, M.T. Coffey, J.W. Hannigan, W.G. Mankin, B. Galle, J. Mellqvist, E. Mahieu, R. Zander, J. Notholt, B. Sen, and G.C. Toon, On the use of HF as a reference for the comparison of stratospheric observations and models, *J. Geophys. Res., 102* (D11), 12901-12919, 1997.

Coheur, P.F., C. Clerbaux, and R. Colin, Spectroscopic measurements of halocarbons and hydrohalocarbons by satellite-borne remote sensors, *J. Geophys.*

Res., 108 (D4), 4130, doi: 10.1029/2002JD002649, 2003.

Conway, T.J. (Ed.), A.E. Andrews, L. Bruhwiler, A. Crotwell, E.J. Dlugokencky, M.P. Hahn, A.I. Hirsch, D.R. Kitzis, P.M. Lang, K.A. Masarie, A.M. Michalak, J.B. Miller, P.C. Novelli, W. Peters, P.P. Tans, K.W. Thoning, B.H. Vaughn, and C. Zhao, Carbon Cycle Greenhouse Gases, in *Climate Monitoring and Diagnostics Laboratory: Summary Report No. 27, 2002-2003*, edited by R.C. Schnell, A.-M. Buggle, and R.M. Rosson, 32-57, NOAA/ Climate Monitoring and Diagnostics Laboratory, Boulder, Colo., 2004.

Cotter, E.S.N., C.E. Canosa-Mas, C.R. Manners, R.P. Wayne, and D.E. Shallcross, Kinetic study of the reactions of OH with the simple alkyl iodides: CH_3I, C_2H_5I, 1-C_3H_7I and 2-C_3H_7I, *Atmos. Environ., 37* (8), 1125-1133, 2003.

Cox, M.L., P.J. Fraser, G.A. Sturrock, S.T. Siems, and L.W. Porter, Terrestrial sources and sinks of halomethanes near Cape Grim, Tasmania, *Atmos. Environ., 38* (23), 3839-3852, 2004.

Cox, M.L., G.A. Sturrock, P.J. Fraser, S.T. Siems, and P.B. Krummel, Identification of regional sources of methyl bromide and methyl iodide from AGAGE observations at Cape Grim, Tasmania, *J. Atmos. Chem., 50* (1), 59-77, 2005.

Cox, P.M., R.A. Betts, C.D. Jones, S.A. Spall, and I.J. Totterdell, Acceleration of global warming due to carbon-cycle feedbacks in a coupled climate model, *Nature, 408* (6809), 184-187, 2000.

Culbertson, J.A., J.M. Prins, E.P. Grimsrud, R.A. Rasmussen, M.A.K. Khalil, and M.J. Shearer, Observed trends for CF_3-containing compounds in background air at Cape Meares, Oregon, Point Barrow, Alaska, and Palmer Station, Antarctica, *Chemosphere, 55* (8), 1109-1119, 2004.

Cunnold, D.M., P.J. Fraser, R.F. Weiss, R.G. Prinn, P.G. Simmonds, B.R. Miller, F.N. Alyea, and A.J. Crawford, Global trends and annual releases of CCl_3F and CCl_2F_2 estimated from ALE/GAGE and other measurements from July 1978 to June 1991, *J. Geophys. Res., 99* (D1), 1107-1126, 1994.

Cunnold, D.M., R.F. Weiss, R.G. Prinn, D. Hartley, P.G. Simmonds, P.J. Fraser, B. Miller, F.N. Alyea, and L. Porter, GAGE/AGAGE measurements indicating reductions in global emissions of CCl_3F and CCl_2F_2 in 1992-1994, *J. Geophys. Res., 102* (D1), 1259-1269, 1997.

Daniel, J.S., S. Solomon, and D.L. Albritton, On the evaluation of halocarbon radiative forcing and global warming potentials, *J. Geophys. Res., 100* (D1),

1271-1285, 1995.

DeMore, W.B., and K.D. Bayes, Rate constants for the reactions of hydroxyl radical with several alkanes, cycloalkanes, and dimethyl ether, *J. Phys. Chem. A*, *103* (15), 2649-2654, 1999.

Dlugokencky, E.J., K.A. Masarie, P.M. Lang, and P.P. Tans, Continuing decline in the growth rate of the atmospheric methane burden, *Nature*, *393* (6684)*,* 447-450, 1998.

Dlugokencky, E.J., S. Houweling, L. Bruhwiler, K.A. Masarie, P.M. Lang, J.B. Miller, and P.P. Tans, Atmospheric methane levels off: Temporary pause or a new steady-state?, *Geophys. Res. Lett.*, *30* (19), 1992, doi: 10.1029/2003GL018126, 2003.

Dufour, G., C.D. Boone, and P.F. Bernath, First measurements of CFC-113 and HCFC-142b from space using ACE-FTS infrared spectra, *Geophys. Res. Lett., 32,* L15S09, doi: 10.1029/2005GL022422, 2005.

Duncan, B.N., R.V. Martin, A.C. Staudt, R. Yevich, and J.A. Logan, Interannual and seasonal variability of biomass burning emissions constrained by satellite observations, *J. Geophys. Res*., *108* (D2), 4100, doi: 10.1029/2002JD002378, 2003.

Dunse, B.L., L.P. Steele, S.R. Wilson, P.J. Fraser, and P.B. Krummel, Trace gas emissions from Melbourne, Australia, based on AGAGE observations at Cape Grim, Tasmania, 1995-2000, *Atmos. Environ., 39* (34)*,* 6334-6344, 2005.

Engel, A., M. Strunk, M. Muller, H.P. Haase, C. Poss, I. Levin, and U. Schmidt, Temporal development of total chlorine in the high-latitude stratosphere based on reference distributions of mean age derived from CO_2 and SF_6, *J. Geophys. Res., 107* (D12), 4136, doi: 10.1029/2001JD000584, 2002.

Ferretti, D.F., J.B. Miller, J.W.C. White, D.M. Etheridge, K.R. Lassey, D.C. Lowe, C.M.M. Meure, M.F. Dreier, C.M. Trudinger, T.D. van Ommen, and R.L. Langenfelds, Unexpected changes to the global methane budget over the past 2000 years, *Science, 309* (5741), 1714-1717, 2005.

Flückiger, J., E. Monnin, B. Stauffer, J. Schwander, T.F. Stocker, J. Chappellaz, D. Raynaud, and J.-M. Barnola, High-resolution Holocene N_2O ice core record and its relationship with CH_4 and CO_2, *Global Biogeochem. Cycles*, *16* (1), 1010, doi: 10.1029/2001GB001417, 2002.

Frankenberg, C., J.F. Meirink, M. van Weele, U. Platt, and T. Wagner, Assessing methane emissions from global space-borne observations, *Science*, *308* (5724), 1010-1014, 2005.

Fraser, P., D. Cunnold, F. Alyea, R. Weiss, R. Prinn, P.

Simmonds, B. Miller, and R. Langenfelds, Lifetime and emission estimates of 1,1,2-trichlorotrifluoroethane (CFC-113) from daily global background observations June 1982 - June 1994, *J. Geophys. Res., 101* (D7), 12585-12599, 1996.

Fraser, P.J., D.E. Oram, C.E. Reeves, S.A. Penkett, and A. McCulloch, Southern Hemispheric halon trends (1978-1998) and global halon emissions, *J. Geophys. Res., 104* (D13), 15985-15999, 1999.

Fraser, P.J., L.W. Porter, S.B. Baly, P.B. Krummel, B.L. Dunse, L.P. Steele, N. Derek, R.L. Langenfelds, I. Levin, D.E. Oram, J.W. Elkins, M.K. Vollmer, and R.F. Weiss, Sulfur hexafluoride at Cape Grim: long term trends and regional emissions, in *Baseline Atmospheric Program (Australia) 2001-2002*, edited by J.M. Cainey, N. Derek, and P.B. Krummel, 18-23, Bureau of Meteorology and CSIRO Division of Atmospheric Research, Melbourne, Australia, 2004.

Freedman, D.L., M. Swamy, N.C. Bell, and M.F. Verce, Biodegradation of chloromethane by Pseudomonas aeruginosa strain NB1 under nitrate-reducing and aerobic conditions, *Appl. Environ. Microbiol.*, *70* (8), 4629-4634, 2004.

Froidevaux, L., N.J. Livesey, W.G. Read, Y.B.B. Jiang, C. Jimenez, M.J. Filipiak, M.J. Schwartz, M.L. Santee, H.C. Pumphrey, J.H. Jiang, D.L. Wu, G.L. Manney, B.J. Drouin, J.W. Waters, E.J. Fetzer, P.F. Bernath, C.D. Boone, K.A. Walker, K.W. Jucks, G.C. Toon, J.J. Margitan, B. Sen, C.R. Webster, L.E. Christensen, J.W. Elkins, E. Atlas, R.A. Lueb, and R. Hendershot, Early validation analyses of atmospheric profiles from EOS MLS on the Aura satellite, *IEEE Trans. Geosci. Remote Sens.*, *44* (5), 1106-1121, 2006.

GLOBALVIEW-CH_4, Cooperative Atmospheric Data Integration Project - Methane. CD-ROM, NOAA CMDL, Boulder, Colo., 2005. Available via anonymous FTP to ftp.cmdl.noaa.gov, Path: ccg/ch4/ GLOBALVIEW.

Gola, A.A., B. D'Anna, K.L. Feilberg, S.R. Sellevag, L. Bache-Andreassen, and C.J. Nielsen, Kinetic isotope effects in the gas phase reactions of OH and Cl with CH_3Cl, CD_3Cl, and $^{13}CH_3Cl$, *Atmos. Chem. Phys.*, *5*, 2395-2402, 2005.

Gros, V., J. Williams, J.A. van Aardenne, G. Salisbury, R. Hofmann, M.G. Lawrence, R. von Kuhlmann, J. Lelieveld, M. Krol, H. Berresheim, J.M. Lobert, and E. Atlas, Origin of anthropogenic hydrocarbons and halocarbons measured in the summertime european outflow (on Crete in 2001), *Atmos. Chem. Phys., 3*, 1223-1235, 2003.

Groszko, W., and R.M. Moore, Ocean-atmosphere exchange of methyl bromide: NW Atlantic and Pacific Ocean studies, *J. Geophys. Res., 103* (D13), 16737-16741, 1998.

Hall, B.D. (Ed.), J.H. Butler, A.D. Clarke, G.S. Dutton, J.W. Elkins, D.F. Hurst, D.B. King, E.S. Kline, J. Lind, L.T. Lock, D. Mondeel, S.A. Montzka, F.L. Moore, J.D. Nance, E.A. Ray, P.A. Romashkin, and T.M. Thompson, Halocarbons and other atmospheric trace species, in *Climate Monitoring and Diagnostics Laboratory: Summary Report No. 26, 2000-2001*, edited by D.B. King, R.C. Schnell, and R.M. Rosson, 106-135, NOAA/Climate Monitoring and Diagnostics Laboratory, Boulder, Colo., 2002.

Hamilton, J.T.G., W.C. McRoberts, F. Keppler, R.M. Kalin, and D.B. Harper, Chloride methylation by plant pectin: An efficient environmentally significant process, *Science*, *301* (5630)*, 206-209, 2003.

Happell, J.D., and M.P. Roche, Soils: A global sink of atmospheric carbon tetrachloride, *Geophys. Res. Lett., 30* (2), 1088, doi: 10.1029/2002GL015957, 2003.

Harnisch, J., and N. Höhne, Comparison of emissions estimates derived from atmospheric measurements with national estimates of HFCs, PFCs and SF_6, *Environ. Sci. Pollut. Res., 9* (5), 315-320, 2002.

Harries, J.E., H.E. Brindley, P.J. Sagoo, and R.J. Bantges, Increase in greenhouse forcing inferred from the outgoing longwave radiation spectra of the Earth in 1970 and 1997, *Nature*, *410*, 355-357 and 1124 (erratum), 2001.

Hoffmann, L., R. Spang, M. Kaufman, and M. Riese, Retrieval of CFC-11 and CFC-12 from Envisat MIPAS observations by means of rapid radiative transfer calculations, *Adv. Space Res.*, *36* (5), 915-921, 2005.

Huang, L., L.L. Zhu, X.X. Pan, J.L. Zhang, O.Y. Bin, and H.Q. Hou, One potential source of the potent greenhouse gas SF_5CF_3: the reaction of SF_6 with fluorocarbon under discharge, *Atmos. Environ., 39* (9), 1641-1653, 2005.

Hurley, M.D., T.J. Wallington, M.P.S. Anderson, D.A. Ellis, J.W. Martin, and S.A. Mabury, Atmospheric chemistry of fluorinated alcohols: Reaction with Cl atoms and OH radicals and atmospheric lifetimes, *J. Phys. Chem. A, 108* (11), 1973-1979, 2004.

Hurst, D.F., P.A. Romashkin, J.W. Elkins, E.A. Oberlander, N.F. Elansky, I.B. Belikov, I.G. Granberg, G.S. Golitsyn, A.M. Grisenko, C.A.M. Brenninkmeijer, and P.J. Crutzen, Emissions of ozone-depleting substances in Russia during 2001, *J. Geophys. Res., 109*, D14303, doi: 10.1029/2004

JD004633, 2004.

Hurst, D.F., J.C. Lin, P.A. Romashkin, B.C. Daube, C. Gerbig, D.M. Matross, S.C. Wofsy, B.D. Hall, and J.W. Elkins, Continuing global significance of emissions of Montreal Protocol-restricted halocarbons in the United States and Canada, *J. Geophys. Res., 111*, D15302, doi: 10.1029/2005JD006785, 2006.

IPCC (Intergovernmental Panel on Climate Change), *Climate Change 2001: The Scientific Basis: Contribution of Working Group I to the Third Assessment Report of the Intergovernmental Panel on Climate Change,* edited by J.T. Houghton, Y. Ding, D.J. Griggs, M. Noguer, P.J. van der Linden, X. Dai, K. Maskell, and C.A. Johnson, 881 pp., Cambridge University Press, Cambridge, U.K., 2001.

IPCC/TEAP (Intergovernmental Panel on Climate Change/Technology and Economic Assessment Panel)*, IPCC/TEAP Special Report on Safeguarding the Ozone Layer and the Global Climate System: Issues Related to Hydrofluorocarbons and Perfluorocarbons*. Prepared by Working Groups I and III of the Intergovernmental Panel on Climate Change, and the Technical and Economic Assessment Panel, Cambridge University Press, Cambridge, U.K. and New York, N.Y., 2005.

Irion, F.W., M.R. Gunson, G.C. Toon, A.Y. Chang, A. Eldering, E. Mahieu, G.L. Manney, H.A. Michelsen, E.J. Moyer, M.J. Newchurch, G.B. Osterman, C.P. Rinsland, R.J. Salawitch, B. Sen, Y.L. Yung, and R. Zander, Atmospheric Trace Molecule Spectroscopy (ATMOS) Experiment Version 3 data retrievals, *Appl. Opt., 41* (33), 6968-6979, 2002.

Kaspers, K.A., R.S.W. van de Wal, J.A. de Gouw, C.M. Hofstede, M.R. van den Broeke, C. van der Veen, R.E.M. Neubert, H.A.J. Meijer, C.A.M. Brenninkmeijer, L. Karlof, and J.G. Winther, Analyses of firn gas samples from Dronning Maud Land, Antarctica: Study of nonmethane hydrocarbons and methyl chloride, *J. Geophys. Res., 109*, D02307, doi: 10.1029/2003JD003950, 2004.

Kaye, J.A., A.R. Douglass, C.H. Jackman, R.S. Stolarski, R. Zander, and G. Roland, Two-dimensional model calculation of fluorine-containing reservoir species in the stratosphere, *J. Geophys. Res., 96* (D7), 12865-12881, 1991.

Keeling, C.D., and T.P. Whorf, Atmospheric CO_2 records from sites in the SIO air sampling network, in *Trends*: *A Compendium of Data on Global Change*, Carbon Dioxide Information Analysis Center, Oak

Ridge National Laboratory, U.S. Department of Energy, Oak Ridge, Tenn., U.S.A., 2005.

Keppler, F., R.M. Kalin, D.B. Harper, W.C. McRoberts, and J.T.G. Hamilton, Carbon isotope anomaly in the major plant C-1 pool and its global biogeochemical implications, *Biogeosciences, 1* (2), 123-131, 2004.

Khalil, M.A.K., and R.A. Rasmussen, Soil-atmosphere exchange of radiatively and chemically active gases, *Environ. Sci. Pollut. Res., 7* (2)*,* 79-82, 2000.

Khalil, M.A.K., R.A. Rasmussen, and M.J. Shearer, Atmospheric nitrous oxide: patterns of global change during recent decades and centuries, *Chemosphere, 47* (8)*,* 807-821, 2002.

Khalil, M.A.K., R.A. Rasmussen, J.A. Culbertson, J.M. Prins, E.P. Grimsrud, and M.J. Shearer, Atmospheric perfluorocarbons, *Environ. Sci. Technol., 37* (19), 4358-4361, 2003.

Khosrawi, F., R. Muller, H. Irie, A. Engel, G.C. Toon, B. Sen, S. Aoki, T. Nakazawa, W.A. Traub, K.W. Jucks, D.G. Johnson, H. Oelhaf, G. Wetzel, T. Sugita, H. Kanzawa, T. Yokota, H. Nakajima, and Y. Sasano, Validation of CFC-12 measurements from the Improved Limb Atmospheric Spectrometer (ILAS) with the version 6.0 retrieval algorithm, *J. Geophys. Res.*, *109,* D06311, doi: 10.1029/2003JD004325, 2004.

King, D.B., J.H. Butler, S.A. Montzka, S.A. Yvon-Lewis, and J.W. Elkins, Implications of methyl bromide supersaturations in the temperate North Atlantic Ocean, *J. Geophys. Res*., *105* (D15), 19763-19769, 2000.

King, D.B., J.H. Butler, S.A. Yvon-Lewis, and S.A. Cotton, Predicting oceanic methyl bromide saturation from SST, *Geophys. Res. Lett., 29* (24), 2199, doi: 10.1029/2002GL016091, 2002.

Kopp, G., H. Berg, T. Blumenstock, H. Fischer, F. Hase, G. Hochschild, M. Höpfner, W. Kouker, T. Reddmann, R. Ruhnke, U. Raffalski, and Y. Kondo, Evolution of ozone and ozone-related species over Kiruna during the SOLVE/THESEO 2000 campaign retrieved from ground-based millimeter-wave and infrared observations, *J. Geophys. Res.*, *108* (D5), 8308, doi: 10.1029/2001JD001064, 2003.

Krieg, J., J. Nothholt, E. Mahieu, C.P. Rinsland, and R. Zander, Sulphur hexafluoride (SF$_6$): comparison of FTIR-measurements at three sites and determination of its trend in the northern hemisphere, *J. Quant. Spectrosc. Radiat. Transfer, 92* (3), 383-392, 2005.

Krol, M., P.J. van Leeuwen, and J. Lelieveld, Global OH trend inferred from methylchloroform measure-ments, *J. Geophys. Res., 103* (D9), 10697-10711, 1998.

Krol, M.C., J. Lelieveld, D.E. Oram, G.A. Sturrock, S.A. Penkett, C.A.M. Brenninkmeijer, V. Gros, J. Williams, and H.A. Scheeren, Continuing emissions of methyl chloroform from Europe, *Nature, 421* (6919), 131-135, 2003.

Krummel, P.B., L.W. Porter, P.J. Fraser, S.B. Daly, B.L. Dunse, and N. Derek, HCFCs, HFCs, halons, minor CFCs, PCE and halomethanes: The AGAGE in situ GC-MS Program at Cape Grim, 1998-2002, in *Baseline Atmospheric Program (Australia) 2001-2002*, edited by J.M. Cainey, N. Derek, and P.B. Krummel, 57-63, Bureau of Meteorology and CSIRO Division of Atmospheric Research, Melbourne, Australia, 2004.

Kurylo, M.J., and J.M. Rodríguez (Lead Authors), M. Andreae, E. Atlas, D. Blake, J. Butler, S. Lal, P. Midgley, S. Montzka, P. Novelli, C. Reeves, P. Simmonds, P. Steele, W.T. Sturges, R. Weiss, and Y. Yokouchi, Short-lived ozone-related compounds, Chapter 2 in *Scientific Assessment of Ozone Depletion: 1998*, *Global Ozone Research and Monitoring Project–Report No. 44*, World Meteorological Organization, Geneva, Switzerland, 1999.

Langenfelds, R.L., P.J. Fraser, R.J. Francey, L.P. Steele, L.W. Porter, and C.E. Allison, The Cape Grim Air Archive: The first seventeen years, 1978-1995, in *Baseline Atmospheric Program (Australia) 1994-95*, edited by R.J. Francey, A.L. Dick, and N. Derek, 53-70, Bureau of Meteorology and CSIRO Division of Atmospheric Research, Melbourne, Australia, 1996.

Lee-Taylor, J.M., and K.R. Redeker, Reevaluation of global emissions from rice paddies of methyl iodide and other species, *Geophys. Res. Lett., 32*, L15801, doi: 10.1029/2005GL022918, 2005.

Lee-Taylor, J.M., S.C. Doney, G.P. Brasseur, and J.-F. Muller, A global three-dimensional atmosphere-ocean model of methyl bromide distributions, *J. Geophys. Res., 103* (D13)*,* 16039-16057, 1998.

Lee-Taylor, J.M., G.P. Brasseur, and Y. Yokouchi, A preliminary three-dimensional global model study of atmospheric methyl chloride distributions, *J. Geophys. Res., 106* (D24), 34221-34233, 2001.

Li, J.L., D.M. Cunnold, H.-J. Wang, R.F. Weiss, B.R. Miller, C. Harth, P. Salameh, and J.M. Harris, Halocarbon emissions estimated from Advanced Global Atmospheric Gases Experiment measured pollution events at Trinidad Head, California, *J. Geophys. Res., 110* (D14308), doi: 10.1029/2004

JD005739, 2005.

Li, Y., K.O. Patten, D.J. Wuebbles, and D. Youn, Potential impacts of CF_3I on ozone as a replacement for CF_3Br in aircraft applications, *Atmos. Chem. Phys. Discuss., 6* (3), 5163-5195, 2006.

Limão-Vieira, P., S. Eden, P.A. Kendall, N.J. Mason, A. Giuliani, J. Heinesch, M.-J. Hubin-Franskin, J. Delwiche, and S.V. Hoffmann, An experimental study of SF_5CF_3 by electron energy loss spectroscopy, VUV photo-absorption and photoelectron spectroscopy, *Int. J. Mass Spectrom., 233* (1-3), 335-341, 2004.

Lobert, J., and J.M. Harris, Trace gases and air mass origin at Kaashidhoo, Indian Ocean, *J. Geophys. Res.*, *107* (D19), 8013, doi: 10.1029/2001JD000731, 2002.

Low, J.C., N.Y. Wang, J. Williams, and R.J. Cicerone, Measurements of ambient atmospheric C_2H_5Cl and other ethyl and methyl halides at coastal California sites and over the Pacific Ocean, *J. Geophys. Res., 108* (D19), 4608, doi: 10.1029/2003JD003620, 2003.

Lowe, D.C., C.A.M. Brenninkmeijer, G.W. Brailsford, K.R. Lassey, A.J. Gomez, and E.G. Nisbet, Concentration and ^{13}C records of atmospheric methane in New Zealand and Antarctica: Evidence for changes in methane sources, *J. Geophys. Res., 99* (D8), 16913-16925, 1994.

MacFarling-Meure, C., The variation of atmospheric carbon dioxide, methane and nitrous oxide during the Holocene from ice core analysis, Ph.D. thesis, University of Melbourne, Australia, 2004.

Mahieu, E., P. Duchatelet, R. Zander, P. Demoulin, C. Servais, C.P. Rinsland, M.P. Chipperfield, and M. De Mazière, The evolution of inorganic chlorine above the Jungfraujoch station: An update, in *Ozone Vol. II, Proceedings of the XX Quadrennial Ozone Symposium*, 1-8 June 2004, Kos, Greece, edited by C.S. Zerefos, 997-998, Int. Ozone Comm., Athens, Greece, 2004.

Maiss, M., and C.A.M. Brenninkmeijer, Atmospheric SF_6: Trends, sources and prospects, *Environ. Sci. Technol.*, *32* (20), 3077-3086, 1998.

Mangani, F., M. Maione, L. Lattanzi, and J. Arduini, A gas chromatographic-mass spectrometric method for trace analysis of chlorofluorocarbons and their replacement compounds in atmospheric samples, *Chromatographia*, *51* (5-6)*, 325-330, 2000.

Manning, A.J., D.B. Ryall, R.G. Derwent, P.G. Simmonds, and S. O'Doherty, Estimating European emissions of ozone-depleting and greenhouse gases using observations and a modeling back-attribution technique, *J. Geophys. Res., 108* (D14), 4405, doi:

10.1029/2002JD002312, 2003.

Markert, F., and O.J. Nielsen, The reactions of OH radicals with chloroalkanes in the temperature range 295-360 K, *Chem. Phys. Lett.*, *194* (1-2), 123-127, 1992.

McCulloch, A., and P.M. Midgley, The history of methyl chloroform emissions: 1951-2000, *Atmos. Environ., 35* (31), 5311-5319, 2001.

McDonald, I.R., K.L. Warner, C. McAnulla, C.A. Woodall, R.S. Oremland, and J.C. Murrell, A review of bacterial methyl halide degradation: Biochemistry, genetics and molecular ecology, *Environ. Microbiol., 4* (4), 193-203, 2002.

Miller, B.R., J. Huang, R.F. Weiss, R.G. Prinn, and P.J. Fraser, Atmospheric trend and lifetime of chlorodifluoromethane (HCFC-22) and the global tropospheric OH concentration, *J. Geophys. Res., 103* (D11), 13237-13248, 1998.

Miller, J.B., K.A. Mack, R. Dissly, J.W.C. White, E.J. Dlugokencky, and P.P. Tans, Development of analytical methods and measurements of $^{13}C/$ ^{12}C in atmospheric CH_4 from the NOAA/Climate Monitoring and Diagnostics Laboratory global air sampling network, *J. Geophys. Res., 107* (D13), 4178, doi: 10.1029/2001JD000630, 2002.

Miller, L.G., K.L. Warner, S.M. Baesman, R.S. Oremland, I.R. McDonald, S. Radajewski, and J.C. Murrell, Degradation of methyl bromide and methyl chloride in soil microcosms: Use of stable C isotope fractionation and stable isotope probing to identify reactions and the responsible microorganisms, *Geochim. Cosmochim. Acta, 68* (15), 3271-3283, 2004.

Millet, D.B., and A.H. Goldstein, Evidence of continuing methyl chloroform emissions from the United States, *Geophys. Res. Lett., 31*, L17101, doi: 10.1029/2004GL020166, 2004.

Montzka, S.A., and P.J. Fraser (Lead Authors), J.H. Butler, D. Cunnold, J. Daniel, D. Derwent, P. Connell, S. Lal, A. McCulloch, D. Oram, C. Reeves, E. Sanhueza, P. Steele, G.J.M. Velders, R.F. Weiss, and R. Zander, Controlled substances and other source gases, Chapter 1 in *Scientific Assessment of Ozone Depletion: 2002, Global Ozone Research and Monitoring Project–Report No. 47*, World Meteorological Organization, Geneva, Switzerland, 2003.

Montzka, S.A., R.C. Myers, J.H. Butler, J.W. Elkins, L.T. Lock, A.D. Clarke, and A.H. Goldstein, Observations of HFC-134a in the remote troposphere, *Geophys. Res. Lett., 23* (2), 169-172, 1996.

Montzka, S.A., J.H. Butler, J.W. Elkins, T.M. Thompson, A.D. Clarke, and L.T. Lock, Present and future

trends in the atmospheric burden of ozone-depleting halogens, *Nature, 398* (6729), 690-694, 1999.

Montzka, S.A., C.M. Spivakovsky, J.H. Butler, J.W. Elkins, L.T. Lock, and D.J. Mondeel, New observational constraints for atmospheric hydroxyl on global and hemispheric scales, *Science*, *288* (5465), 500-503, 2000.

Montzka, S.A, J.H. Butler, B.D. Hall, D.J. Mondeel, and J.W. Elkins, A decline in tropospheric organic bromine, *Geophys. Res. Lett., 30* (15), 1826, doi: 10.1029/2003GL017745, 2003.

Moore, R.M., The solubility of a suite of low molecular weight organochlorine compounds in seawater and implications for estimating the marine source of methyl chloride to the atmosphere, *Chemosphere: Global Change Sci., 2* (1), 95-99, 2000.

Moore, R.M., A. Gut, and M.O. Andreae, A pilot study of methyl chloride emissions from tropical woodrot fungi, *Chemosphere, 58* (2), 221-225, 2005.

Naik, V., A.K. Jain, K.O. Patten, and D.J. Wuebbles, Consistent sets of atmospheric lifetimes and radiative forcings on climate for CFC replacements: HCFCs and HFCs, *J. Geophys. Res.*, *105* (D5), 6903-6914, 2000.

Nassar, R., P.F. Bernath, C.D. Boone, C. Clerbaux, P.F. Coheur, G. Dufour, L. Froidevaux, E. Mahieu, J.C. McConnell, S.D. McLeod, D.P. Murtagh, C.P. Rinsland, K. Semeniuk, R. Skelton, K.A. Walker, and R. Zander, A global inventory of stratospheric chlorine in 2004, *J. Geophys. Res., 111*, D22312, doi: 10.1029/2006JD007073, 2006a.

Nassar, R., P.F. Bernath, C.D. Boone, S.D. McLeod, R. Skelton, K.A. Walker, C.P. Rinsland, and P. Duchatelet, A global inventory of stratospheric fluorine in 2004 based on Atmospheric Chemistry Experiment Fourier transform spectrometer (ACE-FTS) measurements, *J. Geophys. Res.*, *111*, D22313, doi: 10.1029/2006JD007395, 2006b.

Newman, P.A., E.R. Nash, S.R. Kawa, S.A. Montzka, and S.M. Schauffler, When will the Antarctic ozone hole recover?, *Geophys. Res. Lett., 33*, L12814, doi: 10.1029/2005GL025232, 2006.

O'Doherty, S., D.M. Cunnold, A. Manning, B.R. Miller, R.H.J. Wang, P.B. Krummel, P.J. Fraser, P.G. Simmonds, A. McCulloch, R.F. Weiss, P. Salameh, L.W. Porter, R.G. Prinn, J. Huang, G. Sturrock, D. Ryall, R.G. Derwent, and S.A. Montzka, Rapid growth of hydrofluorocarbon 134a, and hydrochlorofluorocarbons 141b, 142b and 22 from Advanced Global Atmospheric Gases Experiment (AGAGE) observations at Cape Grim, Tasmania, and Mace Head, Ireland, *J. Geophys. Res., 109*, D06310, doi:

10.1029/2003JD004277, 2004.

Oram, D.E., Trends of long-lived anthropogenic halocarbons in the Southern Hemisphere and model calculations of global emissions, Ph.D. thesis, University of East Anglia, Norwich, U.K., 1999.

Oram, D.E., C.E. Reeves, S.A. Penkett, and P.J. Fraser, Measurements of HCFC-142b and HCFC-141b in the Cape Grim air archive: 1978-1993, *Geophys. Res. Lett., 22* (20), 2741-2744, 1995.

Oram, D.E., C.E. Reeves, W.T. Sturges, S.A. Penkett, P.J. Fraser, and R.L. Langenfelds, Recent tropospheric growth rate and distribution of HFC-134a (CF_3CH_2F), *Geophys. Res. Lett.*, *23* (15), 1949-1952, 1996.

Oram, D.E., W.T. Sturges, S.A. Penkett, A. McCulloch, and P.J. Fraser, Growth of fluoroform (CHF_3, HFC-23) in the background atmosphere, *Geophys. Res. Lett.,* 25 (1), 35-38, 1998.

Palmer, P.I., D.J. Jacob, L.J. Mickley, D.R. Blake, G.W. Sachse, H.E. Fuelberg, and C.M. Kiley, Eastern Asian emissions of anthropogenic halocarbons deduced from aircraft concentration data, *J. Geophys. Res., 108* (D24), 4753, doi: 10.1029/ 2003JD003591, 2003.

Prather, M., and D. Ehhalt (Co-ordinating Lead Authors), F. Dentener, R. Derwent, E. Dlugokencky, E. Holland, I. Isaksen, J. Katima, V. Kirchhoff, P. Matson, P. Midgley, and M. Wang (Lead Authors), Atmospheric chemistry and greenhouse gases, Chapter 4 in *Climate Change 2001: The Scientific Basis Contribution of Working Group I to the Third Assessment Report of the Intergovernmental Panel on Climate Change*, edited by J.T. Houghton, Y. Ding, D.J. Griggs, M. Noguer, P.J. van der Linden, X. Dai, K. Maskell, and C.A. Johnson, 881 pp., Cambridge University Press, Cambridge, U.K., 2001.

Prinn, R.G., R.F. Weiss, P.J. Fraser, P.G. Simmonds, D.M. Cunnold, F.N. Alyea, S. O'Doherty, P. Salameh, B.R. Miller, J. Huang, R.H.J. Wang, D.E. Hartley, C. Harth, L.P. Steele, G. Sturrock, P.M. Midgley, and A. McCulloch, A history of chemically and radiatively important gases in air deduced from ALE/GAGE/AGAGE, *J. Geophys. Res., 105* (D14), 17751-17792, 2000.

Prinn, R.G., J. Huang, R.F. Weiss, D.M. Cunnold, P.J. Fraser, P.G. Simmonds, A. McCulloch, C. Harth, P. Salameh, S. O'Doherty, R.H.J. Wang, L. Porter, and B.R. Miller, Evidence for substantial variations of atmospheric hydroxyl radicals in the past two decades, *Science, 292* (5523), 1882-1888, 2001.

Prinn, R.G., J. Huang, R.F. Weiss, D.M. Cunnold, P.J.

Fraser, P.G. Simmonds, A. McCulloch, C. Harth, S. Reimann, P. Salameh, S. O'Doherty, R.-H.J. Wang, L.W. Porter, B.R. Miller, and P.B. Krummel, Evidence for variability of atmospheric hydroxyl radicals over the past quarter century, *Geophys. Res., Lett., 32*, L07809, doi: 10.1029/2004 GL022228, 2005.

Qiu, L.X., S.H. Shi, S.B. Xing, and X.G. Chen, Rate constants for the reactions of OH with five halogen-substituted ethanes from 292 to 366 K, *J. Phys. Chem., 96* (2), 685-689, 1992.

Quay, P., J. Stutsman, D. Wilbur, A. Snover, E. Dlugokencky, and T. Brown, The isotopic composition of atmospheric methane, *Global Biogeochem. Cycles, 13* (2), 445-461, 1999.

Rajakumar, B., J.B. Burkholder, R.W. Portmann, and A.R. Ravishankara, Rate coefficients for the OH + CFH_2CH_2OH reaction between 238 and 355 K, *Phys. Chem. Chem. Phys*., *7* (12), 2498-2505, 2005.

Ramaswamy, V. (Co-ordinating Lead Author), O. Boucher, J. Haigh, D. Hauglustaine, J. Haywood, G. Myhre, T. Nakajima, G.Y. Shi, and S. Solomon (Lead Authors), Radiative forcing of climate change, Chapter 6 in *Climate Change 2001: The Scientific Basis*, *Contribution of Working Group I to the Third Assessment Report of the Intergovernmental Panel on Climate Change*, edited by J.T. Houghton, Y. Ding, D.J. Griggs, M. Noguer, P.J. van der Linden, X. Dai, K. Maskell, and C.A. Johnson, 881 pp., Cambridge University Press, Cambridge, U.K., 2001.

Redeker, K.R., K.K. Treseder, and M.F. Allen, Ectomycorrhizal fungi: A new source of atmospheric methyl halides?, *Global Change Biol., 10* (6), 1009-1016, 2004.

Reeves, C.E., Atmospheric budget implications of the temporal and spatial trends in methyl bromide concentration, *J. Geophys. Res.*, *108* (D11), 4343, doi: 10.1029/2002JD002943, 2003.

Reeves, C.E., W.T. Sturges, G.A. Sturrock, K. Preston, D.E. Oram, J. Schwander, R. Mulvaney, J.-M. Barnola, and J. Chappellaz, Trends of halon gases in polar firn air: implications for their emission distributions, *Atmos. Chem. Phys., 5*, 2055-2064, 2005.

Reimann, S., A.J. Manning, P.G. Simmonds, D.M. Cunnold, R.H.J. Wang, J.L. Li, A. McCulloch, R.G. Prinn, J. Huang, R.F. Weiss, P.J. Fraser, S. O'Doherty, B.R. Greally, K. Stemmler, M. Hill, and D. Folini, Low European methyl chloroform emissions inferred from long-term atmospheric measurements, *Nature, 433* (7025), 506-508, 2005.

Rhew, R.C., B.R. Miller, M. Bill, A.H. Goldstein, and R.F. Weiss, Environmental and biological controls on methyl halide emissions from southern California coastal salt marshes, *Biogeochemistry, 60* (2), 141-161, 2002.

Rhew, R.C., L. Ostergaard, E.S. Saltzman, and M.F. Yanofsky, Genetic control of methyl halide production in Arabidopsis, *Curr. Biol., 13* (20), 1809-1813, 2003a.

Rhew, R.C., M. Aydin, and E.S. Saltzman, Measuring terrestrial fluxes of methyl chloride and methyl bromide using a stable isotope tracer technique, *Geophys. Res. Lett., 30* (21), doi: 10.1029/2003 GL018160, 2003b.

Rice, A.L., A.A. Gotoh, H.O. Ajie, and S.C. Tyler, High-precision continuous-flow measurement of delta ^{13}C and delta D of atmospheric CH_4, *Anal. Chem., 73* (17), 4104-4110, 2001.

Rinsland, C.P., R. Zander, E. Mahieu, L.S. Chiou, A. Goldman, and N.B. Jones, Stratospheric HF column abundances above Kitt Peak (31.9 degrees N latitude): trends from 1977-2001 and correlations with stratospheric HCl columns, *J. Quant. Spectrosc. Radiat. Transfer, 74* (2), 205-216, 2002.

Rinsland, C.P., E. Mahieu, R. Zander, N.B. Jones, M.P. Chipperfield, A. Goldman, J. Anderson, J.M. Russell III, P. Demoulin, J. Notholt, G.C. Toon, J.-F. Blavier, B. Sen, R. Sussmann, S.W. Wood, A. Meier, D.W.T. Griffith, L.S. Chiou, F.J. Murcray, T.M. Stephen, F. Hase, S. Mikuteit, A. Schulz, and T. Blumenstock, Long-term trends of inorganic chlorine from ground-based infrared solar spectra: Past increases and evidence for stabilization, *J. Geophys. Res., 108* (D8)*, 4252, doi: 10.1029/2002 JD003001, 2003.

Rinsland, C.P., C. Boone, R. Nassar, K. Walker, P. Bernath, E. Mahieu, R. Zander, J.C. McConnell, and L. Chiou, Trends of HF, HCl, CCl_2F_2, CCl_3F, $CHClF_2$ (HCFC-22) and SF_6 in the lower stratosphere from Atmospheric Chemistry Experiment (ACE) and Atmospheric Trace Molecule Spectroscopy (ATMOS) measurement near 30°N latitude, *Geophys. Res. Lett., 32* (16), L16S03, doi: 10.1029/ 2005GL022415, 2005.

Rinsland, C.P., E. Mahieu, R. Zander, R. Nassar, P. Bernath, C. Boone, and L.S. Chiou, Long-term stratospheric carbon tetrafluoride (CF_4) increase inferred from 1985-2004 infrared space-based solar occultation measurements, *Geophys. Res. Lett.*, *33* (2), L02808, doi: 10.1029/2005GL024709, 2006.

Röckmann, T., J. Kaiser, and C.A.M. Brenninkmeijer, The isotopic fingerprint of the pre-industrial and the

anthropogenic N$_2$O source, *Atmos. Chem. Phys*., *3*, 315-323, 2003.

Ruddiman, W.F., Orbital insolation, ice volume, and greenhouse gases. *Quart. Sci. Rev.*, *22* (15-17), 1597-1629, 2003.

Rummukainen, M., Modeling stratospheric chemistry in a global three-dimensional chemical transport model, SCTM-1: Model development, *Finn. Meteorol. Inst. Contrib., 19*, 206 pp., 1996.

Russell, J.M. III, L.L. Gordley, J.H. Park, S.R. Drayson, W.D. Hesketh, R.J. Cicerone, A.F. Tuck, J.E. Frederick, J.E. Harries, and P.J. Crutzen, The Halogen Occultation Experiment, *J. Geophys. Res., 98* (D6), 10777-10797, 1993.

Russell, J.M. III, L.E. Deaver, M.Z. Luo, R.J. Cicerone, J.H. Park, L.L. Gordley, G.C. Toon, M.R. Gunson, W.A. Traub, D.G. Johnson, K.W. Jucks, R. Zander, and I.G. Nolt, Validation of hydrogen fluoride measurements made by the Halogen Occultation Experiment from the UARS platform, *J. Geophys. Res., 101* (D6), 10163-10174, 1996.

Saltzman, E.S., M. Aydin, W.J. De Bruyn, D.B. King, and S.A Yvon-Lewis, Methyl bromide in preindustrial air: Measurements from an Antarctic ice core, *J. Geophys. Res., 109*, D05301, doi: 10.1029/2003JD004157, 2004.

Sander, S.P., R.R. Friedl, D.M. Golden, M.J. Kurylo, R.E. Huie, V.L. Orkin, G.K. Moortgat, A.R. Ravishankara, C.E. Kolb, M.J. Molina, and B.J. Finlayson-Pitts, *Chemical Kinetics and Photochemical Data for Use in Atmospheric Studies: Evaluation No. 14, JPL Publication 02-25*, Jet Propulsion Laboratory, Pasadena, Calif., 2003.

Sander, S.P., R.R. Friedl, D.M. Golden, M.J. Kurylo, G.K. Moortgat, H. Keller-Rudek, P.H. Wine, A.R. Ravishankara, C.E. Kolb, M.J. Molina, B.J. Finlayson-Pitts, R.E. Huie, and V.L. Orkin, *Chemical Kinetics and Photochemical Data for Use in Atmospheric Studies: Evaluation No. 15, JPL Publication 06-2*, Jet Propulsion Laboratory, Pasadena, Calif., 2006.

Santoro, M.A., Clarifying the SF$_5$CF$_3$ record, *Science*, *290* (5493), 935-935, 2000.

Schafer, H., I.R. McDonald, P.D. Nightingale, and J.C. Murrell, Evidence for the presence of a CmuA methyltransferase pathway in novel marine methyl halide-oxidizing bacteria, *Environ. Microbiol., 7* (6), 839-852, 2005.

Schauffler, S.M., E.L. Atlas, D.R. Blake, F. Flocke, R.A. Lueb, J.M. Lee-Taylor, V. Stroud, and W. Travnicek, Distributions of brominated organic compounds in the troposphere and lower stratosphere, *J. Geophys.*

Res., 104 (D17), 21513-21535, 1999.

Schauffler, S.M., E.L. Atlas, S.G. Donnelly, A. Andrews, S.A. Montzka, J.W. Elkins, D.F. Hurst, P.A. Romashkin, G.S. Dutton, and V. Stroud, Chlorine budget and partitioning during the Stratospheric Aerosol and Gas Experiment (SAGE) III Ozone Loss and Validation Experiment (SOLVE), *J. Geophys. Res., 108* (D5), 4173, doi: 10.1029/2001JD002040, 2003.

Schneider, M., T. Blumenstock, M.P. Chipperfield, F. Hase, W. Kouker, T. Reddmann, R. Ruhnke, E. Cuevas, and H. Fischer, Subtropical trace gas profiles determined by ground-based FTIR spectroscopy at Izaña (28°N, 16°W): Five-year record, error analysis, and comparison with 3-D CTMs, *Atmos. Chem. Phys., 5*, 153-167, 2005.

Shine, K.P., L.K. Gohar, M.D. Hurley, G. Marston, D. Martin, P.G. Simmonds, T.J. Wallington, and M. Watkins, Perfluorodecalin: Global warming potential and first detection in the atmosphere, *Atmos. Environ., 39* (9), 1759-1763, 2005.

Simmonds, P.G., D.M. Cunnold, F.N. Alyea, C.A. Cardelino, A.J. Crawford, R.G. Prinn, P.J. Fraser, R.A. Rasmussen, and R.D. Rosen, Carbon-tetrachloride lifetimes and emissions determined from daily global measurements during 1978-1985, *J. Atmos. Chem., 7* (1), 35-58, 1988.

Simmonds, P.G., D.M. Cunnold, R.F. Weiss, R.G. Prinn, P.J. Fraser, A. McCulloch, F.N. Alyea, and S. O'Doherty, Global trends and emission estimates of carbon tetrachloride (CCl$_4$) from in-situ background observations from July 1978 to June 1996, *J. Geophys. Res., 103* (D13), 16017-16027, 1998.

Simmonds, P.G, R.G. Derwent, A.J. Manning, P.J. Fraser, P.B. Krummel, S. O'Doherty, R.G. Prinn, D.M. Cunnold, B.R. Miller, H.J. Wang, D.B. Ryall, L.W. Porter, R.F. Weiss, and P.K. Salameh, AGAGE observations of methyl bromide and methyl chloride at Mace Head, Ireland, and Cape Grim, Tasmania, 1998-2001, *J. Atmos. Chem., 47* (3), 243-269, 2004.

Simmonds, P.G., A.J. Manning, D.M. Cunnold, A. McCulloch, S. O'Doherty, R.G. Derwent, P.B. Krummel, P.J. Fraser, B. Dunse, L.W. Porter, R.H.J. Wang, B.R. Greally, B.R. Miller, P. Salameh, R.F. Weiss, and R.G. Prinn, Global trends, seasonal cycles, and European emissions of dichloromethane, trichloroethene, and tetrachloroethene from the AGAGE observations at Mace Head, Ireland, and Cape Grim, Tasmania, *J. Geophys. Res.*, *111*, D18304, doi: 10.1029/2006JD007082, 2006.

Simpson, I.J., T.-Y. Chen, D.R. Blake, and F.S. Rowland,

Implications of the recent fluctuations in the growth rate of tropospheric methane, *Geophys. Res. Lett.*, *29* (10), 1479, doi: 10.1029/2001GL014521, 2002.

Solomon, P., J. Barrett, T. Mooney, B. Connor, A. Parrish, and D.E. Siskind, Rise and decline of active chlorine in the stratosphere, *Geophys. Res. Lett., 33*, L18807, doi: 10.1029/2006GL027029, 2006.

Sowers, T., A. Rodebaugh, N. Yoshida, and S. Toyoda, Extending records of the isotopic composition of atmospheric N_2O back to 1800 A.D. from air trapped in snow at the South Pole and the Greenland Ice Sheet Project II ice core, *Global Biogeochem. Cycles*, *16* (4), 1129, doi: 10.1029/2002GB001911, 2002.

Spahni, R., J. Chappellaz, T.F. Stocker, L. Loulergue, G. Hausammann, K. Kawamura, J. Flückiger, J. Schwander, D. Raynaud, V. Masson-Delmotte, and J. Jouzel, Atmospheric methane and nitrous oxide of the late Pleistocene from Antarctic ice cores, *Science, 310* (5752), 1317-1321, 2005.

Spivakovsky, C.M., J.A. Logan, S.A. Montzka, Y.J. Balkanski, M. Foreman-Fowler, D.B.A. Jones, L.W. Horowitz, A.C. Fusco, C.A.M. Brennink-meijer, M.J. Prather, S.C. Wofsy, and M.B. McElroy, Three-dimensional climatological distribution of tropospheric OH: Update and evaluation, *J. Geophys. Res., 105* (D7), 8931-8980, 2000.

Srivastava, A., A.E. Joseph, and S. Devotta, Volatile organic compounds in ambient air of Mumbai - India, *Atmos. Environ.*, *40* (5), 892-903, 2006.

Sturges, W.T, T.J. Wallington, M.D. Hurley, K.P. Shine, K. Sihra, A. Engel, D.E. Oram, S.A. Penkett, R. Mulvaney, and C.A.M. Brenninkmeijer, A potent greenhouse gas identified in the atmosphere: SF_5CF_3, *Science*, *289* (5479), 611-613, 2000.

Sturges, W.T., H.P. McIntyre, S.A. Penkett, J. Chappellaz, J.-M. Barnola, R. Mulvaney, E. Atlas, and V. Stroud, Methyl bromide, other brominated methanes, and methyl iodide in polar firn air, *J. Geophys. Res., 106* (D2), 1595-1606, 2001.

Sturrock, G.A., L.W. Porter, P.J. Fraser, N. Derek, and P.B. Krummel, HCFCs, HFCs, halons, minor CFCs and halomethanes—the AGAGE in situ GC-MS program, 1997-1998, and related measurements on flask air samples collected at Cape Grim, in *Baseline Atmospheric Program (Australia) 1997-98*, edited by N.W. Tindale, R.J. Francey, and N. Derek, 97-100, Bureau of Meteorology, CSIRO Division of Atmospheric Research, Melbourne, Australia, 2001.

Sturrock, G.A., D.M. Etheridge, C.M. Trudinger, P.J. Fraser, and A.M. Smith, Atmospheric histories of halocarbons from analysis of Antarctic firn air: Major Montreal Protocol species, *J. Geophys. Res., 107* (D24), 4765, doi: 10.1029/2002JD002548, 2002.

Sturrock, G.A., C.E. Reeves, G.P. Mills, S.A. Penkett, C.R. Parr, A. McMinn, G. Corno, N.W. Tindale, and P.J. Fraser, Saturation levels of methyl bromide in the coastal waters off Tasmania, *Global Biogeochem. Cycles, 17* (4), 1101, doi: 10.1029/2002GB002024, 2003.

Takahashi, K., T. Nakayama, Y. Matsumi, S. Solomon, T. Gejo, E. Shigemasa, and T.J. Wallington, Atmospheric lifetime of SF_5CF_3, *Geophys. Res. Lett.*, *29* (15), 1712, doi: 10.1029/2002GL015356, 2002.

Taniguchi, N., T.J. Wallington, M.D. Hurley, A.G. Guschin, L.T. Molina, and M.J. Molina, Atmospheric chemistry of $C_2F_5C(O)CF(CF_3)_2$: Photolysis and reaction with Cl atoms, OH radicals, and ozone, *J. Phys. Chem. A, 107* (15), 2674-2679, 2003.

Thompson, T.M. (Ed.), J.H. Butler, B.C. Daube, G.S. Dutton, J.W. Elkins, B.D. Hall, D.F. Hurst, D.B. King, E.S. Kline, B.G. LaFleur, J. Lind, S. Lovitz, D.J. Mondeel, S.A. Montzka, F.L. Moore, J.D. Nance, J.L. Neu, P.A. Romashkin, A. Scheffer, and W.J. Snible, Halocarbons and other atmospheric trace species, Section 5 in *Climate Monitoring and Diagnostics Laboratory: Summary Report No. 27, 2002-2003*, edited by R. Schnell, A.-M. Buggle, and R. Rosson, 115-135, NOAA/Climate Monitoring and Diagnostics Laboratory, Boulder, Colo., 2004.

Tokarczyk, R., E.S. Saltzman, R.M. Moore, and S.A. Yvon-Lewis, Biological degradation of methyl chloride in coastal seawater, *Global Biogeochem. Cycles, 17* (2), 1057, doi: 10.1029/2002GB001949, 2003a.

Tokarczyk, R., K.D. Goodwin, and E.S. Saltzman, Methyl chloride and methyl bromide degradation in the Southern Ocean, *Geophys. Res. Lett., 30* (15), 1808, doi: 10.1029/2003GL017459, 2003b.

Tokarczyk, R., and R.M. Moore, A seasonal study of methyl bromide concentrations in the North Atlantic (35°-60°N), *J. Geophys. Res., 111*, D08304, doi: 10.1029/2005JD006487, 2006.

Toon, G.C., J.-F. Blavier, B. Sen, and B.J. Drouin, Atmospheric $COCl_2$ measured by solar occultation spectrometry, *Geophys. Res. Lett., 28* (14), 2835-2838, 2001.

Trudinger, C.M., D.M. Etheridge, G.A. Sturrock, P.J. Fraser, P.B. Krummel, and A. McCulloch, Atmospheric histories of halocarbons from analysis of Antarctic firn air: Methyl bromide, methyl chloride, chloroform, and dichloromethane, *J. Geophys. Res.,*

109, D22310, doi: 10.1029/2004JD004932, 2004.

UNEP (United Nations Environment Programme), *1998 Report of the Technology and Economic Assessment Panel (TEAP)*, 286 pp., Nairobi, Kenya, 1998.

UNEP (United Nations Environment Programme), *1998 Assessment Report of the Halons Technical Options Committee (HTOC)*, 209 pp., Nairobi, Kenya, 1999.

UNEP (United Nations Environment Programme), *2002 Report of the Methyl Bromide Technical Options Committee 2002 Assessment (MBTOC)*, 437 pp., Nairobi, 2002a.

UNEP (United Nations Environment Programme), *Production and Consumption of Ozone Depleting Substances under the Montreal Protocol 1986-2000*, Ozone Secretariat, Nairobi, Kenya, Available: http://ozone.unep.org, 2002b.

UNEP (United Nations Environment Programme), *Assessment Report of the Halons Technical Options Committee (HTOC)*, 69 pp., Nairobi, Kenya, 2003.

UNEP (United Nations Environment Programme), Information provided by the Parties in accordance with Article 7 of the Montreal Protocol on Substances that Deplete the Ozone Layer, Nairobi, Kenya, 2005.

van der Werf, G.R., J.T. Randerson, G.J. Collatz, L. Giglio, P.S. Kasibhatla, A.F. Arellano Jr., S.C. Olsen, and E.S. Kasischke, Continental-scale partitioning of fire emissions during the 1997 to 2001 El Niño/La Niña period, *Science*, *303* (5654), 73-76, 2004.

Varner, R.K., P.M. Crill, and R.W. Talbot, Wetlands: a potentially significant source of atmospheric methyl bromide and methyl chloride, *Geophys. Res. Lett., 26* (16), 2433-2435, 1999.

Varner, R.K., M.L. White, C.H. Mosedale, and P.M. Crill, Production of methyl bromide in a temperate forest soil, *Geophys. Res. Lett., 30* (10), 1521, doi: 10.1029/2002GL016592, 2003.

Velders, G.J.M., and S. Madronich, (Co-ordinating Lead Authors), C. Clerbaux, R.G. Derwent, M. Grutter, D.A. Hauglustaine, S. Incecik, M.K.W. Ko, J.-M. Libre, O.J. Nielsen, F. Stordal, and T. Zhu (Lead Authors), Chemical and radiative effects of halocarbons and their replacement compounds, Chapter 2 in *IPCC/TEAP Special Report on Safeguarding the Ozone Layer and the Global Climate System*, edited by B. Metz, L. Kuijpers, S. Solomon, S.O. Andersen, O. Davidson, J. Pons, D. de Jager, T. Kestin, M. Manning, and L.A. Meyer, 478 pp., Cambridge University Press, Cambridge, U.K., 2005.

Verdonik, D.P., and M.L. Robin, Analysis of emission data, estimates, and modeling of fire protection agents, *Proceedings of the Earth Technology Forum*, Washington, D.C., 11 pp., 2004.

Volk, C.M., J.W. Elkins, D.W. Fahey, G.S. Sutton, J.M. Gilligan, M. Loewenstein, J.R. Podolske, K.R. Chan, and M.R. Gunson, Evaluation of source gas lifetimes from stratospheric observations, *J. Geophys. Res., 102* (D21), 25543-25564, 1997.

Vollmer, M.K., and R.F. Weiss, Simultaneous determination of sulfur hexafluoride and three chlorofluorocarbons in water and air, *Mar. Chem., 78* (2-3), 137-148, 2002.

von Clarmann, T., N. Glatthor, U. Grabowski, M. Höpfner, S. Kellmann, A. Linden, G.M. Tsidu, M. Milz, T. Steck, G.P. Stiller, H. Fischer, and B. Funke, Global stratospheric HOCl distributions retrieved from infrared limb emission spectra recorded by the Michelson Interferometer for Passive Atmospheric Sounding (MIPAS), *J. Geophys. Res.*, *111*, D05311, doi: 10.1029/2005JD005939, 2006.

Warwick, N.J., J.A. Pyle, and D.E. Shallcross, Global modelling of the atmospheric methyl bromide budget, *J. Atmos. Chem.*, *54* (2), 133-159, 2006.

Waugh, D.W., and T.M. Hall, Age of stratospheric air: Theory, observations, and models, *Rev. Geophys., 40* (4), 1010, doi: 10.1029/2000RG000101, 2002.

Waugh, D.W., D.B. Considine, and E.L. Fleming, Is upper stratospheric chlorine decreasing as expected?, *Geophys. Res. Lett., 28* (7), 1187-1190, 2001.

Wennberg, P.O., S. Peacock, J.T. Randerson, and R. Bleck, Recent changes in the air-sea gas exchange of methyl chloroform, *Geophys. Res. Lett., 31*, L16112, doi: 10.1029/2004GL020476, 2004.

White, M.L., R.K. Varner, P.M. Crill, and C.H. Mosedale, Controls on the seasonal exchange of CH_3Br in temperate peatlands, *Global Biogeochem. Cycles*, *19*, GB4009, doi: 10.1029/2004GB002343, 2005.

Wingenter, O.W., B.C. Sive, D.R. Blake, F.S. Rowland, and B.A. Ridley, Unexplained enhancements of CH_3Br in the Arctic and sub-Arctic lower troposphere during TOPSE spring 2000, *Geophys. Res. Lett., 30* (22), 2160, doi: 10.1029/2003GL018159, 2003.

WMO (World Meteorological Organization), *Scientific Assessment of Ozone Depletion: 1998*, *Global Ozone Research and Monitoring Project–Report No. 44*, Geneva, Switzerland, 1999.

WMO (World Meteorological Organization), *Scientific Assessment of Ozone Depletion: 2002*, *Global Ozone Research and Monitoring Project–Report No. 47*, Geneva, Switzerland, 2003. [referred to as *WMO 2002* in this chapter]

Wu, J.-Y., J.-Y. Liu, Z.-S. Li, and C.-C. Sun, Theoretical study of the reactions of CF_3OCHF_2 with the

hydroxyl radical and the chlorine atom, *ChemPhysChem*, *5* (9), 1336-1344, 2004.

Yokouchi, Y., Y. Noijiri, L.A. Barrie, D. Toom-Sauntry, T. Machida, Y. Inuzuka, H. Akimoto, H.J. Li, Y. Fujinuma, and S. Aoki, A strong source of methyl chloride to the atmosphere from tropical coastal land, *Nature, 403* (6767), 295-298, 2000.

Yokouchi, Y., D. Toom-Sauntry, K. Yazawa, T. Inagaki, and T. Tamaru, Recent decline of methyl bromide in the troposphere, *Atmos. Environ., 36* (32), 4985-4989, 2002.

Yokouchi, Y., T. Inagaki, K. Yazawa, T. Tamaru, T. Enomoto, and K. Izumi, Estimates of ratios of anthropogenic halocarbon emissions from Japan based on aircraft monitoring over Sagami Bay, Japan, *J. Geophys. Res., 110*, D06301, doi: 10.1029/ 2004JD005320, 2005.

Yoshida, Y., Y.H. Wang, T. Zeng, and R. Yantosca, A three-dimensional global model study of atmospheric methyl chloride budget and distributions, *J. Geophys. Res., 109*, D24309, doi: 10.1029/2004 JD004951, 2004.

Yvon-Lewis, S.A., and J.H. Butler, Effect of oceanic uptake on atmospheric lifetimes of selected trace gases, *J. Geophys. Res., 107* (D20), 4414, doi: 10.1029/2001JD001267, 2002.

Yvon-Lewis, S.A., J.H. Butler, E.S. Saltzman, P.A. Matrai, D.B. King, R. Tokarczyk, R.M. Moore, and J.Z. Zhang, Methyl bromide cycling in a warm-core eddy of the North Atlantic Ocean, *Global Biogeochem. Cycles, 16* (4), 1141, doi: 10.1029/ 2002GB001898, 2002.

Yvon-Lewis, S.A., D.B. King, R. Tokarczyk, K.D. Goodwin, E.S. Saltzman, and J.H. Butler, Methyl bromide and methyl chloride in the Southern Ocean, *J. Geophys. Res., 109*, C02008, doi: 10.1029/2003 JC001809, 2004.

Zander, R., C.P. Rinsland, E. Mahieu, M.R. Gunson, C.B. Farmer, M.C. Abrams, and M.K.W. Ko, Increase of carbonyl fluoride (COF_2) in the stratosphere and its contribution to the 1992 budget of inorganic fluorine in the upper stratosphere, *J. Geophys. Res., 99* (D8), 16737-16743, 1994.

Zander, R., E. Mahieu, M.R. Gunson, M.C. Abrams, A.Y. Chang, M. Abbas, C. Aellig, A. Engel, A. Goldman, F.W. Irion, N. Kämpfer, H.A. Michelsen, M.J. Newchurch, C.P. Rinsland, R.J. Salawitch, G.P. Stiller, and G.C. Toon, The 1994 northern midlatitude budget of stratospheric chlorine derived from ATMOS/ATLAS-3 observations, *Geophys. Res. Lett., 23* (17), 2357-2360, 1996.

Zander, R., E. Mahieu, P. Demoulin, P. Duchatelet, C. Servais, G. Roland, L. DelBouille, M. De Mazière, and C.P. Rinsland, Evolution of a dozen non-CO_2 greenhouse gases above central Europe since the mid-1980s, *Environ. Sci.*, *2* (2-3), 295-303, 2005.